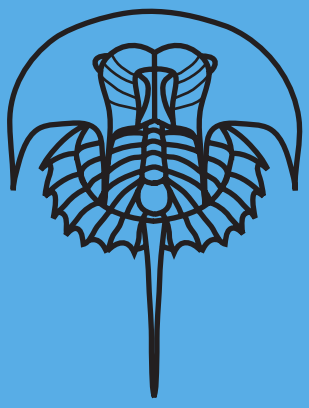

TREATISE ONLINE

Number 158

Part B, Volume 2, Chapter 6: Banded Iron Formations

Adriana Heimann

2021

KU PALEONTOLOGICAL INSTITUTE
The University of Kansas

Lawrence, Kansas, USA
ISSN 2153-4012
paleo.ku.edu/treatiseonline

PART B, VOLUME 2, CHAPTER 6
BANDED IRON FORMATIONS

Adriana Heimann

[East Carolina University, Department of Geological Sciences, Graham 101, Greenville, NC, USA; heimanna@ecu.edu]

INTRODUCTION

Banded iron formations (BIFs) are widespread marine chemical sedimentary rocks typical of the Precambrian with no perfect analogs in chemical composition and volume having formed since then. These enigmatic rocks, characterized by banding defined by the alternation of iron-rich minerals and chert, not only are the testimony of a very different young Earth but also the main source of iron worldwide. Extensive BIFs are used as important indicators of the redox state of the ancient oceans, and their characteristics and variations also reflect the evolution of the biosphere-atmosphere-solid Earth system from the Archean to the present. The literature on BIFs is immense and continues to grow. This chapter provides a summary and review of the current knowledge about BIFs, focusing on the hypotheses of BIF formation, both organic and inorganic, recognizing that such an overview will be far from complete. For a conceptual framework for the deposition of BIFs through time, see Bekker and others (2010) and references therein. For an alternative interpretation of the significance of BIFs in the rock record, see Ohmoto and others (2006). The main characteristics of BIFs, including their classification, temporal and geographic distribution, mineralogy, precursor phases, and geochemistry are presented here, followed by the main hypotheses of BIF genesis, including the sources of iron and silica, the genesis of the banding, inorganic hypotheses for their formation, and the ideas and evidence for the likely role of various bacterial processes in their formation. Geochemical (carbon isotopes, iron isotopes, molecular biomarkers), physical (microfossils), experimental, theoretical (cell calculations), and natural (biofilms) lines of evidence that provide insights into the various hypotheses of BIF formation are reviewed. Finally, possible Phanerozoic and modern environmental analogs to Archean–Proterozoic BIFs and their settings are described.

Although BIFs have been the focus of a huge number of studies, their genesis is still a matter of considerable debate. In particular, the origin of the oxidized iron present in BIFs has been debated for decades. Oxidation and precipitation of iron led to the deposition of some BIFs but exactly how this process operated is yet to be fully deciphered. The origin of the negative carbon isotope composition of carbonate carbon in BIFs, whether biotic or abiotic, has also been debated. Because of their age, BIFs are metamorphosed to various degrees and some are highly deformed. However, some BIFs only experienced a very low degree of metamorphism and a low degree of deformation and are beautifully preserved. Banding occurs at diverse scales, from microbanding (micrometric to millimetric laminations), to mesobanding (centimeter-scale), to macrobanding (meter-scale). How this banding originated has also been debated for decades and is still a matter of controversy. The mineralogy of BIFs is defined by various combinations of the main iron phases (magnetite, hematite, siderite, ankerite, and Fe-silicates) and chert.

Large BIFs range in age from the Eoarchean (~3.8 Ga) Isua BIF from Greenland, to the

Heimann, Adriana. 2021. Part B, Volume 1, Chapter 6: Banded iron formations. Treatise Online 158:1–48, 4 fig., 2 tables.

late Paleoproterozoic (~1.8 Ga) Biwabik and Gunflint BIFs from North America (Canada and USA). The abundance of BIFs in the rock record peaked during the late Archean (2.7–2.5 Ga) and early Proterozoic (2.5–1.8 Ga). After a hiatus of at least 1.1 billion years, BIFs briefly appeared again during the Neoproterozoic (~0.8–0.6 Ga), for example as the ~0.6 Ga BIFs of Urucum, Brazil, and the ~0.75 Ga Rapitan BIFs, Canada. BIFs are most commonly classified based on tectonic setting and age. Algoma-type BIFs are mostly Archean BIFs that formed in active tectonic settings, whereas Superior-type BIFs formed in stable platforms mostly during the Archean–Paleoproterozic. Neoproterozoic BIFs are referred to as Rapitan BIFs and are spatially and temporally associated with Snowball Earth glacial deposits. Snowball Earth refers to a time when Earth's surface is thought to have been entirely or nearly entirely frozen (KIRSCHVINK, 1992). In this chapter, the term BIF is used to refer to all iron formations unless a particular type of BIF is noted. Geographically, BIFs are distributed throughout the planet, but some of the largest and most studied ones include the low metamorphic grade Kuruman BIF from the Transvaal Supergroup in South Africa, the Brockman BIF from the Hamersley Range in Western Australia, and the Biwabik-Gunflint BIF from the Animikie Basin of North America.

The most traditional view holds that BIFs were formed by inorganic chemical and physical processes by which $Fe(II)_{aq}$ emanating from hydrothermal vents would, for example, combine with inorganic bicarbonate dissolved in ocean water and precipitate directly as siderite ($FeCO_3$). Alternatively, after upwelling, $Fe(II)_{aq}$ would become oxidized by small amounts of dissolved O_2 in the upper water column and form hematite (Fe_2O_3) or magnetite (Fe_3O_4) after recrystallization of Fe(III)-hydrated precipitates, such as ferrihydrite. However, based on an increasing body of evidence, other hypotheses have been proposed to explain the formation of BIFs mediated by biological processes. Oxidation of $Fe(II)_{aq}$ and reduction of Fe(III) mediated by various kinds of bacteria, including chemolithoautotrophic iron-oxidizing bacteria, photoferrotrophic bacteria, and dissimilatory iron-reducing bacteria, have been invoked to explain the formation of magnetite, hematite, and siderite.

The disappearance of BIFs from the rock record at ~1.8 Ga, except from the resurgence in the glacial Neoproterozoic successions, is highly debated and has been attributed to various processes. These include the complete oxidation of the atmosphere and oceans after the Great Oxidation Event (GOE) and the increase in seawater sulfate concentration with subsequent expansion of bacterial dissimilatory sulfate reduction and the formation of a sulfidic deep ocean.

Some Phanerozoic ironstones, Phanerozoic iron formations related to massive sulfide deposits (MSDs), and modern siliceous ferric oxide precipitates from marine hydrothermal vents and the Red Sea, are the closest younger equivalents to BIFs. Modern environments that serve as possible analogs to those in which BIF deposition took place in the Precambrian—and where similar processes occur today—include deep ferruginous lakes, such as Lake Matano, Indonesia; iron-rich phototrophic microbial mats, such as those in Yellowstone National Park, USA; and the Iron Mountain acid mine drainage site in California, USA. However, it is important to note that considering size, mineralogy, and environmental conditions together, no real modern analogs of BIFs and their depositional environments occur today on Earth.

A glossary of terms and common abbreviations used in this chapter is on page 37.

TYPES OF BANDED IRON FORMATIONS

Various classification schemes have been used to refer to different varieties of banded iron formations (BIFs), variably considering features such as age, tectonic setting, mineralogy, and texture (JAMES, 1954; GROSS, 1965, 1980; KIMBERLEY, 1978; SIMONSON, 1985). The most currently used classification considers mainly age

and tectonic setting to divide BIFs into two main classes: 1) Algoma-type BIFs, found in volcano-sedimentary sequences of greenstone belts and typical of Eoarchean age; and 2) Superior-type BIFs, formed in stable platform sedimentary successions and characteristic of late Archean to late Paleoproterozoic age (e.g., Gross, 1965; Beukes & Gutzmer, 2008). There are also occurrences of BIFs in the Neoproterozoic related to Snowball Earth (Kirschvink, 1992) glaciogenic sedimentary rocks, which are commonly referred to as Rapitan BIFs (Gross, 1965; Klein, 2005; Macdonald & others, 2010). In addition, BIFs and exhalites occur spatially associated with massive sulfide deposits (MSDs) (e.g., Spry, Peter, & Slack, 2000; Corriveau & Spry, 2013). Exhalites, however, are chemically different than BIFs because they commonly contain a higher metal content (Pb and Zn, for example) compared to normal, non-MSD-related BIFs, and are not included here. Other iron-rich deposits include the Devonian Lahn-Dill-type iron ores in Germany, which occur as lenses and layers of massive iron associated with bimodal and pyroclastic volcanism and carbonate rocks (e.g., Flick, Hesbor, & Behnisch, 1990). The most likely origin of these iron ores is mobilization and redeposition of iron related to secondary diagenetic alteration of pyroclastic rocks (Flick, Hesbor, & Behnisch, 1990). Because some of these iron ores are different than Archean–Proterozoic BIFs, they are not included here. Many Phanerozoic ironstones are different than BIFs in mineralogy and texture but some can be considered similar; therefore, a brief description of these ironstones is included in *Phanerozoic Ironstones* (p. 33–34). Algoma, Superior, and Rapitan BIFs, as well as those associated with massive sulfide deposits (MSDs), are described in separate sections. However, all other mention of BIFs with no specific reference to a particular type imply Archean–Paleoproterozic BIFs and mostly Superior type, and not those related to MSDs.

Texturally, iron formations have been divided into banded iron formations (BIFs) and granular iron formations (GIFs) (see Klein, 2005 and references therein). BIFs are typical of Archean to early Paleoproterozoic successions and formed prior to the rise of atmospheric oxygen during the great oxidation event, ~2.4 Ga (Holland, 1984), whereas GIFs are clastic sedimentary rocks that became abundant after the GOE and are typical of the late Paleoproterozoic (e.g., Klein, 2005). Based on the lack of structures indicative of wave or storm action, Archean BIFs are generally considered to have been deposited in relatively deep water. In contrast, the granular textures typical of late Paleoproterozoic (1.8 Ga) GIFs indicate that they were deposited in shallow water under the influence of waves, likely close to or above storm and fair-weather wave base (e.g., Klein & Beukes, 1992). Granular iron formations can be slaty and cherty and can also be associated with stromatolites (e.g., Pufahl & Fralick, 2004). Both Algoma- and Superior-type BIFs were deposited in open marine environments during high sea level (Simonson & Hassler, 1996; Krapež, Barley, & Pickard, 2003; Fralick & Pufahl, 2006). However, some Superior-type BIFs contain banded and granular textures, the latter of which represent remobilization, transport, and redeposition of BIFs (Beukes & Gutzmer, 2008). GIFs are mainly restricted to Paleoproterozoic continental basins, such as those surrounding the Superior Craton of North America. Examples of BIFs include the giant Brockman Iron Formation of Western Australia (e.g., Klein, 2005), whereas the type examples of GIFs are those from the Lake Superior Region, USA; Labrador Trough, Canada; and Nabberu Basin of Western Australia (James, 1954; Goodwin, 1956; Simonson, 2003; Klein, 2005).

ALGOMA-TYPE BIFs

Algoma-type banded iron formations (BIFs) occur within Eoarchean to early Paleoproterozoic volcano-sedimentary sequences in greenstone belts, range in age from 3.8 Ga to ~2.6 Ga, and are characterized by currently being relatively small occurrences

(lateral extent <10 km, thickness <100 m) (Goodwin, 1973; James, 1983; Isley & Abbott, 1999; Huston & Logan, 2004). These BIFs are typically associated with volcanic rocks and greywackes and formed in tectonically active areas in volcanic arcs and spreading centers (Gross, 1995). Because of this association, scientists have hypothesized that Algoma-type BIFs formed by exhalative hydrothermal processes during pulses of magmatic and hydrothermal activity coeval with the deposition of the volcano-sedimentary successions of greenstone belts (Barley & others, 1998). Many Algoma-type BIFs are typically intensely deformed and folded, in contrast to Lake Superior BIFs that are commonly undeformed. Mineralogically, Algoma-type BIFs are characterized by iron that occurs in ferric and ferrous states in silicates, siderite, magnetite, and hematite.

The ~3.8 Ga Isua BIF, from the Isua Supracrustal Sequence in West Greenland, is an Algoma-type BIF and possibly the oldest BIF in the world. It is found in association with greenstones with low-K tholeiitic characteristics and turbidites, and experienced medium grade (amphibolite facies) metamorphism (Dymek & Klein, 1988; Komiya & others, 1999; Dauphas & others, 2004; Kato, Yamaguchi, & Ohmoto, 2006). Other Algoma-type BIFs include those in the Nulliak supracrustal sequence in Labrador, Canada, dated at ~3.95 Ga (Shimojo & others, 2013) associated with mafic rocks and metamorphosed to amphibolite facies (e.g., Aoki & others, 2013), and those in the 3.13–2.92 Ga Sargur greenstone belt in India, associated with mafic-ultramafic rocks, quartzites, pelites, and calc-silicate rocks and metamorphosed to upper amphibolite-granulite facies (e.g., Kato, Kano, & Kunugiza, 2002; Kato, Yamaguchi, & Ohmoto, 2006).

SUPERIOR-TYPE BIFs

Superior-type banded iron formations (BIFs) mostly formed in the late Archean to late Paleoproterozoic (3.0 to ~1.8 Ga) on stable, passive-margin continental shelf and slope. They are characterized by great areas and lateral extent (up to hundreds of meters thick, >100,000 km^2), are associated with marine siliciclastic (shale and quartzarenite) and carbonate rocks, and lack direct relationships with volcanic rocks (Trendall & Blockley, 1970; Gross, 1983, 1995; Klein, 2005; Kato, Yamaguchi, & Ohmoto, 2006; Beukes & Gutzmer, 2008; Bekker & others, 2010). They are also thought to have formed during periods of global high sea level and during pulses of enhanced magmatic (mantle plumes) and hydrothermal activity (e.g., Bekker & others, 2010). Mineralogically, Superior-type BIFs are characterized by iron in the ferrous state hosted in silicates, siderite, and magnetite, as well as iron in mixed-state minerals (most commonly magnetite) (e.g., Klein & Ladeira, 2004). Late Paleoproterozoic Superior-type BIFs, which have been studied extensively, commonly exhibit granular textures (e.g., Beukes & Gutzmer, 2008), are generally undeformed, and have been metamorphosed to only very low grades (see Klein, 2005; Beukes & Gutzmer, 2008 and references therein).

Examples of Superior-type BIFs include the giant ~2.5 Ga Brockman Iron Formation (Fig. 1.1, see p. 8); the extensive ~2.6 Ga Marra Mamba Iron Formation, and the smaller Weeli Wolli and Boolgeda BIFs of the Hamersley Range, Western Australia; the ~2.5–2.4 Ga Kuruman-Griquatown-Penge Iron Formations of the Kaapvaal craton, South Africa; the ~2.5 Ga BIFs from the São Francisco craton in Minas Gerais, Brazil; the ~2.4 Ga Kursk BIFs from the Kursk magnetic anomaly, Russia; the ~1.88 Ga Biwabik and Gunflint Iron Formations from the Animikie-Marquette basin, North America; and the ~1.88 Ga BIFs from the Yilgarn craton (Nabberu basin), Australia (see Klein, 2005; Beukes & Gutzmer, 2008; Bekker & others, 2010, and references therein).

RAPITAN BIFs

Neoproterozoic (~0.8–0.6 Ga) Rapitan banded iron formations (BIFs) are found

in marginal marine settings, some in broad extensional graben settings, and some are located in mobile belts, such as the Pan African and Brazilian-African belts (Gross, 1995; Trompette, Alvarenga, & de Walde, 1998; Ilyn, 2009). They are typically temporally and spatially associated to Sturtian (~716.5 Ma) and Marinoan (~635 Ma) glacial deposits of global Snowball Earth events (e.g., Kirschvink, 1992; Hoffman & others, 1998). However, studies based on mapping, stratigraphy, and geochemistry of Neoproterozoic BIFs from Namibia and South Africa suggest that all Neoproterozoic iron formations may be of 716.5 Ma Sturtian age (Macdonald & others, 2010). If this is the case, Rapitan BIFs formed as a result of the secular evolution of the redox state of the ocean, which is considered to have been anoxic at the time of iron concentration (Klein & Ladeira, 2004; Macdonald & others, 2010). Because the oceans were covered by ice, hydrothermal iron was able to accumulate in the water and precipitate as ferric oxyhydroxides when mixed with more oxic waters, either derived from subglacial meltwater plumes (Hoffman & others, 1998) or surface waters at the onset of ice melting (Klein & Beukes, 1993).

Rapitan BIFs are commonly associated with diamictite, are typically succeeded by cap carbonates (usually dolomite and rarely limestone), and may contain dropstones (e.g., Bekker & others, 2010; Macdonald & others, 2010). Texturally, these BIFs are commonly laminated, nodular, and oolitic. Mineralogically, Rapitan BIFs consist almost entirely of iron in the ferric state in hematite, in contrast to Archean and Paleoproterozoic BIFs (Klein & Ladeira, 2004). In addition, these iron deposits sometimes host economic manganese concentrations (Klein & Beukes, 1992; Klein & Ladeira, 2004; Halverson & others, 2011). Examples of Neoproterozoic BIFs, some of them large, include the Rapitan BIFs of the Northwestern Territories, Canada; the Urucúm region of Brazil; the Arroyo del Soldado Group, Lavalleja, in Uruguay; the Damara orogen in Namibia; and the Serranía de Mutum in Bolivia (Gross, 1983; Bühn, Stanistreet, & Okrusch, 1992; Klein & Ladeira, 2004; Klein, 2005; Pecoits & others, 2008).

BIFs RELATED TO MASSIVE SULFIDE DEPOSITS

Banded iron formations (BIFs) are commonly associated with metamorphosed base metal (Pb, Zn, Cu) massive sulfide deposits (MSDs) in sedimentary sequences and in felsic volcanic belts (Spry, Peter, & Slack, 2000; Slack, Grenne, & Bekker, 2009; Corriveau & Spry, 2013). These BIFs generally form below, above, in, or along strike from stratiform, exhalative, or volcanogenic ore deposits (e.g., Spry, Peter, & Slack, 2000). Less commonly, they form lateral to the ore deposits and extend for kilometers. Typically, the BIFs form layers less than two meters thick, although they can also reach tens of meters in thickness. They are also normally laminated with varying mineralogy from layer to layer. Geochemical data and diagrams, including those of Al/Al+Fe+Mn vs. Fe/Ti and ternary Al-Fe-Mn, indicate that the BIFs have variable amounts of hydrothermal and detrital components, but usually the detrital content is less than 30 wt% (Corriveau & Spry, 2013). BIFs related to MSDs tend to have a higher detrital component than non-MSD related BIFs but are very similar in most other aspects. Most BIFs associated with sulfide mineralization are chemical sedimentary rocks similar to Algoma-type iron formations and likely formed by venting of hydrothermal fluids into submarine basins (Stanton, 1972, 1976; Spry, Peter, & Slack, 2000).

BIFs occur in spatial association with some of the largest base metal sulfide deposits of the world. The most extensive BIFs associated with massive sulfide deposits (MSDs) are found in volcano-sedimentary sequences of continental rift systems, such as those near the giant Paleoproterozoic (~1.69 Ga) Broken Hill deposit, Australia (Fig. 4.3–4.4) and the Ordovician Bathurst deposit, New Brunswick, Canada (Spry, Peter, & Slack,

2000). BIFs appear close to the Broken Hill and Pinnacles deposits in the southern Curnamona Province of Australia, but also extend laterally and intermittently for about 100 km throughout the province (Stanton, 1972; Plimer, 1988; Parr, 1992; Parr & Plimer, 1993; Spry, Peter, & Slack, 2000; Heimann & others, 2009, 2013). Many of these BIFs do not have a clear temporal relationship with the sulfide ores (Spry, Peter, & Slack, 2000). In the Bathurst mining camp, BIFs and sulfide ore extend for 12 km (Peter & Goodfellow, 1996). Other important occurrences of BIFs associated with large MSDs appear in the Mesoproterozoic Gamsberg and Aggeneys deposits in South Africa and the Bergslagen deposit in Sweden (e.g., Plimer, 1988; Spry, Peter, & Slack, 2000).

Typical lithologies associated with BIFs related to metamorphosed MSDs include metamorphosed clastic sedimentary rocks and felsic volcanic rocks, as well as minor mafic igneous rocks that do not occur within the ore (Spry, Peter, & Slack, 2000). The mineralogy of the BIFs may include carbonates, oxides, silicates, and/or sulfides. Sulfide-bearing iron formation is present at the Gamsberg deposit (South Africa), the carbonate iron formation at the Bathurst deposit (Canada), the oxide-silicate iron formation at the Broken Hill deposit (Australia), and the Bergslagen deposit (Sweden) (Plimer, 1988; Peter & Goodfellow, 1996; Spry, Peter, & Slack, 2000).

SPATIAL AND TEMPORAL DISTRIBUTION OF BIFs

Archean–Paleoproterozoic banded iron formations (BIFs) range in age from ~3.8 Ga to ~1.88 Ga. Recent studies suggest that all Neoproterozoic BIFs may be ~716.5 Ma, although previous studies considered their ages to be ~0.8–0.6 Ga. The oldest BIFs are those (~3.8 Ga) from the Isua Supracrustal Belt of Western Greenland (Appel, 1987; Dymek & Klein, 1988). Other Archean BIFs include the ~3.6–3.2 Ga BIFs from the Sebakwian Group in Zimbabwe and the ~2.8–2.6 Ga BIFs of the Dharwar Supergroup in India (Manikyamba, Balaram, & Naqvi, 1993; Arora & others, 1995; Khan & others, 1996; Kato, Kano, & Kunugiza, 2002). There is some evidence that indicates that the largest peak in Algoma-type BIF deposition is related to a major mantle plume event at 2.75–2.70 Ga (Huston & Logan, 2004). A second peak in BIF deposition occurred at 2.5–2.45 Ga with the deposition of the large Superior-type BIFs of the Ghaap/Chuniespoort Group of the Kaapvaal Craton, South Africa, and the Hamersley Group, Australia (Houston & Logan, 2004; Beukes & Gutzmer, 2008). Another peak in BIF deposition occurred in the late Paleoproterozoic at ~1.88 Ga in the Lake Superior region of the USA and Canada. Studies of BIFs in the Frere Formation of Western Australia, previously thought to be 1.84 Ga, concluded that they are actually ~1.88 Ga, indicating that the deposition of BIFs in the Lake Superior region of North America and those in Western Australia are coeval and likely reflect global ocean chemistry (Rasmussen & others, 2012). These BIFs are coeval with important 1.88 Ga mafic-ultramafic magmatism, a large igneous province (LIP) interpreted to be related to a mantle plume event, juvenile continental and oceanic crust formation, mantle depletion, and volcanogenic MSD formation (Heaman & others, 1986; Condie, 1998; Isley & Abbott, 1999; Condie, 2002; Franklin & others, 2005; Kemp & others, 2006; Parman, 2007; Pearson, Parman, & Nowell, 2007; Hamilton & others, 2009; Heaman, Peck, Toope, 2009; Bekker & others, 2010; Meert & others, 2011). This suggests that BIFs formed as a result of major mantle activity and crustal growth (Rasmussen & others, 2012). After this event, large BIFs disappear from the rock record for more than one billion years (Klein & Beukes, 1993), returning in the Neoproterozoic associated with global glaciations of Snowball Earth distributed on nine separate paleocontinents (Macdonald & others, 2010). After these, BIFs typical of the Precambrian are not present in the rock record.

The present day geographic distribution of BIFs reaches every continent (e.g., Klein, 2005). Algoma-type BIFs are relatively small and commonly less than 10 km in lateral extent (Beukes & Gutzmer, 2008; Bekker & others, 2010). Examples of Algoma-type BIFs occur in India, Singhbhum Group (3.5 Ga) (Muckhopadhyay & others, 2008), and South Africa, Fig Tree Group, Barberton Greenstone Belt (~3.3 Ga) (Hofmann, 2005), among other places. The largest BIFs (10^5 km^2) are Superior-type BIFs, such as the Brockman Iron Formation of the Hamersley Range of Western Australia (~2.6–2.45 Ga) (Trendall & Blockley, 1970; Trendall, 2002; Trendall & others, 2004); the Quadrilátero Ferrífero of the Itabira Group, Minas Gerais, Brazil (~2.6-2.4 Ga) (Klein, 2005); and the Kuruman, Griquatown, and Penge Iron Formations of the Transvaal Supergroup of South Africa (~2.5–2.3 Ga) (Klein & Beukes, 1989) (Fig. 1.1). Paleogeographic reconstructions and detailed geochronological studies suggest that the Asbestos Hills-Penge Iron Formations, Kaapvaal Craton, South Africa (~2.5–2.45 Ga) and the Brockman Iron Formation, Pilbara Craton, Western Australia, were deposited synchronously in the super continent Vaalbara (Cheney, 1996; Zegers & others, 1998; Beukes & Gutzmer, 2008). However, some scientists have suggested, that the similarities, including the stratigraphy, reflect synchronized events on a global scale (Trendall, 1968; Button, 1976; Nelson, Trendall, & Altermann, 1999). Of the late Paleoproterozoic BIFs, the large Gunflint Iron Formation in the Animikie basin of North America (~1.88 Ga) contains the first undisputed microfossils that offer evidence of life on the early Earth (e.g., Barghoorn & Tyler, 1965; Awramik & Barghoorn, 1977). See *Clues from Microfossils,* p. 26–28, for elaboration. The youngest of the Paleoproterozoic BIFs include the ~1.7 Ga Baraboo BIF from the Freedom Formation, Wisconsin, USA (e.g., Weidman, 1904), which has not been studied in detail.

Examples of Neoproterozoic BIFs occur between 0.8 and 0.6 Ga in the Rapitan Group, Yukon and the Northwest Territory, Canada (~0.716 Ga); Jacadigo Group in the Urucúm District, Brazil and Bolivia (~0.6 Ga); the Damara Supergroup, Chuos Formation, Namibia (~0.75–0.65 Ga); and Arroyo del Soldado Group, eastern Uruguay (~0.6 Ga) (Breitkopf, 1988; Klein & Beukes, 1993; Klein & Ladeira, 2004; Klein, 2005; Pecoits & others, 2008). An integrated mapping, stratigraphic, geo-chemical, and geochronological study of Neoproterozoic BIFs and associated rocks in Namibia and South Africa proposed that all Neoproterozoic iron formations may be of Sturtian age (~716.5 Ma) (Mcdonald & others, 2010), instead of some being Marinoan in age (635 Ma) as previously thought (e.g., Frimmel, 2008). An association between Neoproterozoic BIFs and mantle plume events has also been proposed to explain their time-related genesis (e.g., Bekker & others, 2010). See *Hypotheses of BIF Formation,* p. 14–18, for elaboration on this topic.

MINERALOGY AND GEOCHEMISTRY OF BIFs

MINERALOGY AND PRECURSOR PHASES

The main minerals present in banded iron formations (BIFs) include (Table 1): siderite, magnetite, hematite, chert, stilpnomelane, minnesotaite and accessory ankerite, ferroan dolomite, riebeckite, mica (ferri-annite), and chlorite (Klein, 2005). Pyrite may be present as a rare accessory mineral. Some of these minerals, such as siderite and minnesotaite, required low oxygen conditions, whereas others, such as hematite or its precursor Fe oxyhydroxides, clearly required at least some oxygen present in the environment of formation. Some magnetite, siderite, ferrosilicates (minnesotaite), ankerite, and pyrite likely formed during diagenesis and metamorphism (e.g., Ayres, 1972; Perry, Tan, & Morey, 1973). Ankerite, for example, overgrew early, very thin siderite laminations

1

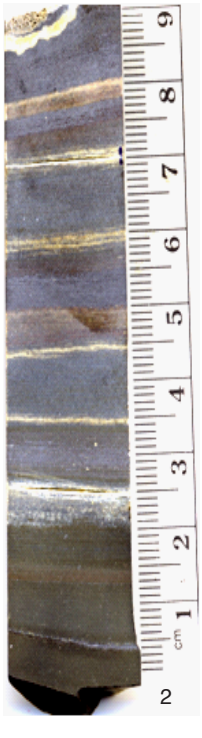

FIG. 1. Selected examples of banded iron formation with different mineralogy from the Brockman Iron Formation, Western Australia (*1–2*) and the Kuruman Iron Formation, South Africa (*3–4*). *1,* View of the Dales Gorge of the giant Brockman Iron Formation (new; image courtesy of Clark M. Johnson). *2,* Core slab sample of banded and laminated oxide and carbonate BIF; magnetite (gray), siderite + stilpnomelane (brown), pure siderite (light tan), Dales

(*continued on facing page*)

TABLE 1. Mineralogy and chemistry of major mineral constituents in Banded Iron Formations.

Mineral Group	Mineral Species	Chemical Composition
Carbonates	Siderite	$FeCO_3$
	Ankerite	$Ca(Fe^{2+},Mg)(CO_3)_2$
	Ferroan dolomite	$(CaMg,Fe^{2+})(CO_3)_2$
Oxides	Magnetite	Fe_3O_4 (or $FeO.Fe_2O_3$)
	Hematite	Fe_2O_3
Silicates	Quartz	SiO_2 (chert or amorphous silica)
	Stilpnomelane	$K(Fe^{2+},Mg,Fe^{3+})_8(Si,Al)_{12}(O,OH)_{27}.n(H_2O)$
	Greenalite	$(Fe^{2+},Fe^{3+})_{2-3}Si_2O_5(OH)_4$
	Minnesotaite	$Fe^{2+}{}_3Si_4O_{10}(OH)_2$
	Riebeckite	$Na_2(Fe^{2+},Mg)_3Fe^{3+}{}_2Si_8O_{22}(OH)_2$
	Ferriannite	$KFe^{2+}{}_3((Fe^{3+},Al)Si_3O_{10})(OH)_2$
	Chlorite	$(Mg,Fe^{2+})_3(Si,Al)_4O_{10}(OH)_2(Mg,Fe^{3+})_3(OH)_6$
	Nontronite	$Na_{0.3}Fe_2(Si,Al)_4O_{10}(OH)_2.nH_2O$
Hydroxides	Ferrihydrite	$Fe^{3+}{}_2O_3.0.5(H_2O)$
	Ferric hydroxide	$Fe^{3+}(OH)_3$
	Goethite	$Fe^{3+}O(OH)$
Sulfides	Pyrite	FeS_2

in the carbonate-rich Kuruman Iron Formation, likely evidencing a late diagenetic origin for ankerite and an early diagenetic origin for siderite (Fig. 1.3–1.4; 2.1–2.2) (BEUKES & KLEIN, 1990; BEUKES & others, 1990; HEIMANN & others, 2010).

The original mineralogy of BIFs has been debated for decades. The original or early diagenetic mineralogy of BIFs likely included the minerals siderite, amorphous or crystalline ferric hydroxides (ferrihydrite, ferric hydroxide, and goethite), greenalite, nontronite, and amorphous silica (Table 1) (e.g., KLEIN, 2005; BEUKES & GUTZMER, 2008). It has also been suggested that most siderite and pyrite in BIFs precipitated within the water column of anoxic basins, but some also formed during early diagenesis (OHMOTO & others, 2006). Silica was also present in the structure of original clays. Thermodynamic calculations and experiments indicate that ferric hydroxides (ferrihydrite or goethite) can be transformed to hematite by dehydration

FIG 1. (*continued from facing page*)

Gorge Member, Brockman Iron Formation, Western Australia, sample DDH#44-19. *3,* Core sample of banded and finely laminated carbonate BIF with siderite-chert laminations (dark black), pure siderite laminations (light brown), and large, diagenetic ankerite (white), Kuruman Iron Formation, Transvaal, South Africa, sample WB98-815 (*2–3,* core samples, Geology Museum, University of Wisconsin-Madison; new, photos, Adriana Heimann). *4a–b,* Iron-carbonate microlaminations, organic matter remains, and mineralogy typical of the Kuruman Iron Formation; *a,* photomicrograph showing siderite mud microlaminae (*Sid,* dark gray-brown), organic matter remains (*OM,* black), and diagenetic ankerite (*Ank,* white, coarser grained), plane polarized ×10, sample WB98-800A; *b*, back-scattered scanning electron microscope image of same sample showing siderite (almost white), coarser diagenetic ankerite (gray), and organic matter (black) remains (new).

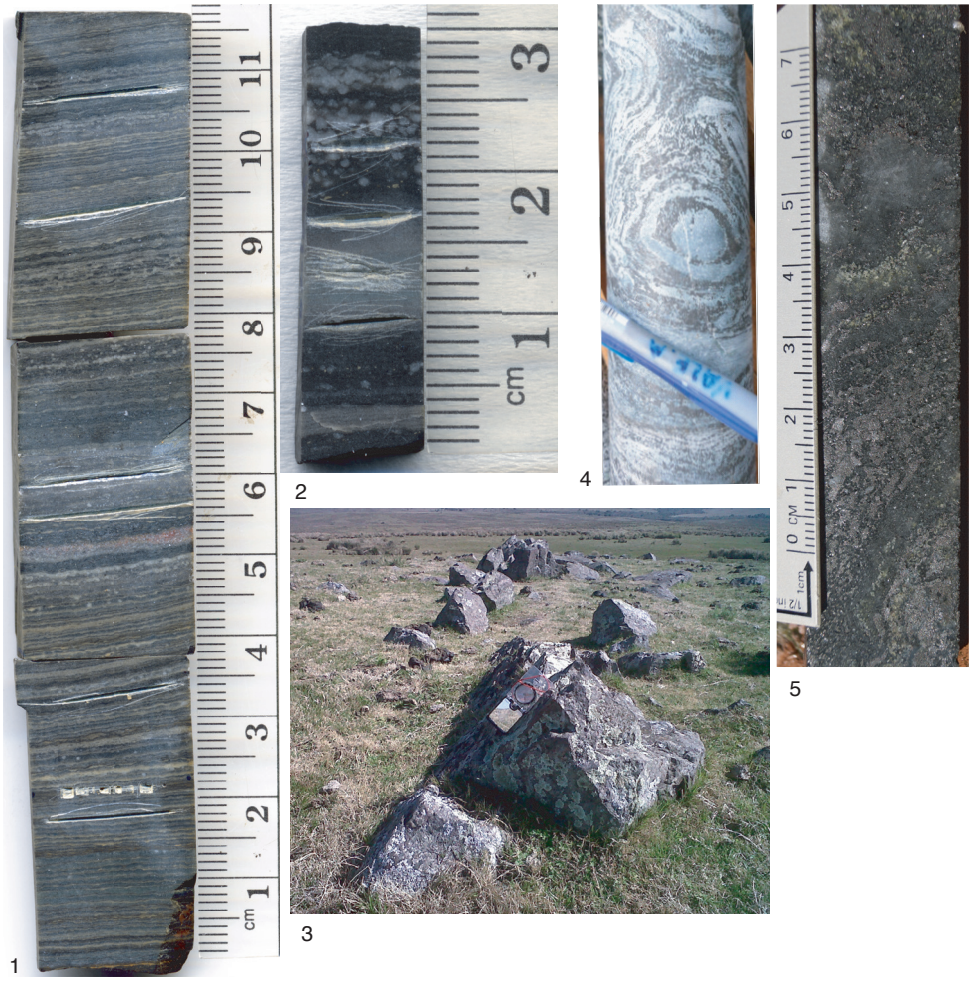

Fig. 2. Selected examples of banded iron formations with different mineralogy from various locations worldwide. *1,* Core slab sample showing banded and finely laminated carbonate BIF of the Kuruman Iron Formation, South Africa, pure siderite laminations (light brown/tan), lamination rich in hematite (reddish), sample DI1-213.8 (Geology Museum, University of Wisconsin-Madison). *2,* Core slab sample of banded carbonate BIF of the Kuruman Iron Formation, siderite (dark), large, late, diagenetic ankerite (white areas), sample AD5-161-9A, Geology Museum, University of Wisconsin-Madison (*1–2,* new; photos, Adriana Heimann). *3,* Field photo of the Valentines Iron Formation, Nico Pérez Terrane, Uruguay, compass for scale (new; photo courtesy of Richard Lateulade). *4,* Core sample of deformed and metamorphosed quartz-magnetite iron formation from the Valentines Iron Formation, quartz (white), magnetite (dark, brown). *5,* Core slab sample of deformed banded quartz-magnetite-pyroxene iron formation, magnetite (reddish brown), quartz (dark), pyroxene (greenish), quartz (coarse, whitish spots), Valentines Iron Formation (new; photo, Heather Lancaster).

and recrystallization reactions during early diagenesis (Berner, 1969; Schwertmann & Cornell, 1991). Nanoscale hematite inclusions found within siderite in the Kuruman BIF have been interpreted as reflecting the origin of siderite in a reaction involving coupled oxidation of organic matter and reduction of Fe(III) hosted in primary hematite or an original Fe(III) hydroxide by bacterial dissimilatory iron reduction (DIR) (Heimann & others, 2010). Similar hematite microspheroids, dusty hematite, or microcrystalline hematite have been reported from other BIFs, including the Bruno's BIF

of the Mount Sylvia Formation, Hamersley Basin (Western Australia), and interpreted to be the result of recrystallization of original ferrihydrite (e.g., Beukes & Gutzmer, 2008).

BIFs were originally classified based on their dominant mineralogy as carbonate, oxide, silicate, and sulfide facies BIFs (James, 1954). Sulfide facies BIFs were originally defined as pyritic and organic carbon-rich black shales with high iron contents (>15 wt%) (James, 1954), although most authors do not consider these as BIFs but as shales (e.g., Bekker & others, 2010). These shales commonly occur stratigraphically above, below, or interbedded with oxide or carbonate. More recently, Beukes and Gutzmer (2008) classified BIF facies into oxide-, hematite-, and siderite-facies BIFs. Some BIFs contain more than one dominant type of mineral. Oxide facies BIFs are comprised predominantly of magnetite, hematite, and chert. The large Superior-type ~2.5 Ga Brockman Iron Formation (Fig. 1.1–1.2) is a good example of an oxide facies BIF but also contains carbonate (siderite)-rich bands and silicates (stilpnomelane) (Ewers & Morris, 1981; Pecoits & others, 2009, and herein). The giant ~2.5 Ga Kuruman Iron Formation is an excellent example of a carbonate-rich BIF primarily composed of siderite, ankerite, and minor ferroan dolomite with local laminations of iron oxides (Fig. 1.3–1.4; Fig. 2.1–2.2) (Klein & Beukes, 1989; Beukes & others, 1990; Heimann & others, 2010). It represents the best-preserved, carbonate-rich BIF, as it has only been affected by very low metamorphism and almost no deformation. It is characterized by millimeter-scale laminations of very fine-grained (up to 5 μm) siderite with interstitial organic matter intercalated with very fine-grained chert (Fig. 1.4a–b). Ankerite appears as an accessory, late diagenetic, medium-grained mineral in the fine-grained, siderite-rich laminations (Fig. 1.4a; Fig. 2.1–2.2). Other BIFs also contain oxide and carbonate minerals. Algoma- and Superior-type BIFs are similar mineralogically, whereas Neoproterozoic BIFs have very simple mineralogies, containing mainly iron oxides and silica (Klein & Beukes, 1992; Klein & Ladeira, 2004).

Most Archean BIFs have experienced metamorphism and deformation and only some have very low or low metamorphic grade mineral assemblages (Fig. 3). Many of the large and most-studied late Archean–early Proterozoic BIFs, such as the Kuruman and Brockman BIFs, have undergone only very low-grade metamorphism and even preserve diagenetic mineral assemblages (Fig. 1.4a) (Klein, 2005). In most cases metamorphism was isochemical, except for dehydration and decarbonation reactions. The BIFs of the Hamersley Basin in Australia have been metamorphosed to sub-greenschist to greenschist facies conditions at estimated burial temperatures of 200–300°C and burial pressures of ~1.2 kbar (Klein & Gole, 1981; Kaufman, Hayes, & Klein, 1990). The burial temperatures of the BIFs from the Kaapvaal Basin in South Africa have been estimated to be one of the lowest, at 100–150°C (Miyano & Klein, 1983).

The mineralogy of silicate-rich BIFs depends on the metamorphic grade. At low metamorphic grades of the biotite zone, the minerals can include greenalite, stilpnomelane, minnesotaite, chamosite, ripidolite, riebeckite, and minor ferriannite. At medium and high pressures and temperatures, amphiboles (cummingtonite, grunerite, actinolite, hornblende), pyroxenes, fayalite, and minor garnet form (Fig. 2.3–2.5; 4.3–4.4) (Klein, 2005).

GEOCHEMISTRY

Most researchers agree that original iron-rich minerals in banded iron formations (BIFs), except some Fe silicates, formed by oxidation and direct precipitation of iron dissolved in seawater as Fe(III) oxyhydroxides in large water bodies (Trendall & Blockley, 1970; Ayres, 1972; Ewers & Morris, 1981; Trendall, 2002). If this is the case, the geochemistry of BIFs can help scientists understand the chemistry

Fig. 3. Photos showing mesoscopic layering and deformation features of various deformed banded iron formations from the southwestern Superior Province, Ontario, Canada (new; all photos, Adriana Heimann). *1,* Outcrop of Neoarchean, Algoma-type, Temagami Iron Formation (2.7 Ga) showing vertical to subvertical layering and minor folding, layers of gray/black hematite (gray), red jasper (chert and hematite), and chert (white); also present, carbonates and iron silicates, Sherman Mine, Cobalt area. *2,* Close-up of outcrop showing deformation features in the Temagami Iron Formation, layers are red jasper (chert with hematite) and black-gray hematite. *3,* Neoarchean BIF (2.7 Ga), Beardmore area, BIF is red and metallic gray and characterized by vertical to subvertical layering of hematite-magnetite (gray) and jasper (red). *4,* Close-up of horizontal face of outcrop of Beardmore iron formation showing thin, deformed, folded layers of specular hematite and magnetite (gray) and chert + hematite (red). *5,* Drill core of laminated Neoarchean (2.7 Ga) Temagami Iron Formation associated with mafic-intermediate volcanic rocks, laminations composed of red hematite, gray magnetite, also a quartz vein with pyrite, Sherman Mine, sample core ORS_1-87, 64 feet.

(*continued on facing page*)

of the water from which they precipitated. In particular, rare earth elements (REEs) in BIFs could serve as redox proxies (e.g., Bau & Möller, 1993; Planavksy & others, 2010). However, there are still some unknowns regarding the fractionation of elements and isotopes during precipitation and the effects of diagenesis and metamorphism. In addition, some scientists have argued and continue to postulate that the precursor sediments of BIFs were not direct chemical precipitates but microgranular muds or Fe-rich, Al-poor silicate microgranules that were resedimented by dilute density currents. The granules were originally comprised of greenalite, chamosite, or nontronite and are now present as stilpnomelane (Table 1, see p. 9) (Krapež, Barley, & Pickard 2003; Rasmussen & others, 2013).

The iron content of BIFs typically ranges from 15 to 35 wt% Fe, and their silica content varies from 34 to 56 wt% SiO_2 (James, 1954; Klein, 2005). The concentrations of CaO, MgO, MnO, Al_2O_3, Na_2O, K_2O, and P_2O_5 are typically low. The Ca, Mg, and Mn contents reflect the presence of carbonate (siderite, ankerite, minor calcite), whereas Al, Na, and K are hosted mainly by silicates (riebeckite, greenalite, stilpnomelane; Klein, 2005). The CaO and MgO values range from 1.8 to 9.0 wt%, whereas those for Na_2O and K_2O are very low (<1.5 wt%). The very low-metamorphic-grade, siderite-rich BIF from the Kuruman Iron Formation has organic carbon contents ranging from 0.05 to 0.2 wt% (see Fig. 1.4) (Klein & Beukes, 1989). Magnetite-rich BIFs from the same sequence have even lower organic carbon contents (Klein, 2005), which has been the focus of debate regarding the role of biologic processes in mediating the deposition of BIF minerals.

It is commonly accepted that, under conditions of low fluid/rock ratios, bulk-rock REE contents are not affected by post-depositional processes, such as diagenesis and metamorphism (e.g., Taylor & McLennan, 1986; McLennan & Taylor, 1991; Bau, 1991). The REE contents and the presence of Ce and Eu anomalies in normalized REE patterns of BIFs have been used to understand their origin and the chemical composition and redox state of the Precambrian oceans. Cerium anomalies are defined as $Ce/Ce^* = Ce_N/(\{La_N+Pr_N\}/2)$ (where N refers to the normalization value of shale composites or the Chondrite concentration, and Ce* to the predicted normalized concentration calculated from the equation) and true negative Ce anomalies have $Ce/Ce^* < 1$ and Pr/Pr^* ($Pr_N/[\{Ce_N+Nd_N\}/2]$) >1 (Bau & Dulski, 1996; Planavsky & others, 2010). Another way of defining the Ce anomaly is using Pr and Nd to avoid utilizing possibly anomalous concentrations of La. Thus, it is defined as $Ce^*_N = Pr^*_N(Pr_N/Nd_N)^2$ (Lawrence & Kamber, 2006). In modern oxygenated seawater, true negative Ce anomalies develop when Ce^{3+} is oxidized and removed as Ce^{4+} by Fe-Mn oxides or hydroxides, organic matter, and clays. Consequently, modern oxic seawater is depleted in Ce and has very large negative Ce anomalies. Suboxic and anoxic waters (0.05–5 μmol O_2 and no dissolved sulfide) lack significant negative Ce anomalies, and some have positive Ce anomalies. These anomalies are the result of reductive dissolution of settling Mn-Fe-rich particles that return Ce back to seawater which is then captured by precipitating Fe-Mn oxides (German & Elderfield, 1990; De Carlo & Green, 2002). Cerium has therefore been used to determine paleooceanic redox conditions. Europium anomalies ($Eu/Eu^*= Eu_N/[\{Sm_N+Gd_N\}/2]$) develop due to an abundance of Eu^{2+} in high-temperature (>250 °C), reduced, hydrothermal fluids and reflect the relative contribution of hydrothermal and riverine influx to the oceans

Fig 3. (*continued from facing page*)
6, Outcrop image from the Beardmore area showing vertical laminations of oxide-rich (magnetite-hematite) Neoarchean iron formation (dark) with interbedded metapelitic rocks (lighter gray). *7,* Close-up outcrop view of Neoarchean Deloro Iron Formation (2,723 Ma) from the Abitibi Greenstone belt, Canada, exhibiting banded magnetite-hematite (gray/black), siderite (brown), and chert (not visible), with crosscutting veins.

(Klinkhammer, Elderfield, & Hudson, 1983; Sverjensky, 1984; Elderfield, 1988). For further discussion of the significance of REE compositions of BIFs as indicators of paleooceanic redox conditions, see p. 17–18.

HYPOTHESES OF BIF FORMATION

The processes responsible for the generation and precipitation of the vast amounts of iron present in banded iron formations (BIFs) have been the subject of extensive study during the last ~60 years (e.g., Gross, 1988; Brown, Gross, & Sawicki, 1995). A summary of some of the main ideas about BIF formation is presented here, followed by a more detailed view of the recent thinking about the source of iron and silicon, the origin of the banding in BIFs, the paleoredox ocean structure, and inorganic and biological hypotheses of BIF formation. Table 2 provides a summary of the current thinking of the processes (organic and inorganic) involved in the formation of some well-studied Precambrian BIFs.

The most accepted view of BIF genesis holds that they formed in Archean and Paleoproterozoic oceans that were characterized by extremely low sulfate and sulfide concentrations and oxygen-free deep waters that contained high amounts of dissolved ferrous Fe [$(Fe(II)_{aq}$] (Canfield, Habicht, & Thamdrup, 2000; Canfield, 2005). Most researchers agree that a large reservoir of marine dissolved Fe(II) (~20 ppm; Ewers, 1980; Veizer, 1983) in the Archean and Paleoproterozoic oceans existed due to a high hydrothermal iron flux and a reduced atmosphere, or one that had a low oxidation potential (Holland, 1973; 1984; 2006; Bekker & others, 2004; Kump & Seyfried, 2005). The low sulfate and sulfide contents were necessary to maintain the large amounts of dissolved iron (Habicht & others, 2002). In such an environment, the accumulation of large volumes of iron took place by oxidation of hydrothermally derived Fe(II) and precipitation (Jacobsen & Pimentel-Klose, 1988; Klein & Beukes, 1992; Holland & Petersen, 1995; Isley, 1995). Cloud (1965) was the first to consider the role of bacterial processes for the generation of Fe(III) in BIFs and invoked oxidation of riverine Fe(II) by O_2 produced by oxygenic photosynthesis (cyanobacteria). A contrasting view of BIF genesis, based on the similarity of ancient BIFs and modern chert-hematite deposits associated with volcanogenic massive sulfide deposits (MSDs), considers that BIFs are the result of local discharge of submarine hydrothermal fluids under a fully oxygenated atmosphere and oceans (except in local basins) since ~3.8 Ga (Ohmoto, 1997, 2004; Ohmoto & others, 2006; Kato & others, 2006).

Considerable effort in the study of the origin of BIFs has centered particularly on the mechanisms of oxidation of Fe(II) to Fe(III), the latter estimated to account for 40% of the total Fe in BIFs (Ohmoto & others, 2006; Konhauser & others, 2007; Beukes & Gutzmer, 2008). Most models of BIF formation invoke two stages of Fe cycling. First, hydrothermal Fe(II) is oxidized in the photic zone of the oceans resulting in the crystallization and deposition of Fe(III) oxides or oxyhydroxides on the seafloor. Then, $Fe(II)_{aq}$ reacts with deposited Fe(III) oxides in the sediment or during diagenesis to produce mixed valence minerals or with carbonate or dissolved silica to produce siderite or Fe(II) silicates (Klein, 2005; Beukes & Gutzmer, 2008; Johnson, Beard, & Roden, 2008). Possible mechanisms of Fe oxidation include abiologic and biologically mediated Fe(II) oxidation by oxygen (Cloud, 1965; Konhauser & others, 2002), UV Fe(II) photo-oxidation (Cairns-Smith, 1978; Braterman, Cairns-Smith, & Sloper, 1983), and anoxygenic phototrophic Fe(II) oxidation (or photoferrotrophy) (Widdel & others, 1993; Kappler & others, 2005). It is more than likely that no single mechanism was responsible for the oxidation, precipitation, and generation of the vast amounts of iron present in Precambrian BIFs (Trouwborst & others, 2007). The generation of the Fe(II) present in BIF

TABLE 2. Summary of the current thinking of the processes (organic and inorganic) involved in the formation of some well-studied Precambrian banded iron formations (*ank*, akerite; *cal*, calcite; *goe*, goethite; *hem*, hematite; *mgt*, magnetite; *qtz*, quartz; *sid*, siderite; *stp*, stilpnomelane).

BIF	Mineralogy	Metamorphism	Age	Type	Processes	References
Isua and Akilia, Greenland	Fe silicates, mgt, qtz	Amphibolite-granulite facies	~3.8 Ga	Algoma	Inorganic or organic mediated by anaerobic photosynthetic oxidation	Dauphas & others, 2004; Whitehouse & Fedo, 2007; Czaja & others, 2013
Carajás BIF, Brazil	Hem, ±mgt, goe, qtz, kerogen	Lower greenschist facies	~2.75 Ga	Superior	Inorganic, organic oxidation (from biomats)	Klein & Ladeira, 2002; Fabre & others, 2011; Ribeiro da Luz & Crowley, 2012
Marra Mamba BIF, Australia	Mgt, hem, qtz	Lower greenschist facies	~2.6 Ga	Superior	Organic	Brocks & others, 1999; Summons & others, 1999
Kuruman BIF, South Africa	Sid, ank, mgt, hem, qtz, kerogen	Lower greenschist facies	~2.5 Ga	Superior	Bacterial DIR (siderite); inorganic precipitation from Fe(II) waters	Johnson & others. 2003; Beukes & Gutzmer, 2008; Heimann & others, 2010; Johnson & others, 2013
Dales Gorge Member, Brockman BIF, Australia	Sid, mgt, hem, stp, qtz	Lower greenschist facies	~2.5 Ga	Superior	Bacterial DIR (siderite); chemolithotrophic or photoferrotrophic Fe(II) oxidation (Fe oxides); inorganic (Fe-rich silicates)	Konhauser & others, 2002; Johnson & others, 2003; Pecoits & others, 2009; Cradock & Dauphas, 2011; Li & others, 2013; Rasmussen & others, 2013
Hotazel BIF, South Africa	Mgt, hem, Fe silicates, qtz, ank, cal	Lower greenschist facies	~2.3 Ga	Superior	Inorganic? oxidation	Tsikos & others, 2010
Gunflint BIF, North America	Hem, qtz, carbonates	Lower greenschist facies	~1.88 Ga	Superior	Bacterial oxidation	Planavsky & others, 2009
Rapitan BIF, Canada	Hem, qtz	Lower greenschist facies	~716.5 Ma	Rapitan	Inorganic? oxidation	Halverson & others, 2011

minerals (magnetite, siderite, Fe silicates) has also been debated and ascribed to either direct inorganic precipitation of Fe(II) (e.g., BEUKES & others, 1990) or bacterial DIR (WALKER, 1984; JOHNSON & others, 2003; JOHNSON & others, 2008; JOHNSON, BEARD, & RODEN, 2008).

One of the most striking discoveries is the temporal relationship between the episodic deposition of giant BIFs and major mantle plume events evidenced by the emplacement of LIPs (KLEIN & BEUKES, 1992; ISLEY, 1995; ISLEY & ABBOTT, 1999). Similarly, a close temporal association of BIFs with volcanogenic MSDs was identified decades ago (e.g., VEIZER, 1976; JAMES, 1983; ISLEY & ABBOTT, 1999; HUSTON & LOGAN, 2004; HUSTON & others, 2010). In a study of BIFs, the association between BIFs of all ages and volcanogenic MSDs was attributed to the interplay among mantle plume events that led to the formation of LIPs, enhanced rates

of midocean ridge spreading, high hydrothermal fluxes in the oceans, and changing surface redox states (Bekker & others, 2010).

The disappearance of large BIFs from the rock record at ~1.8 Ga ago has been attributed to the increase in seawater sulfate concentration as a result of oxic chemical weathering of the continents due to rising atmospheric oxygen contents, the subsequent expansion of bacterial dissimilatory sulfate reduction (DSR), and the formation of a sulfidic ocean in the Proterozoic, which would have favored iron sulfide precipitation over iron oxidation (Canfield, 1998; Habicht & others, 2002; Poulton, Fralick, & Canfield, 2004). Alternatively, their disappearance has simply been attributed to the complete oxidation of the atmosphere (e.g., Holland, 1984, 2006), but this is also a topic of debate. The hypothesis of a sulfidic ocean transition at ~1.84 Ga implies one of the most significant changes in ocean chemistry throughout Earth's history and is largely based on sulfur isotope compositions and iron speciation data from sedimentary rocks in the Paleoproterozoic Animikie Basin of North America (e.g., Poulton, Fralick, & Canfield, 2004). This transition to a global sulfidic ocean, however, was challenged on the basis of new sulfur isotope data in the context of recent tectonic and sedimentologic models from a correlative section in northern Michigan, USA. These data and models suggest that the Animikie Basin studied to support the hypothesis actually records a basin with restricted water circulation and not open circulation with the global ocean (Pufahl, Hiatt, & Kyser, 2010). However, there is also debate as to whether this basin was a restricted basin or open ocean (Fralick, Poulton, & Canfield, 2011; Pufahl, Hiatt, & Kyser, 2011).

SOURCES OF IRON AND SILICA AND THE ORIGIN OF THE BANDING

The source of iron and silicon in banded iron formations (BIFs) is considered to have been oceanic hydrothermal vents mixed with seawater plus a continentally derived freshwater input (Simonson, 1985; Gross, 1993; Hamade & others, 2003; Delvigne & others, 2012). Most studies have focused on the origin of the iron. Earlier ideas proposed a continental-weathering source for iron and that BIFs formed in continental environments by precipitation of iron and silicon due to evaporation of water (Garrels, 1987). In this model, the banding in BIFs represents cyclic episodes similar to those that produce varves (Garrels, 1987). Later studies agree on a hydrothermal iron source (e.g., Jacobsen & Pimentel-Klose, 1988; Bau & Möller, 1993). More recent studies based on the chemical composition of mesobands of the Dales Gorge Member of the Brockman Iron Formation of Western Australia proposed that metal/Si ratios could help distinguish a continental versus a hydrothermal source for the silica (Hamade & others, 2003). Iron-rich mesobands have Ge/Si ratios that reflect a hydrothermal source for the silicon. In contrast, chert-rich mesobands and mesobands with varved laminations have ratios that fall within the continental end-member range of compositions, which suggests a continental source and weathering of a landmass as the predominant source for the silica.

Precambrian ocean waters were silicon-saturated (~120 ppm Si) due to the absence of silica-secreting microorganisms (e.g., diatoms, radiolarians) at that time, which allowed the precipitation of large quantities of amorphous silica (Siever, 1992). The role of microorganisms in generating the silicon component of BIFs has not received much attention because silicon cannot be metabolized by prokaryotes (archaea and bacteria), the only organisms available during the formation of early BIFs (e.g., Koehler, Konhauser, & Kappler, 2010). However, a biological role for silica precipitation has also been proposed because bacteria are known to promote silicification through their metabolic activity (Birnbaum & Wireman, 1985). Some scientists have suggested that all the chert in BIFs is of early diagenetic origin and not a primary precipitate or diagenetic

replacement of earlier silica precipitated from seawater (Krapež, Barkey, & Pickard, 2003; Pickard, Barkley, & Krapež, 2004). In this model, chert was more likely a pore-filling cement and a replacement of sediments.

A later model proposed that silica could have been adsorbed onto the surface of hydrous ferric oxides, which precipitated on the bottom of the ocean along with organic matter (Fischer & Knoll, 2009). Then, once in the sediment pile, reduction of Fe(III) by bacterial respiration released most of the iron as $Fe(II)_{aq}$ and liberated silica to the sediment pores, which ultimately precipitated as a diagenetic mineral (Fischer & Knoll, 2009). Similarly, based on coupled Ge/Si ratios, REE+Y, and silicon isotope studies, a hypothesis for a two-stage precipitation of silica was proposed by Delvigne and others (2012). They envisioned a first stage of silicon adsorption onto Fe oxyhydroxides followed by early diagenetic release of silica to pore fluids from the Fe oxyhydroxides and consequent silica precipitation upon silica saturation at the sediment-water interface. These ideas have important consequences for the interpretation of oxygen and silicon isotope compositions in chert as indicative of a high seawater temperature in the Archean and Proterozoic (Knauth & Lowe, 2003; Robert & Chaussidon, 2006).

During BIF formation, precipitation of iron probably took place episodically, which caused the development of alternating Fe- and Si-rich bands. The origin of these alternating bands, including their presumed lateral continuity for hundreds of kilometers, has also been the matter of extensive research for more than 50 years (Trendall, 1968; Garrels, 1987; Posth & others, 2008). Based on recent detailed studies including modeling, bacteria incubations, and petrographic studies, the main hypotheses currently being considered to explain the banding include: 1) seasonal stratification or yearly climatic cycles, which would allow for periodic upwelling or pulses of hydrothermal Fe(II)-rich waters interrupted by seasonal evaporation and precipitation of silica (Holland, 1973; Garrels, 1987; Jacobsen & Pimentel-Klose, 1988; Siever, 1992; Morris, 1993); 2) temperature fluctuations, which would allow the maximum biogenic Fe(III) precipitation by iron oxidizing microbes (Fe(II)-oxidizing phototrophs) at 20–25 °C and lower Fe oxide precipitation and abiotic silica precipitation at higher or lower temperatures (Posth & others, 2008); and 3) formation and deposition of silt-size iron-rich silicate microgranules accompanied by alternating seafloor silicification during nondeposition and burial compaction of non-silicified lamina sets (Rasmussen & others, 2013). Based on the first two hypotheses, it seems that temperature could have been an important factor controlling BIF formation in the Archean and Proterozoic oceans. However, because temperature estimates for the Archean and Proterozoic are still a matter of considerable debate, this require further studies.

PALEOOCEANIC REDOX STRUCTURE AND THE FORMATION OF BIFS

Secular variations of cerium (Ce) and europium (Eu) anomalies in banded iron formations (BIFs) have been used to understand the redox state and hydrothermal versus riverine input to the Precambrian oceans and the bio-geochemical evolution of Earth (Klein, 2005; Kato, Yamaguchi, & Ohmoto, 2006; Bekker & others, 2010; Planavsky & others, 2010). In general, the concentration of REEs and the size of the positive Eu anomaly in BIFs seem to decrease with decreasing BIF age (Klein, 2005; Kato, Yamaguchi, & Ohmoto, 2006; Planavsky & others, 2010). Pre-2.7 Ga, Algoma-type BIFs (Isua BIF) have very strong positive Eu anomalies. Middle Archean BIFs (Cleaverville, Australia, and Sargur, India BIFs) have distinct positive Eu anomalies but they are smaller than those in the early Archean BIFs (Rao & Naqvi, 1995; Huston & Logan, 2004; Kato, Yamaguchi, & Ohmoto, 2006). Late Paleoproterozoic BIFs have smaller Eu

anomalies. Neoproterozoic BIFs have REE patterns with no or slightly positive Eu anomalies (Fryer, 1976; Klein & Beukes, 1993; Klein & Ladeira, 2004). This trend in Eu anomalies suggests a declining hydrothermal input into the deep ocean from the Eoarchean to the Early Proterozoic, likely linked to falling temperatures of the hydrothermal solutions as a result of lowering upper-mantle temperatures (Bau & Möller, 1993). In addition, no or slightly positive Eu anomalies in Neoproterozoic BIFs indicate the dilution of local hydrothermal fluids by mixing with mildly oxidized seawater in semi-isolated basins (e.g., Maynard, 2003).

New studies show that bulk Archean and early Paleoproterozoic BIFs lack significant shale-normalized negative Ce anomalies, and that strong positive Ce anomalies are only present in BIFs younger than 1.9 Ga (Planavsky & others, 2010). Some earlier studies of smaller samples have suggested that Ce anomalies were also present in Archean and early Paleoproterozoic BIFs (e.g., Kato, Yamaguchi, & Ohmoto, 2006; Ohmoto & others, 2006). However, bulk-rock studies reflect the overall chemistry of the water mass and the latest findings have been used to propose that late Paleoproterozoic BIFs record the shuttle of metal and Ce oxides from oxic shallow seawater to deeper anoxic waters, similar to the process taking place in modern redox-stratified basins (e.g., Planavsky & others, 2010). In this scenario, as the Ce-bearing oxides (mainly Mn) are transported to the deeper part of the water column, they dissolve under anoxic conditions and release Ce to the water, which is later incorporated in Fe oxides that precipitate at the redoxcline or in the shallow oxygenated water, thus resulting in a positive Ce anomaly (Planavsky & others, 2010; Bekker & others, 2010). In contrast, Archean BIFs do not show the effects of an oxide shuttle, implying the absence of a redoxcline before the rise of atmospheric oxygen (Planavsky & others, 2010; Bekker & others, 2010). This model supports the idea that Archean BIFs formed by metabolic oxidation of iron and not by oxidation of iron by free oxygen in shallow ocean environments (Planavsky & others, 2010; Czaja & others, 2013).

INORGANIC HYPOTHESES FOR BIF FORMATION

UV Photo Oxidation of Fe(II) by Radiation of a Young Sun

An inorganic mechanism to explain Fe(II) oxidation in the Archean is photo oxidation by UV radiation (Cairns-Smith, 1978; Braterman, Cairns-Smith, & Sloper, 1983). This process could have been possible due to the high levels of ultraviolet radiation that reached Earth prior to the formation of the protective ozone layer (Cairns-Smith, 1978). UV photolysis would not have required free oxygen to oxidize dissolved ferrous Fe but instead requires absorption of radiation (wavelengths in the ~200–400 nm range) to form dissolved ferric iron:

$$2Fe^{2+}_{(aq)} + 2H^{+} + h\upsilon = 2Fe^{3+}_{(aq)} + H_{2(g)}$$

Dissolved ferric iron is subsequently hydrolyzed to form solid ferric hydroxide at circumneutral pH (Cairns-Smith, 1978; Braterman, Cairns-Smith, & Sloper, 1983). This mechanism has been demonstrated in laboratory experiments (Braterman, Cairns-Smith, & Sloper, 1983), although only for simple aqueous solutions in which other ions were not available for reactions with original dissolved ferrous iron. Experiments with silica- and calcite-saturated solutions that mimic deep water conditions suggested that the process of photo oxidation would have been slower than and inhibited by the formation of ferrous silicate minerals (such as greenalite) and carbonates (siderite) in the silica-saturated Precambrian ocean waters from which BIF minerals precipitated (Konhauser & others, 2007). In addition, the calculated precipitation rates of ferric iron oxides through photo-oxidation obtained from the earlier experiments yield an annual amount of Fe(II) oxidized from 2.3×10^{13} to 1.8×10^{14} mol/yr (Braterman & Cairns-Smith, 1986; François, 1986).

These precipitation rates, however, are faster than sedimentation rates calculated for the Kuruman and Brockman BIFs (compacted sedimentation rates = 22–33 m/myr) (Pickard, 2002, 2003). The consensus seems to be that UV photo oxidation was not likely a dominant process in the formation of ferric oxide minerals in BIFs older than 2.5 Ga (e.g., Koehler, Konhauser, & Kappler, 2010). However, more detailed experiments would help understand the role of this process in the generation of BIFs prior to the rise of atmospheric oxygen.

Abiotic Fe(II) Oxidation by O_2 Produced by Cyanobacteria

A traditional view of Fe(II) oxidation considers inorganic oxidation of dissolved Fe(II) with oxygen produced by photosynthetic cyanobacteria (Cloud, 1965). Prokaryotic microbes, such as oxygenic photosynthesizing cyanobacteria, were likely abundant in the nutrient- and Fe(II)-rich photic zones of nearshore Archean oceans, where Fe(II) and nutrients originated by a combination of continental weathering and upwelling of deep hydrothermal waters (Cloud, 1973). This model envisions an anoxic atmosphere where Fe could have been oxidized by a reaction with O_2 in so-called oxygen oases via oxygenic photosynthesis:

$$CO_2 + H_2O \rightarrow [CH_2O] + O_2$$

followed by:

$$2Fe^{2+}_{aq} + 0.5O_2 + 5H_2O \rightarrow 2Fe(OH)_3 + 4H^+$$

Other studies considered a stratified ocean with a thin upper oxic zone and a lower anoxic ferruginous layer (e.g., James, 1954; Klein & Beukes, 1989). In this model, earlier views considered that Fe^{2+} was provided by continental weathering under an anoxic atmosphere and transported to chemically stratified oceans by rivers (James, 1954), whereas in most modern hypotheses, the Fe^{2+} is derived from hydrothermal alteration of oceanic crust in the deep ocean (e.g., Isley, 1995). Both of these models require the existence of oxygenic photosynthesizers, and several studies have suggested their existence by the Neoarchean (see also *Clues from Molecular Biomarkers,* p. 28). A new model of BIF genesis was recently proposed to explain the formation of BIFs in the ~1.8 Chiall Formation, North America, by inorganic precipitation of Fe oxyhydroxides in riverine systems from Fe derived from terrestrial weathering and coastal upwelling (Pufahl, Pirajno, & Hiatt, 2013).

Low $\delta^{13}C$ values (-57 to -28‰) in preserved organic carbon in ~2.7 to 2.57 Ga shales and carbonates from the Hamersley Province in Western Australia were interpreted as evidence of oxygenated microbial ecosystems comprised of cyanobacteria and aerobic methanotrophs (Eigenbrode & Freeman, 2006; Eigenbrode, Freeman, & Summons, 2008). Additionally, 2.7 Ga stromatolites from the Tumbiana Formation in the same stratigraphic sequence were considered to be evidence of a microbial mat community of cyanobacteria (Buick, 1992). However, this does not explain the formation of earlier BIFs. Further, no single type of bacteria can be assigned unequivocally to the construction of the mats and stromatolites.

In situ observations and quantitative geochemical modeling of oxidation of Fe(II) by cyanobacterial oxygenic photosynthesis in high-Fe(II) anoxic waters buffered by bicarbonate and silica at Chocolate Pots hot springs, Yellowstone National Park, USA, also supported the Cloud (1965, 1973) hypothesis (Parenteau & Cady, 2010). In the Parenteau and Cady study, the contributions to *in situ* Fe(II) oxidation by oxygenic photosynthesis (by cyanobacteria), anoxygenic photosynthesis (by *Chloroflexus* Pierson & Castenholz, 1974, purple bacteria, plus any other bacteriochlorophyll-containing phototrophs), and chemolithotrophy (by e.g., *Gallionella* Ehrenberg, 1838) were assessed, and the results suggest that oxygenic photosynthesis was the sole mechanism of Fe(II) oxidation in the anoxic vent waters. Light intensity was the primary variable affecting the rate of oxygen production and subsequent Fe(II) oxidation in

the benthic cyanobacterial mats that are surrounded by anoxic water (Parenteau & Cady, 2010). However, a large body of evidence suggests that molecular oxygen was very scarce before ~2.4 Ga (Farquhar & Johnston, 2008) and this would have made abiotic Fe(II) oxidation extremely slow (Konhauser, Newman, & Kappler, 2005). Biological oxidation of Fe(II) at low oxygen partial pressure is much faster (Søgaard, Medenwaldt, & Abraham-Peskir, 2000), and Fe(II) chemoautotrophic metabolic oxidation is known to occur in modern microaerophilic environments (e.g., Crowe & others, 2008a, 2008b). However, this mechanism also requires the supply of O_2 (see *Bacterial Metabolic Iron Oxidation,* below, for elaboration).

Direct Precipitation from Seawater

It is possible that some siderite (e.g., spheroidal siderite) formed directly by precipitation from anoxic water by mixing of ferrous iron and bicarbonate originating from a combination of hydrothermal fluids and microbial respiration of sedimented organic carbon (Beukes & others, 1990; Tice & Lowe, 2004; Klein, 2005) via:

$$4Fe^{2+} + 8HCO_3^- \rightarrow 4FeCO_3 + 4H_2O + 4CO_2$$

By this mechanism, siderite precipitates along the chemocline where there is supply of some organic carbon. Magnetite and hematite can precipitate in deeper areas where the organic supply is low and some oxygen is available (Beukes & others, 1990). However, it is difficult to envision enough oxygen to form magnetite and hematite in the deeper parts (below the redoxcline) of the Archean–Paleoproterozoic oceans where BIFs precipitated.

A later petrographic study of the Dales Gorge Member of the Brockman Iron Formation found silt-sized microgranules comprised of stilpnomelane and proposed the inorganic origin of 2.5 Ga BIFs as Fe-rich, Al-poor silicates that formed in the water column or ocean floor (Rasmussen & others, 2013).

BIOLOGICAL HYPOTHESES FOR BIF FORMATION

The hypothesis that biological processes could have an important role in the deposition of iron-rich sediments was first proposed by Ehrenberg (1836). Winogradsky (1888) later showed that a bacterium (*Leptothrix* Kützing, 1843) was able to live and grow only in the presence of ferrous iron in solution. Cloud (1965, 1973), while studying the microfossils of the Paleoproterozoic banded iron formations of the Lake Superior area, suggested that cyanobacteria could have participated in the oxidation and precipitation of Fe. Others proposed that BIF formation was related to carbon-cycling processes in which oxidation of Fe(II) driven by photosynthesis (oxygenic or anoxygenic) led to the contemporaneous deposition of Fe(III) oxides and organic matter. In this model, the formation of BIFs was ultimately the result of coupled organic carbon oxidation and iron reduction by anaerobic bacteria, such as iron-reducing bacteria (Walker, 1984; Konhauser, Newman, & Kappler, 2005; Kappler & others, 2005). Based on new observations of microbes and biofilms living in extreme conditions, such as near hydrothermal vents or deep in boreholes, the realization has occurred that prokaryotes probably also thrived in similar hostile environments in shallow Archean ocean waters and that they also likely utilized iron.

Mechanisms of BIF formation: Fe(II)-oxidizing and Fe(III)-reducing bacteria

Bacterial metabolic iron oxidation. Bacterial microaerophilic (chemolithotrophy) Fe(II) oxidation was likely an important process for the generation of banded iron formations (e.g., Holm, 1989; Konhauser & others, 2002). Iron-metabolic (chemolithotrophy) proteobacteria, such as *Leptothrix* and *Gallionella* are common in iron-rich freshwater streams and groundwater seeps (e.g., Harder, 1919). In addition, microaerophilic Fe(II) oxidizers are widespread in marine environments, including iron-rich hydrothermal vents (Emerson & Moyer, 2002) and at

the chemocline of ferruginous lakes, such as Pavin Lake (France), where Fe-rich sediments are being deposited (e.g., Lehours & others, 2007). These bacteria use oxygen, carbon dioxide, and water to form ferric iron hydroxides, possibly by reactions such as:

$$6Fe^{2+} + 0.5O_2 + CO_2 + 16H_2O \rightarrow CH_2O + 6Fe(OH)_3 + 12H^+$$

This microbial Fe(II) oxidation reaction by microaerophilic bacteria could have dominated the redox Fe cycle in the low-oxygen conditions of the Precambrian oceans because its rate can be 60 times faster than abiotic oxidation reactions (e.g., Søgaard, Medenwaldt, & Abraham-Peskir, 2000). The limitation, however, is that sulfur isotope studies have demonstrated that the oxygen levels of the atmosphere ($<10^{-5}$ present levels) and the surface ocean water layer (<0.003 μmol/liter at 25° C) in the Archean were too low to sustain abiotic oxidation (Farquhar, Bao, & Thiemens, 2000; Pavlov & Kasting, 2002). These low O_2 levels could also have restricted the availability of O_2 for biologic oxidation (Farquhar, Bao, Thiemens, 2000; Pavlov & Kasting, 2002).

Another metabolic Fe(II) oxidation mechanism that has been proposed to explain the origin of Fe(III) deposition in BIFs is anoxygenic photosynthetic oxidation, or photoferrotrophy, in which Fe(II) is used instead of H_2O as an electron donor to produce Fe(III) and biomass (Garrels & Perry, 1974; Ehrenreich & Widdel, 1994; Kappler & others, 2005) via:

$$4Fe^{2+} + 11H_2O + CO_2 \rightarrow CH_2O + 4Fe(OH)_3 + 8H^+$$

The presence of enormous amounts of Fe(II) in Archean seawater suggests that these bacteria could have existed and oxidized ferrous iron to ferric iron within the photic zone of the oceans through photosynthesis involving CO_2 fixation fueled by light energy (Konhauser & others, 2002). Until recently, all Fe(II)-oxidizing anoxygenic phototrophs had been cultured in the laboratory from iron-rich springs, ditches, and other shallow, ephemeral environments (Widdel & others, 1993; Ehrenreich & Widdel, 1994; Heising & Schink, 1998; Heising & others, 1999; Straub, Rainey, & Widdel, 1999). In particular, laboratory cultures of green *Chlorobium ferrooxidans* (Heising & others, 1999) (a green sulfur bacterium) and purple bacteria (α and γ *Proteobacteria*) have shown that they can phototrophically oxidize dissolved Fe(II) for carbon dioxide fixation by using Fe(II) as a reductant (Widdel & others, 1993; Heising & others, 1999; Straub, Rainey, & Widdel, 1999). Later, phototrophic Fe(II)-oxidizing bacteria were found in the photic zone of the water column in two Fe(II)-rich lakes (Lake Matano, Indonesia, and Lake La Cruz, Spain) (Crowe & others, 2008a, 2008b; Walter & others, 2009). Finally, although physical and chemical evidence for the existence of phototrophic Fe(II)-oxidizing bacteria in the Archean is yet to be found, phylogenetic studies of the enzymes that are involved in the biosynthesis of bacteriochlorophyll showed that anoxygenic photosynthetic lineages are more deeply rooted than oxygenic cyanobacterial lineages (Xiong, 2006; Posth, Konhauser, & Kappler, 2011). The main takeaway from these studies is that the anoxygenic photoferrotrophy mechanism of Fe(II) oxidation could have been dominant in the Precambrian oceans when molecular oxygen was absent and could have aided in the formation of BIFs.

Bacterial dissimilatory iron reduction (DIR). Based on evidence from natural observations, a role for DIR in the formation of banded iron formations, such as the Brockman and Kuruman BIFs, has been proposed by several researchers (Walker, 1984; Nealson & Myers, 1990; Lovley, 1991; Coleman & others, 1993; Beard & others, 1999; Johnson & others, 2003; Johnson & others 2008; Johnson, Beard, & Roden, 2008; Konhauser & others, 2002; Konhauser, Newman, & Kappler, 2005). It is known that magnetite and siderite, two abundant Fe minerals present in Archean and Proterozoic

BIFs, are common products of DIR (Lovley & others 1987). Under complete reduction of iron oxides, the reaction to form siderite proceeds via:

$$4Fe(OH)_3 + CH_2O + 3HCO_3^- \rightarrow 4FeCO_3 + 3OH^- + 7H_2O$$

This reaction requires two sources of carbon, organic carbon and seawater carbon, to form siderite. If bicarbonate is not present in excess, Fe reduction is incomplete and Fe^{2+}_{aq} is also formed as a product via:

$$4Fe(OH)_3 + CH_2O + 2HCO_3^- \rightarrow 3FeCO_3 + Fe^{2+}_{aq} + 4OH^- + 6H_2O$$

Similar reactions can be written for different organic carbon vs. inorganic carbon ratios. Mass balance considerations using the values of $\delta^{13}C$ for organic matter and carbonate carbon in the ~2.5 Ga Kuruman BIF, estimated Archean–early Paleoproterozoic seawater $\delta^{13}C$ and $\delta^{56}Fe$ values, and the stoichiometric coefficients of these equations show that the predicted C (~-8‰) and Fe +1‰ to -1‰) isotope compositions for siderite actually match those measured in siderite BIFs (Heimann & others, 2010) (see *Clues from Iron Isotope Investigations,* p. 24, for elaboration). By this mechanism, DIR produces aqueous Fe(II), which was likely present in relatively high concentrations in the Fe(III)-reducing precursor sediments to BIFs (e.g., Johnson & others 2008; Johnson, Beard, & Roden, 2008). High concentrations of Fe(III) present in the sedimentary pile along with organic matter would have suppressed DSR and allowed DIR to dominate and generate the Fe(II) present in BIFs (Walker, 1984).

Magnetite present in BIFs could have also formed by the reaction of Fe^{2+}_{aq} generated by DIR with original ferric oxyhydroxides in an anaerobic setting (Lovley & others, 1987; Lovley, 1991; Brown, Gross, & Sawicki, 1995; Johnson & others, 2003, Johnson & others 2008; Johnson, Beard, & Roden, 2008) via:

$$8Fe^{2+} + 16Fe(OH)_3 + 16OH^- \rightarrow 8Fe_3O_4 + 32H_2O$$

In addition, magnetite could have originated during diagenesis (or metamorphism) through oxidation of Fe(II) in siderite by O_2 via:

$$3FeCO_3 + \tfrac{1}{2}O_2 \rightarrow Fe_3O_4 + 3CO_2$$

or by reaction of siderite with hematite via:

$$Fe_2O_3 + FeCO_3 \rightarrow Fe_3O_4 + CO_2$$

The very low organic carbon content of most BIFs, in particular oxide facies, has been used in support of an inorganic origin for BIFs (e.g., Klein, 2005), or to explain the metamorphic origin of magnetite or siderite by a reaction between organic carbon and iron oxides (e.g., Perry, Tan, & Morey, 1973; Trendall, 2002) such as:

$$6Fe_2O_3 + C \rightarrow 4Fe_3O_4 + CO_2$$

Other mechanisms proposed to explain the loss of organic carbon from the sediment pile include transformation by hydrolysis and fermentation and utilization of some of the organic matter by methanogens (Hayes, 1983; Konhauser, Newman, & Kappler, 2005).

Bacterial DIR provides an alternative and consistent explanation for the formation of the large amount of Fe(II) present in BIFs, the formation of mixed-valence minerals, such as magnetite, as well as the negative $\delta^{13}C$ values measured in BIF carbonates (Johnson & others, 2003, 2008; Heimann & others, 2010; Cradock & Dauphas, 2010; Li & others, 2013). This mechanism also explains the low amount of organic carbon present in BIFs if organic carbon was the limiting factor in the reactions (Walker, 1984; Heimann & others, 2010). Moreover, the finding of a variety of deeply branching, presumably very ancient, hyperthermophilic bacteria and archaea that can reduce Fe(III) to Fe(II) reinforces the idea that DIR is a deeply rooted metabolism (Vargas & others, 1998; Lovley, 2004) that was likely active and played a role during the formation of Archean and Paleoproterozoic BIFs.

Clues from Biological Experiments and Cell Calculations

Two studies investigated the size of the bacterial communities and oxidation rates

necessary to oxidize Fe(II) to Fe(III) in ancient marine settings and form the vast amounts of Fe oxides in Precambrian BIFs (Konhauser & others, 2002; Kappler & others, 2005). These studies showed that these settings would have had enough nutrients and light to sustain a community large enough to generate the necessary iron. It was also shown, by ecophysiological experiments and quantitatively by modeling, that direct chemolithotrophic or photoferrotrophic Fe(II) oxidation by phototrophic bacteria would have been capable of generating most, if not all, of the original ferric iron hosted in BIFs (Konhauser & others, 2002). Konhauser and others (2002) calculated the number of metabolizing cells required to form an annual BIF deposit (layer) based on: 1) the Fe content of iron-rich mesobands in the 2.5 Ga Dales Gorge Member of the Brockman Iron Formation; 2) the density of the layers; 3) estimated maximum annual Fe depositional rates for the Hamersley Basin of ~1 m/700 yr (Morris, 1993), or 1 mm of hematite per year; 4) the area of the basin; and 5) cell production from iron oxidation by *Gallionella* and *Chromatium* Perty, 1852. Konhauser and others (2002) showed that bacterial oxidation could account for most, if not all, of the ferric iron present in BIFs. Kappler and others (2005) also demonstrated experimentally using radiation at wavelengths that penetrate to 100 meters depth in the water column at only 1% surface radiance, that photoferrotrophs could have oxidized Fe(II) down to a few hundred meters of water depth and generate enough Fe(III) to account for all the ferric iron in BIFs. This means that photoferrotrophs could have potentially oxidized all the Fe(II) during upwelling before they reached shallow levels and possibly shallow oxygenated waters (Kappler & others, 2005). These studies also calculated the amount of reduced Fe necessary to produce during diagenesis all the magnetite present in BIFs. Finally, they proposed that a complex bacterial community likely existed on the Archean seafloor, including Fe(III) reducers and possibly methanotrophs that could link Fe(III) reduction to methane oxidation (Konhauser, Newman, & Kappler, 2005).

Clues from Carbon Isotope Studies

Numerous studies have investigated the carbon isotope composition of BIFs (expressed as $\delta^{13}C$, in per mil, ‰, relative to Pee Dee Belemnite (PDB)—a standard for carbon) as a way of understanding their genesis. In particular, abundant data exist for the carbonates and organic matter from the low metamorphic grade ~2.5 Ga Kuruman BIF (Klein & Beukes, 1989; Beukes & Klein, 1990; Kaufman, Hayes, & Klein, 1990; Johnson & others, 2003; Heimann & others, 2010), the ~2.5 Ga Brockman BIF (Becker & Clayton, 1972; Baur & others, 1985; Craddock & Dauphas, 2011), and the ~1.88 Ga Gunflint and Biwabik BIFs (Fig. 4.1) (Perty, 1852; Perry, Tan, & Morey, 1973; Winter & Knauth, 1992). Iron formation carbonates have very negative carbon isotope compositions as low as -12‰, and organic carbon isotope values are extremely negative with values as low as -40‰ (Becker & Clayton, 1972; Walker, 1984; Baur & others, 1985; Kaufman, Hayes, & Klein, 1990; Johnson & others, 2003; 2008; Beukes & Gutzmer, 2008; Fischer & others, 2009; Heimann & others, 2010; Craddock & Dauphas, 2011). In contrast, most Ca-Mg-rich carbonates have near-zero $\delta^{13}C$ values (Beukes & others, 1990; Shields & Veizer, 2002; Fischer & others, 2009; Heimann & others, 2010; Craddock & Dauphas, 2011).

The negative carbonate C isotope values in BIF carbonates have been interpreted in various ways as a result of: 1) direct precipitation of siderite from an iron-rich water column that was stratified with respect to the carbon isotope composition of inorganic carbon (e.g., Beukes & Klein, 1990); 2) a fermentative mechanism and anaerobic respiration in the water column (Perry, Tan, & Morey, 1973; Walker, 1984; Fischer & others, 2009; Johnson & others, 2003; Heimann & others, 2010);

3) a hydrothermal flux dominated by mantle-derived carbon (e.g., Beukes & Klein, 1990); and 4) methane oxidation linked to ferric iron reduction (Konhauser, Newman, & Kappler, 2005). Inorganic mechanisms, such as Fischer-Tropsch processes, can also produce large carbon isotope fractionations (between -50 and -100‰), which make it difficult to be certain that the negative $\delta^{13}C$ values measured in BIF carbonates reflect biologic processes. Most researchers, however, interpret the negative $\delta^{13}C$ values of carbonates as reflecting diagenetic siderite precipitation by microbial oxidation of organic matter derived from photosynthesis coupled to reduction of ferric oxides via DIR (Walker, 1984; Johnson & others, 2003; Heimann & others, 2010; Craddock & Dauphas, 2011).

Clues from Iron Isotope Investigations

Investigations of the iron isotope composition (expressed as $\delta^{56}Fe$ in units of per mil, ‰, relative to igneous rocks) of ancient marine sedimentary rocks have been undertaken in the last 20 years to understand the formation of BIFs and the biogeochemical cycling of iron in the early oceans (Beard & others, 1999, 2003; Johnson & others, 2003; Johnson & others, 2008; Johnson, Beard, & Roden, 2008; Dauphas & others, 2004, 2007; Rouxel, Bekker, & Edwards, 2005; Whitehouse & Fedo, 2007; Planavsky & others, 2009, 2012; Heimann & others, 2010; Tsikos & others, 2010; Steinhoefel & others, 2009; Craddock & Dauphas, 2011; Fabre & others, 2011; Halverson & others, 2011; Czaja & others, 2013; Li & others, 2013). This is possible because iron isotopes fractionate during redox changes when iron species are separated, and iron cycling was extensive in the Archean–Proterozoic Earth. In modern marine environments, DSR is the dominant pathway for the oxidation of sediment organic carbon (Thamdrup, 2000). The sulfide produced by this process reacts with sediment or hydrothermal iron with near-zero $\delta^{56}Fe$ values to form iron sulfides that have near zero or slightly positive $\delta^{56}Fe$ values (e.g., Severmann & others, 2006). In contrast, in the Archean and early Proterozoic oceans, high rates of reactive iron flux and low sulfate and sulfide concentrations, as evidenced by the compositions of BIFs (Klein, 2005), would have favored bacterial DIR over bacterial DSR (e.g., Johnson & others, 2008; Johnson, Beard, & Roden, 2008). This, in turn, would have favored extensive bacterial redox iron cycling and phase separation that resulted in iron isotope fractionation.

Iron isotope studies of millimeter scale samples reveal processes that took place in the sediment pile during the formation of BIFs prior to lithification (Johnson & others, 2003; Heimann & others, 2010). Bulk-rock analyses (e.g., Planavsky & others, 2009, 2012), however, give an average of different processes that possibly operated in various places and at different scales, and provide an estimate of the bulk or average iron isotope composition of BIFs. The record through time of iron isotope compositions of marine sedimentary rocks, including pyrite in shales, bulk BIFs, and BIF minerals, shows a large, slightly positive to highly negative (~ -3‰) excursion at ~2.7–2.5 Ga (Rouxel, Bekker, & Edwards, 2005; Johnson & others, 2008; Johnson, Beard, & Roden, 2008; Planavsky & others, 2012; Li & others, 2013). In contrast, $\delta^{56}Fe$ values are mostly near zero to positive in the Eoarchean 3.8 Ga BIFs from Isua in Greenland, the Nuvvuagittuq greenstone belt in northern Quebec, Canada (Dauphas & others, 2004, 2007; Whitehouse & Fedo, 2007; Johnson & others, 2008; Johnson, Beard, & Roden, 2008; Czaja & others, 2013), and the ~1.88 Ga late Paleoproterozoic Gunflint and Biwabik BIFs from the Animikie basin of North America (Planavsky & others, 2009). The majority of younger rocks have near-zero $\delta^{56}Fe$ values. These variations in iron isotope compositions have been interpreted as reflecting inorganic processes and direct precipitation of iron-rich minerals from seawater or the dominance of bacterial DIR in the Precambrian oceans and their

role during BIF formation. Specifically, the iron isotope variations in Precambrian marine sedimentary rocks have been interpreted by some authors to reflect inorganic oxidation of Fe(II) and precipitation of iron oxides and to record changes in the δ^{56}Fe values of ancient seawater (Rouxel, Bekker, & Edwards, 2005) and not the interplay of biologic and geologic processes in the sedimentary pile prior to lithification (e.g., Yamaguchi & others, 2005). The negative δ^{56}Fe values of minerals (siderite, magnetite, and pyrite) could result from partial abiotic oxidation of near-zero δ^{56}Fe iron in the water column (Rouxel, Bekker, & Edwards, 2005) or partial Fe(II) utilization during abiotic pyrite precipitation (Guilbaud, Butler, & Ellam, 2011), which would leave behind low-δ^{56}Fe Fe^{2+} to form these minerals. A counter argument to the abiotic partial oxidation hypothesis is that the wide range in δ^{56}Fe values of marine precipitates at small scales cannot directly record the iron isotope composition of seawater due to the large size of the iron pool and its expected long residence time in Archean and early Paleoproterozoic seawater (Johnson & others, 2008). Finally, although abiotic pyrite formation may explain some iron isotope variations, the idea has been questioned for most low-δ^{56}Fe samples on the grounds of detailed studies of the depositional setting, mineralogy, and geologic history of Precambrian sedimentary rocks (Czaja & others, 2012).

The positive δ^{56}Fe values of Eoarchean BIFs from Greenland have been interpreted to reflect incomplete oxidation of near-zero δ^{56}Fe hydrothermal Fe(II), possibly via anaerobic photosynthetic oxidation by bacteria (Dauphas & others, 2004; Johnson, Beard, & Roden, 2008; Czaja & others, 2013), although the Fe isotope fractionations alone could not be taken as a biosignature (Bullen & others, 2001; Dauphas & others, 2004). Similarly, the positive δ^{56}Fe values in the late Paleoproterozoic Gunflint and Biwabik BIFs seem to reflect the cycling of Fe by iron-oxidizing microbial ecosystems in redox-stratified oceans (Planavsky & others, 2009). The excursion in Fe isotope compositions toward negative values at ~2.7–2.5 Ga, as measured in the giant ~2.5 Ga Kuruman and Brockman BIFs, has been interpreted to represent the expansion of DIR bacteria in the Precambrian oceans starting as early as 2.9 Ga (Johnson & others, 2003; Johnson & others, 2008; Johnson, Beard, & Roden, 2008), which points to the antiquity of this anaerobic respiratory pathway. The decrease in iron isotope variations in BIFs after the GOE at ~2.4 Ga (Rouxel, Bekker, & Edwards, 2005) has been interpreted as indicating a change from the peak of DIR activity at 2.7–2.5 Ga to an increase in seawater sulfate and the expansion of DSR bacteria in the oceans with the consequent removal of Fe(II) by pyrite after that (Johnson & others, 2008; Johnson, Beard, & Roden, 2008). This interpretation is also consistent with the change in sulfur isotope composition of sulfides in marine sedimentary rocks toward negative values and disappearance of strong sulfur mass-independent fractionation effects at ~2.4 Ga, which are evident at > ~2.5 Ga (e.g., Canfield, 2001; Ono & others, 2003; Farquhar & Wing, 2003; 2005; Johnson, Beard, & Roden, 2008). Furthermore, this change in isotope compositions also coincides with a shift from extremely negative carbon isotope compositions of kerogens (δ^{13}C down to -60‰) toward less negative values, which all together suggest some major changes in geobiological processes and isotope pathways at this time (Johnson, Beard, & Roden, 2008).

Experimental work on iron isotope fractionation during iron oxidation and reduction with and without bacteria and observations of natural environments provide the needed basis for the interpretation of the large iron isotope excursion toward negative δ^{56}Fe values at 2-7–2.5 Ga. Based on laboratory experiments and evidence from natural environments, the majority of highly negative δ^{56}Fe Fe^{2+}_{aq} is derived from biogenic reduction of Fe(III) by DIR (Beard & others,

1999, 2003; Crosby & others, 2005, 2007; Croal & others, 2004; Johnson & others, 2005; Tangalos & others, 2010; Wu & others, 2012). Experiments show that the iron isotope fractionation factor between Fe^{2+}_{aq} in a simulated Archean seawater analog and Fe(III) in iron-silica co-precipitates (analogous to the ones assumed to have formed BIFs) is up to -4‰ (Wu & others, 2012). These experiments indicate that the highly negative $\delta^{56}Fe$ values (~ -2.0 ‰) measured in BIF minerals (magnetite, siderite) and pyrite in black shales could have resulted from a multi-stage process involving the generation of low-$\delta^{56}Fe$ Fe^{2+}_{aq} by bacterial DIR [Reaction: $4Fe(OH)_3 + CH_2O + 2HCO_3^- \rightarrow 3FeCO_3 + Fe^{2+}_{aq} + 4OH^- + 6H_2O$ (see p. 22)] and its mobilization (e.g., Johnson & others, 2003; Johnson & others, 2008; Johnson, Beard, & Roden, 2008; Heimann & others, 2010). In a second stage, the $Fe(II)_{aq}$ produced by DIR would have reacted with bicarbonate to form siderite, or could have been mobilized in the sediment pile and reacted with near-zero $\delta^{56}Fe$ ferric oxides to form magnetite [Reaction: $8Fe^{2+} + 16Fe(OH)_3 + 16OH^- \rightarrow 8Fe_3O_4 + 32H_2O$ (see p. 22)] or reacted with sulfur to form pyrite. These minerals would have retained the negative $\delta^{56}Fe$ value of the $Fe(II)_{aq}$ generated by DIR (Johnson & others, 2003; Johnson & others, 2008; Johnson, Beard, & Roden, 2008; Heimann & others, 2010). In this view, the original Fe(III) oxyhydroxides had near-zero $\delta^{56}Fe$ values that resulted from complete or near-complete oxidation, either biologic or abiologic, of hydrothermal Fe(II) with $\delta^{56}Fe$ values similar to modern-day hydrothermal Fe(II) at ~ 0‰ (Beard & others, 2003; Johnson, Beard, & Roden, 2008).

Near-complete reduction of ~0‰ $\delta^{56}Fe$ Fe(III) oxides by DIR would result in Fe(II) with negative $\delta^{56}Fe$ values, as noted above, and would leave behind ferric oxides enriched in the heavy iron isotopes. A study of coupled iron, carbon, and oxygen isotope compositions of millimeter scale samples of carbonates from the ~2.5 Ga Kuruman BIF found that in laminations where the carbonates (siderite) did not have negative but positive $\delta^{56}Fe$ values, they had micrometric inclusions of hematite, which were interpreted as remains of the original iron oxides (Heimann & others, 2010). All carbonates had negative $\delta^{13}C$ values (> -8‰) indicative of incorporation of oxidized organic matter. The iron and carbon isotope values of these carbonates do not reflect precipitation in equilibrium with ancient seawater but are exactly what is expected from near-complete reduction of Fe(III) in original ferric hydroxides by bacterial DIR coupled to organic matter oxidation (Heimann & others, 2010) (see *Bacterial Dissimilatory Iron Reduction*, p. 21). Furthermore, Sr isotope studies of the same siderite BIF samples also indicate that the carbonates did not precipitate in equilibrium with seawater (Johnson & others, 2013). Therefore, these data point to the likely participation of bacterial DIR in the formation of at least these BIF carbonates.

Clues from Microfossils

Microfossils have been found in chert layers of Precambrian banded iron formations (e.g., Tyler & Barghoorn, 1954), as well as in other older cherts not associated with BIFs (e.g., Schopf, 2006). This section deals only with the former. The first assemblage of structurally preserved microorganisms was discovered in dense black cherts of the 1.88 Ga Gunflint Iron Formation of southern Ontario, Canada (Fig. 4.1–4.2) (Tyler & Barghoorn, 1954; Barghoorn & Tyler, 1965; Cloud, 1965; Awramik & Barghoorn, 1977). The Gunflint BIF also contains siliceous and calcitic stromatolites of various morphologies (Fig. 4.2) (Hoffman, 1969; Fralick, 1989; Sommers, Awramik, & Woo, 2000; Planavsky & others, 2009). The microorganisms were described in detail in the black cherts that owe their color to the presence of fine-grained pyrite and organic matter (Barghoorn & Tyler, 1965). Spherical structures, filaments, spore-

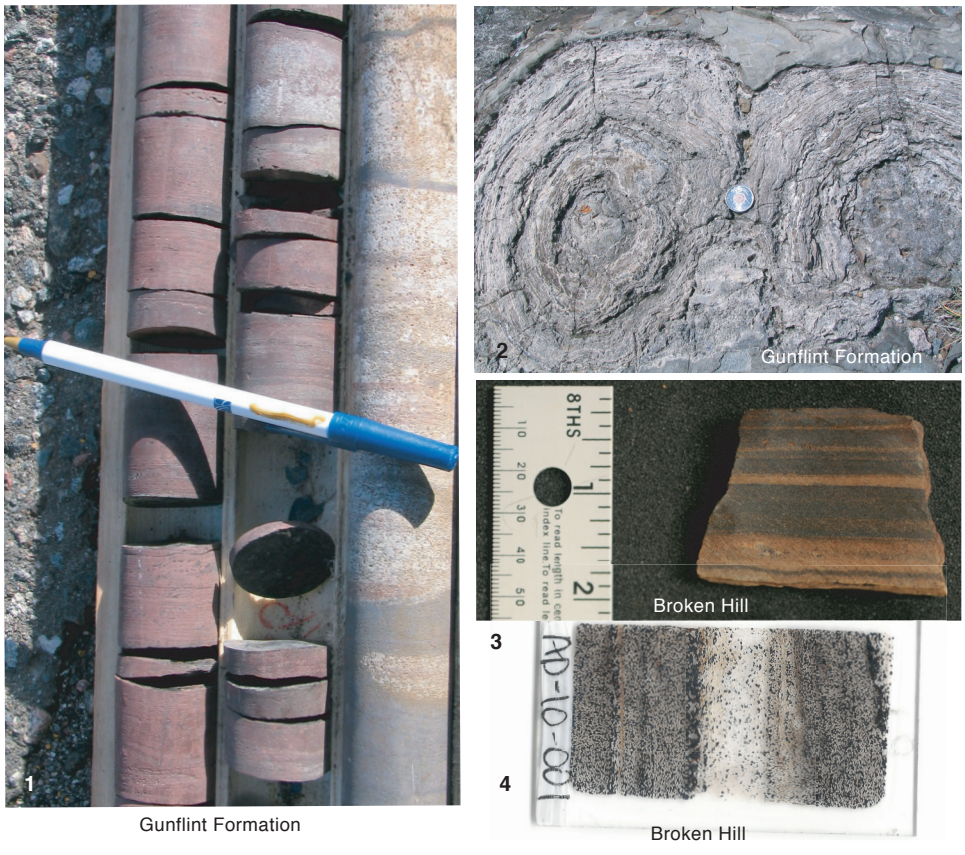

FIG. 4. *1,* Drill core of the Gunflint Formation, Ontario, Canada, showing red, magnetite-rich laminated chemical sediments of the late Paleoproterozoic (1,878 Ma) Gunflint Iron Formation (red/brown) overlaying light color, coarse grained sandstone with magnetite-rich laminations (reddish), drill core 89-mc-1 at ~160 m, Ministry of Northern Development and Mines Core Library (new; photo, Adriana Heimann). *2,* Stromatolites of the Gunflint Formation, coin for scale (new; photo, Adriana Heimann). *3,* Core slab sample of metamorphosed banded iron formation spatially associated with massive sulfide mineralization near the giant late Paleoproterozoic (1.69 Ga) Broken Hill Pb-Zn-Ag deposit, Curnamona Province, Australia, metamorphosed to granulite facies; brown is garnet in quartz, black is magnetite and minor quartz and/or garnet, sample AD-10-010, sample provided by Paul G. Spry (new; photo, Erica Serna). *4,* Scanned polished thin section of BIF near the Broken Hill deposit showing the delicate nature of the magnetite-rich laminations; black is magnetite, clear is quartz, brownish is garnet, sample AD-10-001 (new; image, Erica Serna).

like bodies, and other organic structures are preserved (BARGHOORN & TYLER, 1965).

The most abundant microfossils in the Gunflint chert are filaments ranging from 0.5 to 6.0 μm in diameter. The best-preserved filaments appear to be both septate and nonseptate. The grossly septate filaments were placed in a new genus, *Gunflintia* BARGHOORN & TYLER, 1965 and divided by the authors into two species (*G. grandis* and *G. minuta*). These are the most abundant microfossils, are characterized by randomly oriented filaments, and occur preferentially in stromatolites (PLANAVSKY & others, 2009). Some of the finely septate types of filaments exhibit a basic morphology comparable to that present in extant filamentous blue-green algae (cyanobacteria), such as *Oscillatoria* GOMONT, 1892 and *Lyngbya* GOMONT, 1892 and were grouped into a new taxon, *Animikiea septata* by BARGHOORN and TYLER, 1965. Some of the non-septate filaments include very uncommon forms that contain spores and endogonidia and

were grouped by the authors into a new taxon, *Entosphaeroides amplus*. These structures have a morphology comparable to a few extant genera of cyanobacteria and the iron bacteria *Crenothrix* Cohn, 1870. The spheroidal spore-like organisms that are ubiquitous in the chert exhibit a variety of sizes (1–16 μm), structures, and shapes and were grouped into a new genus, *Huroniospora* Barghoorn & Tyler, 1965, and subdivided by the authors into three species based on the wall-sculpturing pattern.

Other organisms were also found and assigned to a genus, but these were more rare and of unclear relationship to any known living group. In particular, some types of organisms are characterized by segmented or septated filaments radiating from a central structure of poorly defined morphology, and are grouped into the new genus *Eoastrion,* defined by Barghoorn and Tyler, 1965. Rare spiral threads (<1 μm in diameter, <35 μm length), either single corkscrew-like filaments or interwoven pairs, have a gross morphology that resembles spiral threads secreted by the living iron bacterium *Gallionella* (see Cloud, 1965). Although some of the biota appear to be planktonic (coccoidal forms), other forms, such as dense intertwined filaments of *Gunflintia,* appear to be benthic (Planavsky & others, 2009).

Earlier studies considered that the microfossils reflected the dominance of oxygenic photosynthesis in the early Precambrian (Barghoorn & Tyler, 1965; Cloud, 1965; Awramik & Barghoorn, 1977). However, a later study concluded that many of the Gunflint-type microfossils that were interpreted as oxygenic photosynthesizers were more likely to be metabolic iron oxidizers (Golubic & Seong-Joo, 1999). A more recent study that combined iron isotope compositions and REEs in microfossil-rich stromatolites from the Gunflint BIF also suggested that the late Paleoproterozoic environment likely hosted an iron-oxidizing microbial ecosystem and not cyanobacteria (Planavsky & others, 2009). It is more likely that the ecosystem present during the formation of the Gunflint BIF was actually quite complex.

Clues from Molecular Biomarkers

Biomarkers are fossil remains of chemically stable organic molecules derived from the carbon skeletons of precursor lipids preserved in the rock record (Waldbauer & others, 2009). They have been found in sedimentary rocks associated with BIFs and in BIFs themselves, and have been used to infer the presence and role of bacteria during their formation (Brocks & others, 1999, 2003a, 2003b; Summons & others, 1999; Waldbauer & others, 2009). For example, fossil hopanes and steranes (biomarkers typically present in eukaryotes) were found in the 2.6 Ga sedimentary rocks of the Transvaal Supergroup, South Africa (Waldbauer & others, 2009). The biosynthesis of steranes requires free oxygen, implying that oxygen was readily available at 2.6 Ga, or about 0.1 Ga before the formation of the Kuruman BIF, one of the largest BIF deposits that occurs in the same Transvaal Supergroup, and 0.2 Ga before the full oxygenation of the atmosphere took place (Noffke, 2009). In another study, 2a-methylhopanes, organic molecules present in membranes of modern cyanobacteria, were extracted from bitumen in the ~2.6 Ga very low metamorphic grade shales of the Marra Mamba Iron Formation and underlying 2.7 Ga rocks of the Hamersley Group, Western Australia (Brocks & others, 1999; Summons & others, 1999). This finding was interpreted as indicative of the existence of cyanobacteria, or oxygen-producing bacteria, 300–200 million years before the rise of atmospheric oxygen. This may also indicate that the BIFs of the Hamersley Group formed as the result of bacterial production of oxygen (Brocks & others, 1999). However, the hopane molecules found in the Marra Mamba shales were also identified in anoxygenic phototrophic Fe(II)-oxidizing bacteria (Rashby & others, 2007) and, therefore, are not an unequivocal fingerprint for the presence of cyanobacteria at the time the rocks formed.

Furthermore, it was later found that the carbon isotope composition of pyrobitumen and kerogen extracted from the same rocks is 10–20‰ lighter than the extracted hydrocarbons, providing a strong argument against the indigenous origin of the biomarkers (Rasmussen & others, 2008). Thus, there is much work to be done on molecular biomarkers to determine unequivocally the first appearance of oxygenic photosynthesis and the role of this bacterial metabolism in the formation of BIFs.

The Possible Role of Iron-enriched Biofilms

Iron-enriched biofilms or mats can be considered as possible precursors to the formation of finely laminated banded iron formation deposits. For example, recent studies of ~2.75 Ga BIFs in the Carajás mining district, Carajás Formation, Grão Pará Group, Brazil, presented evidence (morphology, carbon content, and very negative C isotope compositions) for the biogenicity of stromatolitic structures present in these Neoarchean BIFs that strongly suggests that the BIFs could have originated as biomats (Ribeiro da Luz & Crowley, 2012). The hypothesis is that Fe(III) precipitation would have taken place through Fe oxidation by contact of Fe(II) with bacterial slime and chemical reactions with organic compounds (Ribeiro da Luz & Crowley, 2012). The Fe(III) is considered to have been available later for dissimilatory Fe(III) reduction.

Bacterial processes related to iron oxide deposition in some modern bacterial mats give us clues about similar processes in the Archean–Proterozoic oceans where BIFs formed. In nutrient-limited environments, bacteria form biofilms that preferentially grow as slime-encased microbes on the surface of rocks instead of as free-swimming (planktonic) organisms (ZoBell, 1943). For example, in modern environments, photosynthetic bacteria and filamentous bacteria form laminated mats next to hydrothermal vents and hot springs, where they can be several millimeters thick (Walter, Bauld, & Brock, 1972; Walter & others, 1992; Doemel & Brock, 1977; Brown, Gross, & Sawicki, 1995; Little, Glynn, & Mills, 2004). Bacteria act as substrate or polyionic trap for the precipitation of minerals, promote mineral crystallization by metabolically generating products (e.g., OH^-, CO_2, H^+) that combine with dissolved metallic ions, or mediate enzymatic oxidation of others (e.g., Fe^{2+} to Fe^{3+}) (Konhauser, 1997, 1998; Thompson & Ferris, 1990; Ghiorse & Ehrlich, 1992; Brown, Gross, & Sawicki, 1995).

Modern microbial mats are commonly associated with the formation of iron hydroxides where bacterial biomineralization takes place (Pierson, Parenteau, & Griffin, 1999; Konhauser, 2000; Little, Glynn, & Mills, 2004; Parenteau & Cady, 2010). Studies of hot springs, active black smokers, and deep hydrothermal areas indicate: 1) that the iron-rich mats are mainly comprised of living cells and remains of bacteria (for example, *Gallionella ferruginea* Ehrenberg, 1836) (Boström & Widenfalk, 1984; Holm, 1987); 2) that microbial mats are the favored sites of deposition of iron hydroxides; and 3) that iron oxides form biogenically in areas of low O_2 and slightly acidic pH (Baross & Deming, 1985; Tunnicliffe & Fontaine, 1987; Karl, Brittain, & Tillbrook, 1989; Pierson, Parenteau, & Griffin, 1999; Little, Glynn, & Mills, 2004; Parenteau & Cady, 2010).

Earth's possibly oldest fossil cyanobacterial mats found in sandy deposits of a tidal environment in the 2.9 Ga Nhlazatse Section, Pongola Supergroup, South Africa, suggest the existence and diversification of cyanobacteria as early as the Mesoarchean (Noffke, 2010). Therefore, modern microbial mats and biofilms, including relatively young (Pleistocene) fossilized mat-forming prokaryote examples, are possibly one of the keys to understanding ancient benthic microbial communities and their habitats (Brown, Gross, & Sawicki, 1995; Noffke, 2010). Particular examples are described

below. The question still remains, however, as to exactly what kind of microbial communities formed these mats, because the mechanism of formation of the mats is not unique to oxygenic photosynthetic bacteria (Tice, 2008).

POSSIBLE PHANEROZOIC AND MODERN ENVIRONMENT ANALOGS

There is no perfect analog for Archean–Proterozoic banded iron formations (BIFs) in chemical composition, environment of formation (physicochemical conditions), and genesis. Paleozoic siliceous iron oxyhydroxide deposits, Phanerozoic hematite-quartz ironstones, and iron-oxide chemical precipitates that form in the modern oceans and deep lakes from hydrothermal fluids and brines are the closest analogs and are described below. In addition, continental sites where iron oxyhydroxides currently form under somewhat similar environmental conditions (low sulfate, low oxygen) as those in Archean–Proterozoic oceans and where biogenic Fe(III) reduction takes place are also included because even though they are terrestrial environments, they have been considered modern environmental analogs to those in Archean–Proterozoic times where BIFs formed.

MODERN SILICEOUS IRON OXYHYDROXIDE MARINE DEPOSITS

Iron Deposits of Marine Hydrothermal Vents

In modern marine environments, siliceous iron oxyhydroxide deposits commonly form spatially and genetically related to hydrothermal activity; examples occur at the Juan de Fuca Ridge (northeast Pacific Ocean), the Lilliput hydrothermal field on the Mid Atlantic Ridge, Trans-Atlantic Geotraverse (TAG), Loihi seamount hydrothermal vents (Hawaii), Coriolis Troughs (southwest Pacific), Red Sea Mount, and the Jan-Mayen vent fields in the Arctic-Ocean Ridge System (Rona & others, 1986; Alt, 1988; Emerson & Moyer, 2002; Little, Glynn, & Mills, 2004; Toner & others, 2009; Dekov & others, 2010; Moeller & others, 2013). In some of these settings, for example at the Jan-Mayen vent field, iron oxyhydroxides precipitate at depths greater than 1,000 m from diffuse, low-temperature hydrothermal fluids that emanate at the seafloor through fissures and faults distal to high-temperature hydrothermal vents (e.g., Moeller & others, 2013). The siliceous iron oxyhydroxide layers in all these locations consist of iron-rich amorphous phases or ferrihydrite and minor amounts of crystalline iron oxides, such as goethite, with up to 50 wt% Fe_2O_3 in bulk analysis and are intimately associated with filamentous structures of biogenic origin (e.g., Little, Glynn, & Mills, 2004; Moeller & others, 2013). All of the vents, for example at Loihi, are surrounded by microbial mats with a gelatinous texture and are encrusted with iron oxides (Emerson & Moyer, 2002; Little, Glynn, & Mills, 2004).

It has been shown that iron-oxidizing bacteria—for example species similar to *Mariprofundus ferrooxidans* Emerson & others, 2007—play a key role in mediating the oxidation of Fe(II) derived from the low temperature hydrothermal fluids (Emerson & Moyer, 2002; Toner & others, 2009; Moeller & others, 2013). At TAG, the filaments have been described as identical to the iron oxide encrusted stalks of *Gallionella* spp and *Leptothrix ochracea* Kützing 1843 (e.g., Little, Glynn, & Mills, 2004). What is more, studies at Loihi showed that up to 60% of the iron oxyhydroxides occur as filaments or sheaths interpreted to be direct deposition by bacteria (Emerson & Moyer, 2002).

Because of their similarities, modern deep-sea hydrothermal vent iron deposits are considered analogs of Ordovician to late Eocene jaspers, which points to a record of bacteriogenic iron oxide precipitation at marine hydrothermal vent sites of at least 490 million years (Little, Glynn, & Mills, 2004). Even though there are environmental differences between the origin of ancient

BIFs and modern siliceous Fe oxyhydroxides, their Si-Fe enrichment and chemical precipitation from hydrothermal fluids makes them the closest modern analogs to ancient BIFs. If we consider the setting near hydrothermal vents, then these Si-Fe precipitates can be considered closer analogs to Algoma-type BIFs, which formed in tectonically active areas and probably close to hydrothermal vents, than to Superior-type BIFs, which formed in stable platforms away from hydrothermal vent sites. The fact that biologic oxidation mediates the precipitation of these iron oxyhydroxides in modern settings also supports the idea of a link between iron precipitation and organic mediation during the formation of BIFs in the ancient oceans.

Iron Deposits of the Red Sea

The Red Sea rift system is characterized by active tectonics and igneous and hydrothermal activities and by a stratified body of water comprised of denser, saline anoxic bottom water overlain by lighter, less saline, cooler, oxic surface water. The deep water that penetrates the sediments achieves a high salinity by leaching of Miocene evaporates and a high temperature by a geothermal gradient and interaction with hot basaltic rocks (e.g., Cocherie, Calvez, & Oudin-Dunlop, 1994). The hot brine that discharges into the basin creates a stratified system with a lower hot (56–67 °C) layer enriched in Fe and Mn (81 mg/kg for each) and with a pH between ~5.5 and 6.4 depending on the location, and an upper, cooler (44°–56 °C) water layer (Taitel-Goldman, Ezrsky, & Mogilyanski, 2009). The Discovery Deep and the Atlantis II Deep are 5 km apart and separated by a sill at a depth of ~1990 m below sea level (Taitel-Goldman, Ezrsky, & Mogilyanski, 2009, and references therein). The lower layer brine flows into various deeps through a fracture and fissure system. The Fe oxyhydroxide minerals crystallize as authigenic minerals and occur at water depths between 2000 and 2216 m.

The mineralogy of the Atlantis II Deep includes Mn-Fe carbonates and rounded particles of Si-associated Fe oxyhydroxides, including well crystallized hematite (α-Fe_2O_3), goethite (α-FeO(OH)), and clusters of ferrihydrite ($Fe_5^{3+}OH_8 \cdot 4H_2O$), as well as feroxyhyte (δFeO(OH)), lepidocrocite (γ-$Fe^{3+}O(OH)$), and Mn oxyhydroxides (Taitel-Goldman, Ezrsky, & Mogilyanski, 2009). Pure hematite is thought to result from the recrystallization of a former phase, whereas the other oxides are original Si-associated Fe and Mn oxyhydroxides (Titel-Goldman, 2009). A lepidocrocite-goethite association crystallizes out of the hot hydrothermal brine with no Mn impurities, whereas the presence of Mn components reflects precipitation from the upper layer or the transition zone. In addition, silicon also discharges from the brine system and precipitates in association with Fe and Mn authigenic phases (Taitel-Goldman, Ezrsky, & Mogilyanski, 2009).

The clusters of hematite, or hematite microspheroids, and the Si-associated rounded particles of Fe oxyhydroxides that form in the Red Sea are similar to fine-grained hematite microspheroids, some containing pore-filling inclusions of early diagenetic silica, present in banded iron formations (Trendall & Blockley, 1970). This similarity suggests that the formation of the Red Sea Fe oxyhydroxides can be considered a close analog to that of BIFs. Because the Fe oxides also coexist with Mn oxides, these modern deposits can be compared with the BIFs and Mn deposits of the 2.4–2.2 Ga Hotazel Formation of South Africa that formed after the Kuruman Iron Formation and close to the timing of the GOE (e.g., Tsikos & others, 2010).

LAKE MATANO, INDONESIA

Lake Matano is located on Sulawesi Island, Indonesia (Crowe & others, 2008a), and is the eighth deepest (>590 m) lake in the world. The steep margins, great depth, and the geographic location, characterized by the lack of strong seasonal temperature

changes, allow the existence of a persistent pycnocline at ~100 m depth that separates an oxic surface layer from anoxic bottom waters. Sulfate concentrations are low (<20 µmol/liter) in the surface mixed layer and the rates of sulfate reduction within the anoxic waters of the chemocline are slow (<0.015 µmol/liter/day) (Crowe & others, 2008a). The slow sulfate reduction rates within the chemocline are fast enough to reduce all the sulfate and remove it from the surface waters, which results in deep waters with sulfate concentrations below detection limits. This also results in very low but detectable sulfide concentrations (including free sulfide, sulfide-bearing colloids, and larger particles of NiS and FeS). The low sulfur results in the accumulation of high concentrations of dissolved ferrous iron (~150 µmol/l). A low, suspended load of inorganic particulate matter, scavenging of phosphate by allogenic and authigenic iron (hydr)oxides, and low primary productivity in the surface mixed layer allows light to penetrate well into the anoxic bottom waters (Crowe & others, 2008a, 2008b).

The presence and abundance peaks with depth of the dominant photosynthetic pigment bacteriochlorophyll *e* (BChl *e*), a light-harvesting pigment used by brown-colored phototrophic green sulfur bacteria (GSB) of the family Chlorobiaceae, which are specially well adapted to low light conditions, indicate that GSB are an important component of the phototrophic bacterial community in Lake Matano (Crowe & others, 2008a). Molecular fingerprinting by Crowe and others (2008a) indicated the existence of an abundant and mixed bacterial community between 110 and 120 m depth, including several phyllogenetically distinct members of Chlorobiaceae. Lake Matano clones have up to 95% sequence similarity to a known photoferrotroph, *Chlorobium ferrooxidans* Heising & others, 1999 (Crowe & others, 2008a). In contrast to most known Chlorobiaceae (obligate photolithoautotrophs that fix carbon using sulfide as an electron donor), *C. ferrooxidans* is an exception that uses ferrous iron as electron donor (Heising & others, 1999).

Unlike other water bodies, such as anoxic sulfidic lakes and euxinic marine basins like the Black Sea, the extremely low dissolved sulfide concentrations in Lake Matano suggest that the community of GSB is sustained by using the abundant concentration of Fe(II) as electron donor (Crowe & others, 2008a). The concentration of free sulfide is considered too low to sustain sulfide-fueled anoxygenic phototrophy by GSB. What is more, calculations of the irradiance in the lake at ~110 m show that the light flux is sufficient to phototrophically oxidize the entire Fe(II) flux through the chemocline (Crowe & others, 2008a). The rates of Fe(II) oxidation are also consistent with the rates of oxidation of known photoferrotrophs. Therefore, the population of GSB is largely sustained by photoferrotrophy, and this mechanism could explain BIF deposition in Archean and Proterozoic oceans. This hypothesis remains to be fully proven, however, because Fe(II) oxidizing GSB have yet to be isolated and cultured in the laboratory (Crowe & others, 2008a). Studies also concluded that iron oxides currently precipitate from the water column in Lake Matano, including the mixed ferrous-ferric mineral green rust, at the oxycline, and that authigenic magnetite formation takes place in the water column and during diagenesis (Poulton, 2011). This has been used to argue that similar processes of formation under anoxic, ferruginous conditions could have formed BIFs in ancient oceans (Poulton, 2011). Further investigations of the paths of formation of these minerals will also help improve our understanding of the cycling of iron in the Archean–Proterozoic oceans and the formations of BIFs.

Because of its high ferrous iron concentration, low sulfate content, deep light penetration, and presence of a mixed upper layer and bottom anoxic layer, as well as other physical and chemical characteristics, Lake Matano is a good modern analog for the chemistry

and biology of Archean and early Proterozoic oceans (Crowe & others, 2008a). This setting at Lake Matano can be compared to that of the Archean–Proterozoic oceans where Superior-type BIFs formed in stable basins from a stratified water column. It is important to note, however, that the size of the system is small and the salinity is much lower compared to Archean–Proterozoic marine environments where BIFs formed.

PHANEROZOIC IRONSTONES

Phanerozoic iron-rich sedimentary rocks, called ironstones, are rocks with relatively high iron contents (>15% Fe) and some of them can be considered younger analogs to banded iron formations. Ironstones are rare, temporally related to marine anoxic events and mainly restricted to the Ordovician–Devonian and Jurassic–Paleogene and to modern local areas of closed to semi-closed basins (Van Houten, 1985; Van Houten & Arthur, 1989; Bekker & others, 2010; Ciobotă & others, 2011; Salama, Aref, & Gaupp, 2012, 2013). Many are temporally associated with peaks in abundance of volcanogenic massive sulfide deposits (MSDs), sea level rise, major anoxic events, and volcanic episodes (Van Houten & Arthur, 1989; Maynard & Van Houten, 1992; Burkhalter, 1995; Taylor & others, 2002; Peter, 2003; Franklin & others, 2005; Garzani, 1993; Bekker & others, 2010; Ciobotă & others, 2011; Salama, Aref, & Gaupp, 2012, 2013). The temporal association between ironstones and volcanogenic MSDs has been used to suggest a hydrothermal origin for the iron and that the deposition of ironstones was linked to global ocean anoxic periods and superplume events (see Bekker & others, 2010 and references therein).

Ironstones are commonly small (most <2 m thick, some 20 m thick) but large examples (>1,000 km) occur along ancient continental margins in Fennoscandia (covers present-day Finland, Norway, Sweden, and the Kola Peninsula in Russia) and the Himalayas (Garzani, 1993; Sturesson, Dronov, & Saadre, 1999; Sturesson, 2003). Large examples of Phanerozoic oolitic ironstones include the Jurassic Minnette deposits of central and western Europe, and the Silurian Clinton ores of North America. Phanerozoic ironstones are comprised of oolites of Fe oxyhydroxides (goethite and limonite), Fe silicates (chamosite and berthierite), and minor amounts of amorphous silica (less chert than BIFs) and are typically enriched in phosphorous. Some ironstones are non-cherty, sandy, fine-grained siliciclastic or siliciclastic-carbonate rocks (e.g., Petránek & Van Houten, 1997).

Even though the genesis of some ironstones is likely different than that of BIFs, others, for example the Phanerozoic deposits from the Løkken ophiolite and the Eocene ironstones of Egypt, have similarities to older jaspers and modern Fe-Si deposits with origins closely linked to Fe(II) oxidation by bacterial processes (Salama, Aref, & Gaupp, 2012; Moeller & others, 2013). This suggests that they can be considered younger equivalents of BIFs. The Phanerozoic Ordovician hematite-quartz deposits from the Løkken ophiolite complex in Norway, which have been metamorphosed to lower greenschist facies, are related to volcanogenic MSDs and associated hydrothermal feeders (e.g., Grenne & Slack, 2005). The rocks consist of fine-grained hematite microspheroids comprised of cryptocrystalline hematite and quartz in a quartz matrix (e.g., Grenne & Slack, 2005). The jasper deposits have soft-sediment deformation structures that along with the presence of the cryptocrystalline hematite reflect their formation as gel-like amorphous iron oxyhydroxides, such as ferrihydrite (Grenne & Slack, 2003). They are interpreted as siliceous ferrihydrite fallout deposits formed from a hydrothermal plume during times of oxic or suboxic conditions in a preponderantly widespread anoxic period (Grenne & Slack, 2005). Therefore, this kind of Phanerozoic ironstone may be somewhat similar to BIFs in its formation. If we take into account the association with volcanogenic MSDs and the occurrence in the ophiolite, the genesis of these ironstones

would resemble that of Algoma-type BIFs rather than that of Superior-type BIFs.

Some recent studies also suggest that at least some Phanerozoic ferruginous and stromatolitic ironstones, such as those in the Eocene ironstones of the Western Desert in Egypt, formed by similar processes as those described for hot springs and other hydrothermal venting areas (e.g., Ciobotă & others, 2011; Salama, Aref, & Gaupp, 2013). The Egypt ironstones are interpreted to be genetically linked to iron-oxidizing bacteria and their biofilms, where oxidation of Fe^{2+} in solution by these bacteria in shallow water with near acidic pH and low fO_2 precipitated a hydrous ferric gel that was also colonized by bacteria (Salama, Aref, & Gaupp, 2013). Ferruginous ooids and oncoids, now comprised of goethite, which coexist with ferruginous stromatolitic microbialites, seem to have been formed *in situ* and later reworked from shallow marine areas during storms to form the ironstones (Salama, Aref, & Gaupp, 2013). Based on the association with stromatolitic rocks, the genesis of these ironstones can be compared with that of Superior-type BIFs, such as the ~2.75 Ga Carajás (Brazil) BIF (Ribeiro da Luz & Crowley, 2012).

IRON MOUNTAIN MINE DRAINAGE SITE, NORTHERN CALIFORNIA

Iron Mountain Mine is a group of mines on Iron Mountain, Shasta County, northern California, USA (Alpers, Nordstrom, & Spitzley, 2003). The acid drainage effluent from Iron Mountain Mine has extremely low pH (-3.6) within the Richmond mine portal, ranging to pH values of +1 to +4 in drainage tributaries, such as Spring Creek (Nordstrom & Alpers, 1999; Edwards, Gihring, & Banfield, 1999; Norstrom & others 2000; Alpers, Nordstrom, & Spitzley, 2003). Concentrations of total dissolved solids in the effluent can exceed 900 g/L, and the waters are iron rich (Nordstrom, 2000). Mixing of neutral pH waters from an upstream reservoir with the iron-rich water of the acid mine drainage from Spring Creek has formed three large surface accumulation piles (>260,000 m^3 total volume) comprised of fine-grained Fe(III) oxide-rich sediment. Minerals present in the piles include ferrihydrite [$Fe(OH)_3$], goethite [α-FeO(OH)], and minerals with structures similar to synthetic schwertmannite [$Fe(III)_8O_8(OH)_6(SO_4)$] (Nordstrom & Alpers, 1999). The concentration of iron in the wet sediments ranges from 4% to 47% and the pore waters have extremely high concentrations of aqueous Fe(II) up to 36 mM (Nordstrom & Alpers, 1999). The pore waters have pH values of 5.5–6.5 and sulfate concentrations of 10 mM (Nordstrom & Alpers, 1999).

Iron Mountain iron-rich sediments represent a potential modern analog to early diagenetic BIF minerals formed in Archean and Proterozoic marine environments (Tangalos & others, 2010). Although the setting where the sediments form is an aerobic continental environment, it is characterized by high concentrations of reactive Fe(III) oxide that result in the dominance of dissimilatory iron reduction (DIR) over dissimilatory sulfate reduction (DSR) in early sediment diagenesis and large quantities of mobile Fe(II) in the pore waters. Additionally, the sediments contain significant concentrations of sulfate (4–23 mM), but there is an absence of acid volatile sulfides and a very low content of Cr(II)-extracted reduced inorganic sulfur (pyrite and/or elemental sulfur) compared with dilute HCl-extractable Fe(II). The sediments also have a relatively high ratio of nonsulfide-associated reactive iron to reduced inorganic sulfur, which are significantly higher than those in most modern marine sediments but similar to oxide and siderite BIFs from the Kuruman BIF and the Dales Gorge Member of the Brockman BIF (Tangalos & others, 2010). These characteristics and the chemical composition of the Iron Mountain sediments make the environment a good analog to study the processes that operated in the sedimentary pile prior to diagenesis and authigenic formation of magnetite and siderite in Archean BIFs (Tangalos & others, 2010). In particular, this site is

a natural example of the diagenetic process of bacterial DIR that likely took place in the sedimentary pile during the formation of siderite and magnetite in Superior-type BIFs, such as the Kuruman Iron Formation (Heimann & others, 2010).

Tangalos and others (2010) considered that the high amounts of $Fe(II)_{aq}$ in the Iron Mountain sediment pore water were generated by bacterial DIR of Fe(III) minerals (goethite and ferrihydrite) in the sediments. This is based on the assumption that DIR predominates over DSR due to the high concentration of reactive Fe(III) oxides, which allows dissimilatory iron-reducing microorganisms to outcompete dissimilatory sulfate-reducing bacteria for organic electron donors (Lovley & Phillips, 1987; Tangalos & others, 2010). The sediments also contain 1.5%–4% (dry weight) particulate organic carbon, derived from primary production in the overlying water or inputs of organic matter from the surrounding terrestrial environment, which is thought to serve as electron donors for DIR. The dominance of DIR was confirmed by gene sequencing of cultures of the material in the sediments and pore waters that showed that the sediments contained gene sequences closely related (97% similarity) to known dissimilatory iron-reducing microorganisms (*Geobacter* Lovley & others 1993 and *Geothrix* Coates & others, 1999). Four different culture isolates of *Geothrix fermentans* Coates & others, 1999 were also obtained, which also confirm that dissimilatory iron-reducing microorganisms are active in the Iron Mountain materials (Tangalos & others, 2010).

Iron isotope analysis indicates that $Fe(II)_{aq}$ from the sediments pore water at Iron Mountain has negative $\delta^{56}Fe$ values (-0.8% to -1.2‰), in contrast to the near-zero $\delta^{56}Fe$ values for the bulk Fe sediments that are isotopically similar to the average crust (Tangalos & others, 2010). The near-zero $\delta^{56}Fe$ values of the bulk sediments indicate that complete oxidation of Fe(II) took place in the near-neutral ~6.5 pH environment prior to the deposition of the Fe(III) oxide sediment. Isotopic fractionations between Fe(II)aq and Fe(III) extractable are similar to those measured in pure culture DIR experiments with Fe(III) oxides that showed the generation of low-$\delta^{56}Fe$ Fe(II) generated by DIR (Crosby & others, 2005, 2007). These *in situ* results were also reproduced in the laboratory with cultured iron oxides (Crosby & others, 2005, 2007). The less negative isotopic composition of $Fe(II)_{aq}$, compared to those measured in modern marine sediments (-1.3‰ to -3‰) (e.g., Severmann & others, 2006; Bergquist & Boyle, 2006) or stratified water bodies (Teutsch & others, 2009), are likely due to differences in the iron redox cycle and redistribution, which are more limited in the Iron Mountain sedimentary piles than they were in Archean and Proterozoic marine environments. At Iron Mountain, therefore, DIR is linked directly to the generation of large quantities of isotopically light, mobile $Fe(II)_{aq}$, which suggests that DIR could have led to the formation of low-$\delta^{56}Fe$ iron-bearing minerals (siderite, magnetite) during early diagenesis of Precambrian BIFs (Tangalos & others, 2010).

CHOCOLATE POTS HOT SPRINGS, YELLOWSTONE NATIONAL PARK

Iron-rich sediments are actively being deposited at Chocolate Pots hot springs, Yellowstone National Park, USA (Pierson, Parenteau, & Griffin, 1999). Colorful, iron-rich phototrophic microbial mats form a boundary layer at the interface between the iron-rich sediment surface and flowing spring water that contains high concentrations (~100 μM) of ferrous iron at the source (Pierson, Parenteau, & Griffin, 1999; Klatt & others, 2013; Wu & others, 2013). The source waters have a near-neutral pH and lack sulfide. Beneath the surface of the microbial mat-water interface the environment is anoxic and rich in Fe(II). Although in a terrestrial surficial location, this site serves as an analog for the extensive anoxic environments of and processes operating in

the Precambrian oceans where iron oxides formed (e.g., Pierson, Parenteau, & Griffin, 1999; Wu & others, 2013).

The microbial mats are comprised mainly of filamentous gliding phototrophs that stabilize oxidized iron and enhance the accumulation of sediments that are later compacted to form the iron deposits (Pierson, Parenteau, & Griffin, 1999). The intimate association between the filamentous phototrophs and the iron minerals, as well as the observation that the motility and orientation of the filaments may be important in trapping and stabilizing the sediments to produce the iron formation, is most evident in an olive green-color mat consisting of a narrow (cyanobacteria) *Oscillatoria* sp. (Pierson, Parenteau, & Griffin, 1999).

Measurements in the olive mat indicate that both under light and in the dark, ferrous iron stimulates bicarbonate uptake (photosynthesis), with the highest stimulation taking place at Fe contents of 1.0 mM, whereas Fe(II) concentrations of 5 mM inhibited photosynthesis (Pierson, Parenteau, & Griffin, 1999). What is not known with certainty is whether Fe(II)-stimulated photosynthesis in anoxygenic phototrophs (*Chloroflexus* filaments) occurs in the cyanobacterial mat suspensions or only in the cyanobacteria themselves (Pierson, Parenteau, & Griffin, 1999). Isolation of Chocolate Pots mat phototrophs and experiments performed with pure cultures may help resolve which bacteria are stimulated by Fe(II) (Pierson, Parenteau, & Griffin, 1999). Newer studies indicate that the Fe isotope compositions measured at Chocolate Pots could be important to predict those on a limited-oxygen early Earth or on Mars (Wu & others, 2013). This is because the range of Fe isotopic compositions (-1.57‰ to +0.88‰) measured in the iron oxides and hot springs at Chocolate Pots do not reflect simple equilibrium oxidation or Rayleigh oxidation of Fe(II) but rather reflect different extents and rates of Fe(II) oxidation as well as the possible reduction of iron by dissimilatory Fe(III)-reducing bacteria (Wu & others, 2013). Because of the link between iron oxide precipitation, microbial mats, and bacterial iron oxidation, the processes operating at Chocolate Pots hot springs can be considered analogs to those taking place during BIF formation.

FUTURE DIRECTIONS

The following are a few lines of research that will help improve our understanding of the genesis of banded iron formations (BIFs) and the role of various biological processes directly and indirectly involved in their formation. The search for new physical biosignatures in low-metamorphic grade oxide-facies BIFs older than the Gunflint BIF in North America—for example, permineralized cells similar to those present in iron-rich modern microbial mats (e.g., Klein, 2005; Parenteau & Cady, 2010)—will help elucidate the role of bacterial processes in the generation of BIFs (Walter & Hoffman, 1983). Further search for stromatolitic structures and organic matter in BIFs, similar to the ones described from the ~2.75 Carajás BIFs from Brazil (Ribeiro da Luz & Crowley, 2012), will help determine if biomats and BIFs could have a strong genetic link. A common aspect to most, if not all, modern water environments where iron oxide precipitation takes place is their intrinsic association with bacterial mats and biofilms. Further studies of modern environments and BIFs will help to understand the likely role of these bacterial structures in the formation of BIFs, especially the striking extremely fine-scale laminations of iron oxides and chert.

The search in Archean BIFs for chemical fingerprints unique to Fe(II)-oxidizing phototrophs will provide the physical evidence for the existence of these organisms in Archean oceans. For example, the discovery of biomarkers of pigments involved in photosynthesis and radical scavenging (radicals that form during Fe-Fenton reactions), which are two processes important in systems where photosynthetic Fe(II) oxidizers exist, would provide definite clues

about their presence during the Archean (Koehler, Konhauser, & Kappler, 2010). Similarly, isolation and culture in the laboratory of Fe(II) oxidizing green sulfur bacteria (GSB) that occur in modern analogs to Archean marine environments, such as the deep Lake Matano, are needed (Crowe & others, 2008a). Culturing of Fe(II)-oxidizing GSB will improve our understanding of the physiology and metabolism of the GSB, help prove that photoferrotrophy is the responsible bacterial process oxidizing iron in the lake (Crowe & others, 2008a), and provide clues as to what bacterial metabolism likely existed and played a role during the formation of BIFs.

Geochemical investigations of iron isotopes to fill the gaps in the iron isotope record through time as well as in modern natural environments will help prove that large variations in iron isotope compositions, observed particularly at ~2.7–2.5 Ga, indicate the expansion of bacterial dissimilatory iron reduction (DIR) in the Precambrian oceans and its likely role during BIF formation. More detailed iron isotope studies similar to the ones conducted at Chocolate Pots, Yellowstone National Park (Wu & others, 2013) will help to understand the processes responsible for the fractionation of iron isotopes in oxygenated and oxygen-limited environments and the implications for the formation of iron deposits on early Earth and Mars. In addition, studies of iron, carbon, and sulfur isotopes on the same rocks in Archean–Proterozoic sequences, including multiple sulfur isotopes to detect mass-independent sulfur isotope effects, will help test the hypothesis that these isotopic records are coupled and reflect photosynthesis and heterotrophic respiration (e.g., Johnson, Beard, & Roden, 2008). Furthermore, basin-wide scale iron isotope studies of BIFs, similar to those undertaken in other sedimentary rocks (mostly shale and carbonate) from Western Australia (e.g., Czaja & others, 2010), will help improve our understanding of the biogeochemical cycling of iron in ancient oceans. Finally, new rare earth element studies of BIFs, coupled with iron and carbon isotopes, as well as isotopes of other redox metals, may also help elucidate the presence or absence of a redoxcline in Archean oceans and the role of bacterial iron oxidation and reduction in the formation of different BIFs in the Archean–Paleoproterozoic and in the late Paleoproterozoic (Planavsky & others, 2010).

ACKNOWLEDGEMENTS

I wish to thank Steve Culver for comments and suggestions made on an earlier manuscript and Terri Woods for a thorough revision of the text and recommendations, both of which helped improve the chapter. This chapter greatly benefited from detailed and constructive criticism provided by reviewers Jens Gutzmer and Christopher Fedo, for which I am very thankful. I also thank Clark Johnson for kindly providing an image of BIFs. Finally, I thank Nora Noffke for organizing this volume and for handling the manuscript and Elizabeth Black for careful editorial corrections and handling of the chapter.

GLOSSARY OF TERMS AND ABBREVIATIONS

BIF: banded iron formation
DIR: dissimilatory iron reduction
DSR: dissimilatory sulfate reduction
Fe-Fenton reaction: catalytic process that forms hydroxyl free radicals from ferrous Fe
Fischer-Tropsch processes: chemical reactions that convert a mixture of carbon monoxide and hydrogen into hydrocarbons
GIF: granular iron formation
GOE: Great Oxidation Event
GSB: green sulfur bacteria
LIP: large igneous province
MSD: massive sulfide deposit
PDB: Pee Dee Belemnite, a standard used for C isotope analysis, based on the Cretaceous marine fossil *Belemnitella americana* from the Peedee Formation in South Carolina
Rayleigh oxidation: distillation, kinetic or non-equilibrium oxidation
REE: rare earth element
Snowball Earth: Earth mostly covered by ice

REFERENCES

Alpers, C. N., D. K. Nordstrom, & John Spitzley. 2003. Extreme acid mine drainage from a pyritic massive sulfide deposit: The Iron Mountain end member. *In* J. L. Jambor, D. W. Blowes, & A. I. M. Ritchie, eds., Environmental Aspects of Mine-Wastes. Mineralogical Association of Canada, Ottawa. p. 407–430.

Alt, J. C. 1988. Hydrothermal oxide and nontronite deposits on seamounts in the eastern Pacific. Marine Geology 81:227–239.

Aoki, Shogo, Masanori Shimojo, Shuhei Sakata, Shinji Yamamoto, Akira Ishikawa, Takafumi Hirata, & Tsuyoshi Komiya. 2013. Geology, lithostratigraphy and geochemistry of the oldest Eoarchaean BIFs, northern Labrador. Mineralogical Magazine (Abstract) 77:601.

Appel, P. W. U. 1987. Geochemistry of the early Archean Isua iron-formations, West Greenland. *In* P. W. U. Appel & G. L. LaBerge, eds., Precambrian Iron-formations. Theophrastus Publications. Athens. p. 31–67.

Arora, M., P. K. Govil, S. N. Charan, B. Uday Raj, C. Manikyamba, A. K. Chatterjee, & S. M. Naqvi. 1995. Geochemistry and origin of Archean banded iron-formation from the Bababudan schist belt, India. Economic Geology 90:2040–2057.

Awramik, S. M., & E. S. Barghoorn. 1977. Gunflint microbiota. Precambrian Research 5:121–142.

Ayres, D. E. 1972. Genesis of iron-bearing minerals in banded iron formation mesobands in the Dales Gorge Member, Hamersley Group, Western Australia. Economic Geology 67:1214–1233.

Barghoorn, E. S., & S. A. Tyler. 1965. Microorganisms from the Gunflint Chert. Science 147:563–575.

Barley, M. E., Robert Kerrich, Bryan Krapež, & D. I. Groves. 1998. The 2.72–2.60 Ga bonanza: Metallogenic and environmental consequences of the interaction between mantle plumes, lithospheric tectonics and global cyclicity. Precambrian Research 91:65–90.

Baross, J. A., & J. W. Deming. 1985. The role of bacteria in the ecology of black-smoker environments. Hydrothermal vent of the Eastern Pacific: An overview. (M. L. Jones, ed.). Bulletin of the Biological Society of Washington 6:355–371.

Bau, Michael. 1991. Rare-earth element mobility during hydrothermal and metamorphic fluid-rock interaction and the significance of the oxidation state of europium. Chemical Geology 93:219–230.

Bau, Michael, & Peter Dulski. 1996. Distribution of yttrium and rare-earth elements in the Penge and Kuruman Iron-Formations, Transvaal Supergroup, South Africa. Precambrian Research 7:37–55.

Bau, Michael, & Peter Möller. 1993. Rare earth element systematics of the chemically precipitated component in Early Precambrian iron-formations and the evolution of the terrestrial atmosphere-hydrosphere-lithosphere system. Geochimica et Cosmochimica Acta 57:2239–2249.

Baur, M. E., J. M. Hayes, S. A. Studley, & M. R.Walter. 1985. Millimeter-scale variations of stable isotope abundances in carbonates from banded iron-formations in the Hamersley Group of Western Australia. Economic Geology 80:270–282.

Beard, B. L., C. M. Johnson, Lea Cox, Henry Sun, K. H. Nealson, & Carmen Aguilar. 1999. Iron isotope biosignatures. Science 285:1889–1892.

Beard, B. L., C. M. Johnson, K. L. Von Damm, & R. L. Poulson. 2003. Iron isotope constraints on Fe cycling and mass balance in oxygenated Earth oceans. Geology 31:629–632.

Becker, R. H., & R. N. Clayton. 1972. Carbon isotopic evidence for the origin of a banded iron-formation in Western Australia. Geochimica et Cosmochimica Acta 36:577–595.

Bekker, Andrey, H. D. Holland, P. L.Wang, Douglas Rumble, H. J. Stein, J. L. Hannah, L. L. Coetzee, & N. J. Beukes. 2004. Dating the rise of atmospheric oxygen. Nature 427:117–120.

Bekker, Andrey, J. F. Slack, Noah Planavsky, Bryan Krapež, Axel Hofmann, K. O. Konhauser, & O. J. Rouxel. 2010. Iron formation: The sedimentary product of a complex interplay among mantle, tectonic, oceanic, and biospheric processes. Economic Geology 105:467–508.

Bergquist, B. A., & E. A. Boyle. 2006. Iron isotopes in the Amazon River system: Weathering and transport signatures. Earth and Planetary Science Letters 248:54–68.

Berner, R. A. 1969. Goethite stability and the origin of red beds. Geochimica et Cosmochimica Acta 33:267–273.

Beukes, N. J., & Jens Gutzmer. 2008. Origin and paleoenvironmental significance of major iron formations at the Archean-Paleoproterozoic boundary. Reviews in Economic Geology 15:5–47.

Beukes, N. J., & Cornelis Klein. 1990. Geochemistry and sedimentology of a facies transition—from microbanded to granular iron-formation—in the Early Proterozoic Transvaal Supergroup, South Africa. Precambrian Research 47:99–139.

Beukes, N. J., Cornelis Klein, A. J. Kaufman, & J. M. Hayes. 1990. Carbonate petrography, kerogen distribution, and carbon and oxygen isotope variations in an Early Proterozoic transition from limestone to iron-formation deposition: Transvaal Supergroup, South Africa. Economic Geology 85:663–690.

Birnbaum, S. J., & J. W. Wireman. 1985. Sulfate-reducing bacteria and silica solubility: A possible mechanism for evaporate diagenesis and silica precipitation in banded iron formations. Canadian Journal of Earth Sciences 22:1904–1909.

Boström, Kurt, & Lennart Widenfalk. 1984. The origin of iron-rich muds at the Kameni Islands, Santorini, Greece. Chemical Geology 42:203–218.

Braterman, P. S., & A. G. Cairns-Smith. 1986. Photoprecipitation and the banded iron-formations: Some quantitative aspects. Origins of Life and Evolution of Biospheres 17:221–228.

Braterman, P. S., A. G. Cairns-Smith, & R. W. Slope. 1983. Photooxidation of hydrated Fe^{2+}: Significance for banded iron formations. Nature 303:163–164.

Breitkopf, J. H. 1988. Iron formations related to mafic volcanism and ensialic rifting in the southern margin

zone of the Damara orogen, Namibia. Precambrian Research 38:111–130.
Brocks, J. J., R. Buick, G.A. Logan, & R. E. Summons. 2003a. Composition and syngeneity of molecular fossils from the 2.78 to 2.45 billion-year-old Mount Bruce Supergroup, Pilbara Craton, Western Australia. Geochimica et Cosmochimica Acta 67:4289–4319.
Brocks, J. J., R. Buick, R. E. Summons, & G. A. Logan. 2003b. A reconstruction of Archean biological diversity based on molecular fossils from the 2.78 to 2.45 billion-year-old Mount Bruce Supergroup, Hamersley Basin, Western Australia. Geochimica et Cosmochimica Acta 67:4321–4335.
Brocks, J. J., G. A. Logan, R. Buick, & R. E. Summons. 1999. Archean molecular fossils and the early rise of Eukaryotes. Science 285:1033–1036.
Brown, D. A., G. A. Gross, & J.A. Sawicki. 1995. A review of the microbial geochemistry of banded-iron formations. Canadian Mineralogist 33:1321–1333.
Bühn, B., I. G. Stanistreet, & M. Okrusch. 1992. Late Proterozoic outer shelf manganese and iron deposits at Otjosondu (Namibia) related to the Damaran oceanic opening. Economic Geology 87:1393–1411.
Buick, Roger. 1992. The antiquity of oxygenic photosynthesis: Evidence from stromatolites in sulphate-deficient Archaean lakes. Science 255:74–77.
Bullen, T. D., A. F. White, C. W. Childs, D. V. Vivit, & M. S. Schulz. 2001. Demonstration of significant abiotic iron isotope fractionation in nature. Geology 29:699–702.
Burkhalter, R. M. 1995. Ooidal ironstones and ferruginous microbialites: Origin and relation to sequence stratigraphy (Aalenian and Bajocian, Swiss Jura Mountains). Sedimentology 42:57–74.
Button, A. 1976. Transvaal and Hamersley Basins-review of basin development and mineral deposits. Minerals Science and Engineering 8:262–293.
Cairns-Smith, A. G. 1978. Precambrian solution photochemistry, inverse segregation, and banded iron formations. Nature 76:807–808.
Canfield, D. E. 1998. A new model for Proterozoic ocean chemistry. Nature 396:450–453.
Canfield, D. E. 2001. Biogeochemistry of sulfur isotopes. Reviews in Mineralogy and Geochemistry 4:607–36.
Canfield, D. E. 2005. The early history of atmospheric oxygen: Homage to Robert Garrels. The Annual Review of Earth and Planetary Sciences 33:1–36.
Canfield, D. E., K. S. Habicht, & B. Thamdrup. 2000. The Archean sulfur cycle and the early history of atmospheric oxygen. Science 288:658–61.
Coates, J. D., D. J. Ellis, C. V. Gaw, & D. R. Lovley. 1999. *Geothrix fermentans* gen. nov., sp. nov., a novel Fe(III)-reducing bacterium from a hydrocarbon-contaminated aquifer. International Journal Systematic and Evolutionary Microbiology 49:1615–1622.
Cheney, E. S. 1996. Sequence stratigraphy and plate tectonic significance of the Transvaal succession of southern Africa and its equivalent in Western Australia. Precambrian Research 79:3–24.
Ciobotă, Valerian, Walid Salama, Nicolae Tarcea, Petra Rösch, Mourtada El Aref, Reinhard Gauppc, & Jürgen Popp. 2011. Identification of minerals and organic materials in Middle Eocene ironstones from the Bahariya Depression in the Western Desert of Egypt by means of micro-Raman spectroscopy. Journal of Raman Spectroscopy 43:405–410.
Cloud, P. E. 1965. Significance of Gunflint (Precambrian) microflora—photosynthetic oxygen may have had important local effects before becoming a major atmospheric gas. Science 148:27–35.
Cloud, P. E. Jr. 1973. Paleoecological significance of banded iron-formation. Economic Geology 68:1135–1143.
Cocherie, Alain. J. Y. Calvez, & E.Oudin-Dunlop. 1994. Hydrothermal activity as recorded by Red Sea sediments: Sr-Nd isotopes and REE signatures. Marine Geology 118:291–302.
Cohn, F. 1870. Über den Brunnenfaden (*Crenothrix polyspora*) mig Bemerkungen über die mikroskopische analyse des Brunnenwassers. Beitrage zur Biologie der Pflanzen 1:108–131.
Coleman, M. L., D. B. Hedrick, D. R. Lovley, D. C. White, & Kenneth Pye. 1993. Reduction of Fe(III) in sediments by sulphate-reducing bacteria. Nature 361:436–438.
Condie, K. C. 1998. Episodic continental growth and supercontinents: A mantle avalanche connection? Earth and Planetary Science Letters 163:97–108.
Condie, K. C. 2002. Continental growth during a 1.9-Ga superplume event. Journal of Geodynamics 34:249–264.
Corriveau, L., & P. G. Spry. 2014. Metamorphosed hydrothermal ore deposits. *In* S. D. Scott, ed., Geochemistry of Mineral Resources. Treatise on Geochemistry. 2nd Edition. Vol. 13. Elsevier. New York. p. 175–194.
Cradock, P. R., & Nicolas Dauphas. 2011. Iron and carbonisotope evidence for microbial iron respiratio throughout the Archean. Earth and Planetary Science Letters 303:121–132.
Croal, L. R., C. M. Johnson, B. L. Beard, & D. K. Newman. 2004. Iron isotope fractionation by Fe(II)-oxidizing photoautotrophic bacteria. Geochimica et Cosmochimica Acta 68:1227–1242.
Crosby, H. A., C. M. Johnson, B. L. Beard, & E. E. Roden. 2007. The mechanisms of iron isotope fractionation produced during dissimilatory Fe(III) reduction by Shewanella putrefaciens and Geobacter sulfurreducens. Geobiology 5:169–189.
Crosby, H. A., C. M. Johnson, E. E. Roden, & B. L. Beard. 2005. Fe(II)-Fe(III) electron atom exchange as a mechanism for Fe isotope fractionation during dissimilatory iron oxide reduction. Environmental Science and Technology 39:6698–6704.
Crowe, S. A. J., C. Katsev, S. Magen, A. H. O'Neill, A. H. Sturm, D. E. Canfield, G. D. Haffner, A. Mucci, B. Sundby, & D. A. Fowle. 2008a. Photoferrotrophs thrive in an Archean ocean analogue. Proceedings of the National Academy of Sciences 105:15937–15943.
Crowe, S. A., A. H. O'Neill, S. Katsev, P. Hehanussa, G. D. Haffner, B. Sundby, A. Mucci, & D. A. Fowl. 2008b. The biogeochemistry of tropical lakes: A case

study from Lake Matano, Indonesia. Limnology and Oceanography 53:319–331.

Czaja, A. D., C. M. Johnson, B. L. Beard, J. L. Eigenbrode, K. H. Freeman, & K. E. Yamaguchi. 2010. Iron and carbon isotope evidence for ecosystem and environmental diversity in the ~2.7 to 2.5 Ga Hamersley Province, Western Australia. Earth and Planetary Science Letters 292:170–180.

Czaja, A. D., C. M. Johnson, B. L. Beard, E. E. Roden, W. Li, & S. Moorbath. 2013. Biological Fe oxidation controlled deposition of banded iron formation in the ca. 3770 Ma Isua Supracrustal Belt (West Greenland). Earth Planetary Science Letters 363:192–203.

Czaja, A. D., C. M Johnson, K. E. Yamaguchi, & B. L. Beard. 2012. Comment on 'Abiotic pyrite formation produces a large Fe isotope fractionation'. Science 335:538–c.

Dauphas, Nicolas, N. L. Cates, S. J. Mojzsis, & Vincent Busigny. 2007. Identification of chemical sedimentary protoliths using iron isotopes in the >3750 Ma Nuvvuagittuq supracrustal belt, Canada. Earth and Planetary Science Letters 254:357–376.

Dauphas, Nicolas, M. van Zuilen, M. Wadhwa, A. M. Davis, B. Marty, & P. E. Janne. 2004. Clues from Fe isotope variations on the origin of Early Archean BIFs from Greenland. Science 306:2077–2080.

De Carlo, E. H., & W. J. Green. 2002. Rare earth elements in the water column of Lake Vanda, McMurdo Dry Valleys, Antarctica. Geochimica et Cosmochimica Acta 66:1323–1333.

Delvinge, C., D. Cardinal, A. Hofmann, & L. André. 2012. Stratigraphic changes of Ge/Si, REE+Y and silicon isotopes as insights into the deposition of a Mesoarchean banded iron formation. Earth and Planetary Science Letters 355–356:109–118.

Dekov, V. M., Sven Petersen, C.-D. Garbe-Schonberg, G. D. Kamenov, Mirjam Perner, Erno Kuzmann, & Mark Schmidt. 2010. Fe-Si-oxyhydroxide deposits at a slow-spreading centre with thickened oceanic crust: The Lilliput hydrothermal field (9°33′S, Mid-Atlantic Ridge). Chemical Geology 278:186–200.

Doemel, W. N., & T. D. Brock. 1977. Structure, growth, and decomposition of laminated algal-bacterial mats in alkaline hot springs. Applied and Environmental Microbiology 34:433–452.

Dymek, R. F., & Cornelis Klein. 1988. Chemistry, petrology, and origin of banded iron formation lithologies from the 3800 Ma Isua supracrustal belt, West Greenland. Precambrian Research 39:247–302.

Edwards, K. J., T. M. Gihring, & J. F. Banfield. 1999. Seasonal variations in microbial populations and environmental conditions in an extreme acid mine drainage environment. Applied and Environmental Microbiology 65:3627–3632.

Ehrenberg, D. C. G. 1836. Vorläufige Mittheilungen über das wirkliche Vorkommen fossiler Infusorien und ihre grosse Verbreitung. Annalen der Physik und Chemie 38:213–227.

Ehrenberg, D. C. G. 1838. Die Infusionsthierchen als vollkommene Organismen. Voss. Leipzig. 577 p.

Ehrenreich, Armin, & Friedrich Widdel. 1994. Anaerobic oxidation of ferrous iron by purple bacteria, a new type of phototrophic metabolism. Applied and Environmental Microbiology 60:4517–4526.

Eigenbrode, J. L., & K. H. Freeman. 2006. Late Archean rise of aerobic microbial ecosystems. Proceedings of the National Academy of Sciences 103:15759–15764.

Eigenbrode, J .L., K. H. Freeman, & R. E. Summons. 2008. Methylhopane biomarker hydrocarbons in Hamersley Province sediments provide evidence for Neoarchean aerobiosis. Earth and Planetary Science Letters 273:323–331.

Elderfield, Henry. 1988. The oceanic chemistry of the rare-earth elements. Royal Society of London Philosophical Transactions (series A) 325:105–126.

Emerson, David, & C. L. Moyer. 2002. Neutrophilic Fe-oxidizing bacteria are abundant at the Loihi seamount hydrothermal vents and play a major role in Fe oxide deposition. Applied and Environmental Microbiology 68:3085–3093.

Emerson, David, J. A. Rentz, T. G. Lilburn, R. E. Davis, H. Aldrich, C. Chan, & C. L. Moyer. 2007. A novel lineage of Proteobacteria involved in formation of marine Fe-oxidizing microbial mat communities. Plos One 2(8):e667.

Ewers, W. E. 1980. Chemical conditions for the precipitation of banded iron-formations. *In* P. A. Trudinger, M. R. Walter, & B. J. Ralph, eds., Biogeochemistry of Ancient and Modern Environments. Springer-Verlag. Netley, Australia. p. 83–92.

Ewers, W. E., & R. C. Morris. 1981. Studies of the Dales Gorge Member of the Brockman Iron Formation, Western Australia. Economic Geology 76:1929–1953.

Fabre, S., A. Nédélec, F. Poitrasson, H. Strauss, C. Thomazo, & A. Nogueira. 2011. Iron and sulphur isotopes from the Carajás mining province (Pará, Brazil): Implications for the oxidation of the ocean and the atmosphere across the Archaean–Proterozoic transition. Precambrian Research 289:124–139.

Farquhar, James, Huiming Bao, & Mark Thiemens. 2000. Atmospheric influence of Earth's earliest sulfur cycle. Science 289:756–758.

Farquhar, James, & D. T. Johnston. 2008. The oxygen cycle of the terrestrial planets: Insights into the processing and history of oxygen in surface environments. Reviews in Mineralogy and Geochemistry 68:463–492.

Farquhar, James, & B. A. Wing. 2003. Multiple sulfur isotopes and the evolution of the atmosphere. Earth and Planetary Science Letters 213:1–13.

Farquhar, James, & B. A. Wing. 2005. The terrestrial record of stable sulphur isotopes: A review of the implications for evolution of Earth's sulphur cycle. Geological Society Special Publication 248:167–177.

Fischer, W. W., & A. H. Knoll. 2009. An iron shuttle for deep-water silica in Late Archean and early Paleoproterozoic iron formation. Geological Society of America Bulletin 121:222–235.

Fischer, W. W., S. Schroeder, J. P. Lacassie, N. J. Beukes, T. Goldberg, H. Strauss, U. E. Horstmann, D. P. Schrag, & A. H. Knoll. 2009. Isotopic constraints on the Late Archean carbon cycle from the Transvaal Supergroup along the western margin of the

Kaapvaal craton, South Africa. Precambrian Research 169:15–27.

Flick, H, H. D. Nesbor, & R. Behnisch. 1990. Iron ore of the Lahn-Dill type formed by diagenetic seeping of pyroclastic sequences: A case study on the Schalstein section at Gänsberg (Weilburg). International Journal of Earth Sciences 79:1401–415.

Fralick, P. W. 1989. Microbial bioherms, Lower Proterozoic Gunflint Formation, Thunder Bay, Ontario. *In* H. H. J. Geldsetzer, N. P. James, & G. E. Tebbutt, eds., Reefs: Canada and Adjacent Areas. Memoirs, Canadian Society of Petroleum Geologists. p. 24–29.

Fralick, P. W., S. W. Poulton, & D. E. Canfield. 2011. Does the Paleoproterozoic Animikie Basin record the sulfidic ocean transition? Comment. Geology 39 (5):e241, available online:[doi:10.1130/G31747C.1].

Fralick, P. W., & P. K. Pufahl. 2006. Iron formation in Neoarchean deltaic successions and the microbially mediated deposition of transgressive systems tracts. Journal of Sedimentary Research 76:1057–1066.

François, L. M. 1986. Extensive deposition of banded iron formations was possible without photosynthesis. Nature 320:352–354.

Franklin, J. M., H. L. Gibson, I. R. Jonasson, & A. G. Galley. 2005. Volcanogenic massive sulfide deposits. Economic Geology, 100th Anniversary Volume. p. 523–560.

Frimmel, H. E. 2008. The Gariep Belt. *In* R. M. Miller, ed., The Geology of Namibia. Handbook of the Geological Survey of Namibia, Geological Survey of Namibia. p. 1–39.

Fryer, B. J. 1976. Rare earth evidence in iron-formations for changing Precambrian oxidation states. Geochimica et Cosmochimica Acta 41:361–367.

Garrels, R. M. 1987. A model for the deposition of the microbanded Precambrian iron formations. American Journal of Science 287:81–106.

Garrels, R. M., & E. A. J. Perry. 1974. Cycling of carbon, sulfur, and oxygen through geologic time. *In* E. A. Goldberg, ed., The Sea. Wiley. New York. p. 303–336.

Garzani, E. 1993. Himalayan ironstones, "superplumes," and the breakup of Gondwana. Geology 21:105–108.

German, C. R. & Henry Elderfield. 1990. Application of the Ce-anomaly as a paleoredox indicator: The ground rules. Paleoceanography 5:823–833.

Ghiorse, W. C., & H. L. Ehrlich. 1992. Microbial biomineralization of iron and manganese. *In* H. C. W. Skinner & R. W Fitzpatrick, eds., Biomineralization. Processes of iron and manganese. Cremlingen. Catena Supplement 21:75–99.

Golubic, Stjepko, & Seong-Joo Lee. 1999. Early cyanobacterial fossil record: preservation, paleoenvironments and identification. European Journal of Phycology 34:339–348.

Gomont, M. 1892. Monographie des Oscillariées (Nostocacées Homocystées). Deuxième partie. Lyngbyées. Annales des Sciences Naturelles, Botanique (série 7) 16:91–264, pl 1–7.

Goodwin, A. M. 1956. Facies relations in the Gunflint iron-formation. Economic Geology 51:565–595.

Goodwin, A. M. 1973. Archean iron-formations and tectonic basins of the Canadian Shield. Economic Geology 68:915–933.

Grenne, Tor, & J. F. Slack. 2003. Bedded jaspers of the Ordovician Løkken ophiolite, Norway: Seafloor deposition and diagenetic maturation of hydrothermal plume-derived silica-iron gels. Mineralium Deposita 38:625–639.

Grenne, Tor, & J. F. Slack. 2005. Geochemistry of jasper beds from the Ordovician Løkken ophiolite, Norway: Origin of proximal and distal siliceous exhalites. Economic Geology 100:1511–1527.

Gross, G. A. 1965. Geology of iron deposits in Canada. Volume I. General Geology and Evaluation of Iron Deposits. Geological Survey of Canada Economic Report 22, 181 p.

Gross, G. A. 1980. A classification of iron-formation based on depositional environments. Canadian Mineralogist 18:215–222.

Gross, G. A. 1983. Tectonic systems and the deposition of iron-formation. Precambrian Research 20:171–187.

Gross, G. A. 1988. A comparison of metalliferous sediments, Precambrian to Recent. Krystalinikum 19:59–74.

Gross, G. A. 1993. Element distribution patterns as metallogenetic indicators in siliceous metalliferous sediments. Resource Geology Special Issue 17:96–107.

Gross, G. A. 1995. The distribution of rare earth elements in iron-formations. Global Tectonics and Metallogeny 5:63–68.

Guilbaud, Romain, I. B. Butler, & R. M. Ellam. 2011. Abiotic pyrite formation produces a large Fe isotope fractionation. Science 332:1548–1551.

Habicht, K. S., Michael Gade, Bo Thamdrup, Peter Berg, & D. E. Canfield. 2002. Calibration of sulfate levels in the Archean ocean. Science 298:2372–2374.

Halverson, G. P., Franck Poitrasson, P. H. Hoffman, Anne Nedelec, J.-M. Montel, & Jason Kirby. 2011. Fe isotope and trace element geochemistry of the Neoproterozoic syn-glacial Rapitan iron formation. Earth and Planetary Science Letters 309:100–112.

Hamade, Tristan, K. O. Konhauser, R. Raiswell, R. C. Morris, & S. Goldsmith. 2003. Using Ge:Si ratios to decouple iron and silica fluxes in Precambrian banded iron formations. Geology 31:35–38.

Hamilton, M. A., K. L. Buchan, R. E. Ernst, & G. M. Stott. 2009. Widespread and short-lived 1870 Ma mafic magmatism along the northern Superior craton margin. EOS Transactions, American Geophysical Union, 2009 Joint Assembly, Toronto, Canada, Abstract GA11A-01.

Harder, E. C. 1919. Iron-depositing bacteria and their geological relations. U.S. Geological Survey Professional Paper 113. 89 p.

Hayes, J. M. 1983. Geochemical evidence bearing on the origin of aerobiosis: a speculative hypothesis. *In* J. W. Schopf, ed., Earth's Earliest Biosphere: Its Origin and Evolution. Princeton University Press. Princeton. p. 291–301.

Heaman, L. M., N. Machado, T. E. Krogh, & W. Weber. 1986. Precise U-Pb zircon ages for the Molson dyke swarm and the Fox River sill: Constraints for Early Proterozoic crustal evolution in northeastern

Manitoba, Canada. Contributions to Mineralogy and Petrology 94:82–89.

Heaman, L. M., Dave Peck, & Kimberly Toope. 2009. Timing and geochemistry of 1.88 Ga Molson igneous events, Manitoba: Insights into the formation of a craton-scale magmatic and metallogenic province. Precambrian Research 172:143–162.

Heimann, Adriana, C. M. Johnson, B. L. Beard, J. Valley, E. E. Roden, M. J. Spicuzza, & N. J. Beukes. 2010. Fe, C, and O isotope compositions of banded iron formation carbonates demonstrate a major role for dissimilatory iron reduction in ~2.5 Ga marine environments. Earth and Planetary Science Letters 294:8–18.

Heimann, Adriana, P. G. Spry, G. S. Teale, C. H. H. Conor, & W. R. Leyh. 2009. Geochemistry of garnet-rich rocks in the Southern Curnamona Province, Australia, and their genetic relationship to Broken Hill-type Pb-Zn-Ag mineralization. Economic Geology 104:687–712.

Heimann, Adriana, P. G. Spry, G. S. Teale, W. R. Leyh, C. H. H. Conor, Germán Mora, & J. J. O'Brien. 2013. Geochemistry and genesis of low grade metasediment-hosted Zn-Pb-Ag mineralization, southern Proterozoic Curnamona Province, Australia. Journal of Geochemical Exploration 128:97–116.

Heising, Silke, Lothar Richter, Wolfgang Ludwig, & B. Schink. 1999. *Chlorobium ferrooxidans* sp. nov., a phototrophic green sulfur bacterium that oxidizes ferrous iron in coculture with a "Geospirillum" sp. Strain. Archives of Microbiology 172:116–124.

Heising, Silke, & B. Schink. 1998. Phototrophic oxidation of ferrous iron by a Rhodomicrobium vannielii strain. Microbiology 144:2263–2269.

Hofmann, Axel. 2005. The geochemistry of sedimentary rocks from the Fig Tree Group, Barberton greenstone belt: Implications for tectonic, hydrothermal and surface processes during mid-Archaean times. Precambrian Research 143:23–49.

Hofmann, H. J. 1969. Stromatolites from the Proterozoic Animikie and Sibley Groups. Geological Survey of Canada Paper, Geological Survey of Canada. p. 68.

Hoffman, P. F., A. J. Kaufman, G. P. Halverson, & D. P. Schrag. 1998. A Neoproterozoic snowball Earth. Science 281:1342–1346.

Holland, H. D. 1973. The oceans: A possible source of iron in iron-formations. Economic Geology 68:1169–1172.

Holland, H. D. 1984. The Chemical Evolution of the Atmosphere and Oceans. Princeton University Press. New York. 582 p.

Holland, H. D. 2006. The oxygenation of the atmosphere and oceans. Philosophical Transactions of the Royal Society (series B) 361:903–915.

Holland, H. D., & Ulrich Petersen. 1995. Living dangerously. Princeton University Press. Princeton. 490 p.

Holm, N. G. 1987. Biogenic influences on the geochemistry of certain ferruginous sediments of hydrothermal origin. Chemical Geology 63:45–57.

Holm, N. G. 1989. The $^{13}C/^{12}C$ ratios of siderite and organic matter of a modern metalliferous hydrothermal sediment and their implications for banded iron formations. Chemical Geology 63:45–57.

Huston, D. L., & G. A. Logan. 2004. Barite, BIFs and bugs: Evidence for the evolution of the Earth's early hydrosphere. Earth and Planetary Science Letters 220:41–55.

Huston, D. L., S. Pehrsson, B. M. Eglington, & K. Zaw. 2010. The geology and metallogeny of volcanic-hosted massive sulfide deposits: Variations through geologic time and with tectonic setting. Economic Geology 105:571–591.

Ilyn, A. V. 2009. Neoproterozoic banded iron formations. Lithology and Mineral Resources 44:78–86.

Isley, A. E. 1995. Hydrothermal plumes and the delivery of iron to banded iron formation. Journal of Geology 10:169–185.

Isley, A. E., & Abbott, D. H. 1999. Plume-related mafic volcanism and the deposition of banded iron formation. Journal of Geophysical Research 104: 15461–15477.

Jacobsen, S. B., & M. R. Pimentel-Klose. 1988. A Nd isotopic study of the Hamersley and Michipicoten banded iron formations: The source of REE and Fe in Archean oceans. Earth and Planetary Science Letters 87:29–44.

James, H. L. 1954. Sedimentary facies of iron-formation. Economic Geology 49:235–293.

James, H. L. 1983. Distribution of banded iron-formation in space and time. *In* A. F. Trendall & R. C. Morris, eds., Iron-formation: Facts and Problems. Elsevier. Amsterdam. p. 471–490.

Johnson, C. M., B. L. Beard, N. J. Beukes, Cornelis Klein, & J. M. O'Leary. 2003. Ancient geochemical cycling in the Earth as inferred from Fe isotope studies of banded iron formations from the Transvaal craton. Contributions to Mineralogy and Petrology 144:523–547.

Johnson, C. M., B. L. Beard, Cornelis Klein, N. J. Beukes, & E. E. Roden. 2008. Iron isotopes constrain biologic and abiologic processes in banded iron formation genesis. Geochimica et Cosmochimica Acta 72:151–169.

Johnson, C. M., B. L. Beard, & E. E. Roden. 2008. The iron isotope fingerprints of redox and biogeochemical cycling in the modern and ancient Earth. Annual Reviews of Earth and Planetary Sciences 36:457–493.

Johnson, C. M., J. M. Ludois, B. L. Beard, N. J. Beukes, & Adriana Heimann. 2013. Iron formation carbonates: Paleoceanographic proxy or recorder of microbial diagenesis? Geology 41:1147–1150.

Johnson, C. M., E. E. Roden, S. A. Welch, & B. L. Beard. 2005. Experimental constraints on Fe isotope fractionation during magnetite and Fe carbonate formation coupled to dissimilatory hydrous ferric oxide reduction. Geochimica et Cosmochimica Acta 69:963–993.

Kappler, Andreas, Claudia Pasquer, K. O. Konhauser, & D. K. Newman. 2005. Deposition of banded iron formations by anoxygenic phototrophic Fe(II)-oxidizing bacteria. Geology 33:865–868.

Karl, D. M., A. M. Brittain, & B. D. Tillbroo. 1989. Hydrothermal and microbial processes at Loihi Seamount, a mid-plate hot-spot volcano. Deep-Sea Research 36:1655–1673.

Kato, Yasuhiro, Takashi Kano, & Keitaro Kunugiza. 2002. Negative Ce anomaly in the Indian banded iron formations: Evidence for the emergence of oxygenated deep-sea at 2.9–2.7 Ga. Resource Geology 52:101–110.

Kato, Yasuhiro, K. E. Yamaguchi, & Hiroshi Ohmoto. 2006. Rare earth elements in Precambrian banded iron formations: Secular changes of Ce and Eu anomalies and evolution of atmospheric oxygen. *In* S. E. Kesler & Henry Ohmoto, eds., Evolution of the Early Earth's Atmosphere, Hydrosphere, and Biosphere: Constraints from Ore Deposits. Geological Society of America Memoir 198:269–289.

Kaufman, A. J., J. M. Hayes, & Cornelis Klein. 1990. Primary and diagenetic controls of isotopic compositions of iron-formation carbonates. Geochimica et Cosmochimica Acta 54:3461–3473.

Kemp, A. I. S., C. J. Hawkesworth, B. A. Paterson, & P. D. Kinny. 2006. Episodic growth of the Gondwana supercontinent from hafnium and oxygen isotopes in zircon. Nature 439:580–583.

Khan, R. M. K., S. Das Sharma, D. J. Patil, & S. M. Naqvi. 1996. Trace, rare-earth elements, and oxygen isotope systematics for the genesis of banded iron-formations: Evidence from Kushtagi schist belt, Archean Dharwar Craton, India. Geochimica et Cosmochimica Acta 60:3285–3294.

Kimberley M. M. 1978. Palaeoenvironmental classification of iron formations. Economic Geology 73:215–229.

Kirschvink, J. L. 1992. Late Proterozoic low-latitude global glaciation: The Snowball Earth. *In* J. W. Schopf & C. Klein eds, The Proterozoic Biosphere: A Multi-disciplinary Study. Cambridge University Press. New York. p. 51–52.

Klatt, C. G., W. P. Inskeep, M. J. Herrgard, Z. J. Jay, D. B. Rusch, S. G. Tringe, M. N. Parenteau, D. M. Ward, S. M. Boomer, D. A. Bryant, & S. R. Miller. 2013. Community structure and function of high-temperature chlorophototrophic microbial mats inhabiting diverse geothermal environments. Frontiers in Microbiology 4:1–23 [DOI:10.3389/fmicb.2013.00106]

Klein, Cornelis. 2005. Some Precambrian banded iron-formations (BIFs) from around the world: Their age, geologic setting, mineralogy, metamorphism, geochemistry, and origin. Presidential Address to the Mineralogical Society of America, Boston. American Mineralogist 90:1473–1499.

Klein, Cornelis, & N. J. Beukes. 1989. Geochemistry and sedimentology of a facies transition from limestone to iron-formation deposition in the early Proterozoic Transvaal Supergroup, South Africa. Economic Geology 84:1733–1774.

Klein, Cornelis, & N. J. Beukes. 1992. Proterozoic iron formations. *In* K. C. Condie, ed., Proterozoic Crustal Evolution. Elsevier. Amsterdam. p. 383–418.

Klein, Cornelis, & N. J. Beukes. 1993. Sedimentology and geochemistry of the glaciogenic late Proterozoic Rapitan Iron-Formation in Canada. Economic Geology 88:542–565.

Klein, Cornelis, & M. J. Gole. 1981. Mineralogy and petrology of parts of the Marra Mamba iron-formation, Hamersley Basin, Western Australia. American Mineralogist 66:507–525.

Klein, Cornelis, & E. A. Ladeira. 2002. Petrography and geochemistry of the least altered banded iron-formation of the Archean Carajás Formation, Northern Brazil. Economic Geology 97:643–651.

Klein, Cornelis, & E. A. Ladeira. 2004. Geochemistry and mineralogy of Neoproterozoic banded iron-formations and some selected, siliceous manganese formations from the Urucum district, Mato Grosso do Sul, Brazil. Economic Geology 99:1233–1244.

Klinkhammer, G., Henry Elderfield, & A. Hudson. 1983. Rare-earth elements in seawater near hydrothermal vents. Nature 305:185–188.

Knauth, L. P., & D. R. Lowe. 2003. High Archean climatic temperature inferred from oxygen isotope geochemistry of cherts in the 3.5 Ga Swaziland Supergroup, South Africa. Geological Society of America Bulletin 115:566–580.

Koehler, Inga, Kurt Konhauser, & Andreas Kappler. 2010. Role of microorganisms in banded iron formations. *In* L. L. Barton, Martin Mandl, & Alexander Loy, eds., Geomicrobiology: Molecular and Environmental Perspective. Springer Science+Business Media BV. Dordrecht.

Komiya, Tsuyoshi, Shigenori Maruyama, Toshiaki Masuda, Susumu Nohda, Mamoru Hayashi, & Kazuaki Okamoto. 1999. Plate tectonics at 3.8-3.7 Ga: Field evidence from the Isua accretionary complex, southern West Greenland. Journal of Geology 107:515–554.

Konhauser, K. O. 1997. Bacterial iron biomineralization in nature. FEMS Microbiology Reviews 20:315–326.

Konhauser, K. O. 1998. Diversity of bacterial iron mineralization. Earth Science Reviews 43:91–121.

Konhauser, K. O. 2000. Hydrothermal bacterial biomineralization: Potential modern-day analogues for banded iron formations. Marine Authigenesis: From Global to Microbial, SEPM Special Publication 66:133–145.

Konhauser, K. O., Larry Amskold, S. V. Lalonde N. R. Posth, Andreas Kappler & Ariel Anbar. 2007. Decoupling photochemical Fe(II) oxidation from shallow-water BIF deposition. Earth and Planetary Science Letters 258:87–100.

Konhauser, K. O., Tristan Hamade, R. C. Morris, F. G. Ferris, Gordon Southam, Rob Raiswell, & Donald Canfield. 2002. Could bacteria have formed the Precambrian banded iron formations? Geology 30:1079–1082.

Konhauser, K. O., D. K. Newman, & Andreas Kappler. 2005. Fe(III) reduction in BIFs: The potential significance of microbial Fe(III) reduction during deposition of Precambrian banded iron formations. Geobiology 3:167–177.

Krapež, Bryan, M. E. Barley, & A. L. Pickard. 2003. Hydrothermal and resedimented origins of the precursor sediments to banded iron formations: Sedimentological evidence from the early Palaeoproterozoic Brockman Super-sequence of Western Australia. Sedimentology 50:979–1011.

Kump, L. R., & W. E. Seyfried. 2005. Hydrothermal Fe fluxes during the Precambrian: Effect of low oceanic sulfate concentrations and low hydrostatic pressure on the composition of black smokers. Earth and Planetary Science Letters 235:654–662.

Kützing, F. T. 1843. Phycologia Generalis. Leipzig. xxiv + 458 p.

Lawrence, M. G., & B. S. Kamber. 2006. The behaviour of the rare earth elements during estuarine mixing-revisited. Marine Chemistry 100:147–161.

Lehours, A. C., Paul Evans, Corinne Bardot, Keith Joblin, & Gérard Fonty. 2007. Phylogenetic diversity of Archaea and Bacteria in the anoxic zone of a meromictic lake (Lake Pavin, France). Applied and Environmental Microbiology 73:2016–2019.

Li, W., J. Huberty, B. L.Beard, J. Valley, & C. Johnson. 2013. Contrasting behavior of oxygen and iron isotopes in banded iron formations as determined by in situ isotopic analysis. Earth and Planetary Science Letters 384:132–143.

Little, C. T. S., S. E. J. Glynn, & R. A. Mills. 2004. Four-hundred-and-ninety-million-year record of bacteriogenic iron oxide precipitation at sea-floor hydrothermal vents. Geomicrobiology Journal 21:415–429.

Lovley, D. R. 1991. Dissimilatory Fe(III) and Mn(IV) reduction. Microbiology Reviews 55:259–287.

Lovley, D. R. 2004. Potential role of dissimilatory iron reduction in the early evolution of microbial respiration. *In* J. Seckbach, ed., Origins, Evolution, and Biodiversity of Microbial Life. Kluwer. The Netherlands. p. 301–313.

Lovley D. R., S. J. Govannoni, D. C. White, J. E Champine, E. J. P. Phillips, Y. A. Gorby & S. Goodwin. 1993. Geobacter metallireducens gen. nov., sp. nov., a microorganism capable of coupling the complete oxidation of organic compounds to the reduction of iron and other metals. Archives of Microbiology 159:336–344.

Lovley, D. R., & E. J. P. Phillips. 1987. Competitive mechanisms for inhibition of sulfate reduction and methane production in the zone of ferric iron reduction in sediments. Applied and Environmental Microbiology 53:2636–2641.

Lovley, D. R., J. F. Stolz, G. L. Nord, & E. J. P. Phillips. 1987. Anaerobic production of magnetite by a dissimilatory iron-reducing microorganism. Nature 330:252–254.

Macdonald, F. A., J. V. Strauss, C. V. Rose, F. O. Dudás, & D. P. Schrag. 2010. Stratigraphy of the Port Nolloth Group of Namibia and South Africa and implications for the age of Neoproterozoic iron formations. American Journal of Science 310:862–888.

Manikyamba, C., V. Balaram, & S. M. Naqvi. 1993. Geochemical signatures of polygenetic origin of a banded iron formation (BIF) of the Archaean Sandur greenstone belt (schist belt) Karnataka nucleus, India. Precambrian Research 61:137–164.

Maynard, J. B. 2003. Manganiferous sediments, rocks, and ores. Treatise on Geochemistry 7:289–308.

Maynard, J. B., & F. B. Van Houten. 1992. Descriptive model of oolitic ironstones. U.S. Geological Survey Bulletin 2004:39–40.

McLennan, S. M., & S. R. Taylor. 1991. Sedimentary rocks and crustal evolution: Tectonic setting and secular trends. Journal of Geology 99:1–21.

Meert, J. G., M. K. Pandit, V. R. Pradhan, & G. Kamenov. 2011. Preliminary report on the paleomagnetism of 1.88 Ga dykes from the Bastar and Dharwar cratons, peninsular India. Gondwana Research 20:335–343.

Moeller, Kirsten, R. Schoenberg, Tor Grenne, I. H. Thorseth, K. Drost, & R. B. Pedersen. 2013. Comparison of iron isotope variations in modern and Ordovician siliceous Fe oxyhydroxide deposits. Geochimica et Cosmochimica Acta 126:422–440.

Miyano, Takashi, & Cornelis Klein. 1983. Evaluation of the stability relations of amphibole asbestos in metamorphosed iron-formations. Mining Geology 33:213–222.

Morris, R. C. 1993. Genetic modeling for banded iron-formation of the Hamersley Group, Pilbara craton, Western Australia. Precambrian Research 60:243–286.

Mukhopadhyay, Joydip, N. J. Beukes, R. A. Armstrong, Udo Zimmermann, Gautam Ghosh, & R. A. Medda. 2008. Dating the oldest greenstone in India: A 3.51-Ga precise U-Pb SHRIMP zircon age for dacitic lava of the southern Iron Ore Group, Singhbhum craton. Journal of Geology 116:449–461.

Nelson, D. R., A. F. Trendall, & W. Altermann. 1999. Chronological correlations between the Pilbara and Kaapvaal Cratons. Precambrian Research 97:165–189.

Nealson, K. H., & C. R. Myers. 1990. Iron reduction by bacteria: A potential role in the genesis of banded iron formations. American Journal of Science 290:35–45.

Noffke, Nora. 2009. An astrobiologist considers life's oldest oxygen. Nature 457:939.

Noffke, Nora. 2010. Geobiology: Microbial mats in sandy deposits from the Archean era to today. Springer. Berlin. 205 p.

Nordstrom, D. K. 2000. Advances in the hydrogeochemistry and microbiology of acid mine waters. International Geology Review 42:499–515.

Nordstrom, D. K., & C. N. Alpers. 1999. Negative pH, efflorescent mineralogy, and consequences for environmental restoration at the Iron Mountain superfund site, California. Proceedings of the National Academy of Sciences 96:3455–3462.

Nordstrom, D. K., C. N. Alpers, C. J. Ptacek, and D. W. Blowes. 2000. Negative pH and extremely acidic mine waters from Iron Mountain, California. Environmental Science and Technology 34:245–258.

Ohmoto, Hiroshi. 1997. When did the Earth's atmosphere become oxic? Geochemical News 93:12–13; 26–28.

Ohmoto, Hiroshi. 2004. Archean atmosphere, hydrosphere, and biosphere. *In* P. G. Erickson, Wladyslaw Altermann, D. R. Nelson, W. U. Mueller, & Octavian Catuneanueds, The Precambrian Earth: Tempos and Events. Developments in Precambrian Geology. Volume 12. Elsevier. Amsterdam. p. 361–368.

Ohmoto, Hiroshi., Yumiko Watanabe, & Kazumasa Kumazawa. 2004. Evidence from massive siderite

beds for a CO_2-rich atmosphere before approximately 1.8 billion years ago. Nature 429:395–399.

Ohmoto, Hiroshi, Yumiko Watanabe, K. E. Yamaguchi, H. Naraoka, M. Haruna, T. Kakegawa, K. Hayashi, & Y. Kato. 2006. Chemical and biological evolution of early Earth: Constraints from banded iron formations. *In* S. E. Kesler & Hiroshi Ohmoto, eds., Evolution of early Earth's atmosphere, hydrosphere, and biosphere: Constraints from ore deposits. Geological Society of America Memoir 98:291–331.

Ono, Shuhei, J. L. Eigenbrode, A. A. Pavlov, P. Kharech, D. Rumble, J. F. Kasting, & K. H. Freeman. 2003. New insights into Archean sulfur cycle from mass-independent sulfur isotope records from the Hamersley Basin, Australia. Earth and Planetary Science Letters 213:15–30.

Parenteau, M. N., & S. L. Cady. 2010. Microbial biosignatures in iron-mineralized phototrophic mats at Chocolate Pots Hot Springs, Yellowstone National Park, United States. Palaios 25:97–111.

Parman, S. W. 2007. Helium isotopic evidence for episodic mantle melting and crustal growth. Nature 446:900–903.

Parr, J. M. 1992. Rare-earth element distribution in exhalites associated with Broken Hill type mineralisation at the Pinnacles deposit, New South Wales, Australia. Chemical Geology 100:73–91.

Parr, J. M., & I. R. Plimer. 1993. Models for Broken Hill-type lead-zinc-silver deposits. Geological Association of Canada Special Paper 40:253–288.

Pavlov, A. A., & J. F. Kasting. 2002. Mass-independent fractionation of sulfur isotopes in Archean sediments: Strong evidence for an anoxic Archean atmosphere. Astrobiology 2:27–41.

Pearson, D. G., Parman, S. W., & G. M. Nowell. 2007. A link between large mantle melting events and continent growth seen in osmium isotopes. Nature 449:202–205.

Pecoits, Ernesto, M. K. Gingras, Natalie Aubet, & K. O. Konhauser. 2008. Ediacaran in Uruguay: Palaeoclimatic and palaeobiologic implications. Sedimentology 55:689–719.

Pecoits, Ernesto, M. K. Gingras, M. E. Barley, Andreas Kappler, N. R. Posth & K. O. Konhauser. 2009. Petrography and geochemistry of the Dales Gorge banded iron formation: paragenetic sequence, source and implications for palaeo-ocean chemistry. Precambrian Research 172:163–187.

Perry, E. C., F. C. Tan, & G. B. Morey. 1973. Geology and stable isotope geochemistry of Biwabik Iron Formation, northern Minnesota. Economic Geology 68:1110–1125.

Peter, J. M. 2003. Ancient iron formations: Their genesis and use in the exploration for stratiform base metal sulphide deposits, with examples from the Bathurst mining camp. Geological Association of Canada, Geotext 4:145–176.

Peter, J. M., & W. D. Goodfellow. 1996. Mineralogy, bulk and rare earth element geochemistry of massive sulphide-associated hydrothermal sediments of the Brunswick Horizon, Bathurst Mining Camp, New Brunswick. Canadian Journal of Earth Sciences 33:252–283.

Petránek, J., & F. B. Van Houten. 1997. Phanerozoic ooidal ironstones. Czech Geological Survey Special Paper 7:1–71.

Perty, M. 1852. Zur Kenntnis kleinster Lebensformen. Jent and Reinert. Bern. i–vvv, +228 p.

Pickard, A. L. 2002. SHRIMP U–Pb zircon ages of tuffaceous mudrocks in the Brockman Iron Formation of the Hamersley Range, Western Australia. Australian Journal of Earth Sciences 49:491–507.

Pickard, A. L. 2003. SHRIMP U-Pb zircon ages for the Palaeoproterozoic Kuruman Iron Formation, Northern Cape Province, South Africa: Evidence for simultaneous BIF deposition on Kaapvaal and Pilbara cratons. Precambrian Research 125:275–315.

Pickard, A. L., M. E. Barley, & Bryan Krapež. 2004. Deep-marine depositional setting of banded iron formation: Sedimentological evidence from interbedded clastic sedimentary rocks in the early Paleoproterozoic Dales Gorge Member of Western Australia. Sedimentary Geology 170:37–62.

Pierson, B. K., and Castenholz, R.W. 1974. A phototrophic gliding filamentous bacterium of hot springs, *Chloroflexus aurantiacus*, gen. and sp. nov.. Archives of Microbiology 100:5–24.

Pierson, B. K., M. N. Parenteau, & B. M. Griffin. 1999. Phototrophs in high-iron-concentration microbial mats: Physiological ecology of phototrophs in an iron-depositing hot spring. Applied and Environmental Microbiology 65:5474–5483.

Planavsky, Noah, Andrey Bekker, O. J. Rouxel, B. Kamber, A. Hofmann, A. Knudsen, & T. W. Lyons. 2010. Rare earth element and yttrium compositions of Archean and Paleoproterozoic Fe formations revisited: New perspectives on the significance and mechanisms of deposition. Geochimica et Cosmochimica Acta 74:6387–6405.

Planavsky, Noah, O. J. Rouxel, Andrey Bekker, Axel Hofmann, C. T. S. Little, & T. W. Lyons. 2012. Iron isotope composition of some Archean and Proterozoic iron formations. Geochimica et Cosmochimica Acta 80:158–169.

Planavsky, Noah, O. J. Rouxel, Andrey Bekker, Russell Shapiro, P. W. Fralick, & Andrew Knudsen. 2009. Iron-oxidizing microbial ecosystems thrived in late Paleoproterozoic redox-stratified oceans. Earth and Planetary Science Letters 286:230–242.

Plimer, I. R. 1988. Broken Hill, Australia and Bergslagen, Sweden: Why God and Mammon bless the anthipodes! *In* The Bergslagen Province, central Sweden: Structure, stratigraphy and ore-forming processes. Geologie en Mijnbouw. Netherlands Journal of Sciences 67:265–278.

Posth, N. R., Florian Hegler, K. O. Konhauser, & Andreas Kappler. 2008. Alternating Si and Fe deposition caused by temperature fluctuations in Precambrian oceans. Nature Geoscience 1:703–708.

Posth, N. R., K. O. Konhauser, & Andreas Kappler. 2011. Banded iron formations. *In* Volker Thiel & Joachim Reitner, eds., Encyclopedia of Geobiology. Encyclopedia of Earth Science Series. Springer. The Netherlands. p. 92–103.

Poulton, S. W. 2011. Iron mineralization in anoxic, non-sulphidic systems. Mineralogical Magazine 75.3:1662.

Poulton, S. W., P. W. Fralick, & D. E. Canfield. 2004. The transition to a sulphidic ocean 1.84 billion years ago. Nature 43:173–177.

Pufahl, P. K., & P. W. Fralick. 2004. Depositional controls on Palaeoproterozoic iron formation accumulation, Gogebic Range, Lake Superior region, USA. Sedimentology 51:791–808.

Pufahl, P. K., E. E. Hiatt, & T. K. Kyser. 2010. Does the Paleoproterozoic Animikie Basin record the sulfidic ocean transition? Geology 38.7:659–662.

Pufahl, P. K., E. E. Hiatt, & T. K. Kyser. 2011. Does the Paleoproterozoic Animikie Basin record the sulfidic ocean transition? Reply. Geology 39:e242–243.

Pufahl, P. K., Franco Pirajno, & E. E. Hiatt. 2013. Riverine mixing and fluvial iron formation: A new type of Precambrian biochemical sediment. Geology G34812.1. [doi: 10.1130/G34812.1].

Rao, T. G., & S. M. Naqvi. 1995. Geochemistry, depositional environment and tectonic setting of the BIF's of the Late Archaean Chitradurga Schist Belt, India. Chemical Geology 121:217–243.

Rashby, S. E., A. L. Sessions, R. E. Summons, & D. K. Newman. 2007. Biosynthesis of 2-ethylbacteriohopanepolyols by an anoxygenic phototroph. Proceedings of the National Academy of Sciences USA 104:15099–15104.

Rasmussen, Birger, I. R. Fletcher, Andrey Bekker, J. R. Muhling, C. J. Gregory, & A. M. Thorne. 2012. Deposition of 1.88-billion-year-old iron formations as a consequence of rapid crustal growth. Nature 484:498–501.

Rasmussen, Birger, I. R. Fletcher, J. J. Brocks, & M. R. Kilburn. 2008. Reassessing the first appearance of eukaryotes and cyanobacteria. Nature 455:1101–1104.

Rasmussen, Birger, D. B. Meier, Bryan Krapež, & J. R. Muhling. 2013. Iron silicate microgranules as precursor sediments to 2.5-billion-year-old banded iron formations. Geology 4:435–438.

Ribeiro da Luz, B., & J. K. Crowley. 2012. Morphological and chemical evidence of stromatolitic deposits in the 2.75 Ga Carajás banded iron formation, Brazil. Earth and Planetary Science Letters 355-356:60-72.

Robert, François, & Marc Chaussidon. 2006. A palaeotemperature curve for the Precambrian oceans based on silicon isotopes in cherts. Nature 443:969–972.

Rona, P. A., G. Klinkhammer, T. A. Nelsen, J. H. Trefrey, and Henry Elderfield. 1986. Blacksmokers, massive sulphides and vent biota at the mid-Atlantic ridge. Nature 321:33-37.

Rouxel, O. J., Andrey Bekker, & K. J.Edwards. 2005. Iron isotope constraints on the Archean and Paleoproterozoic ocean redox state. Science 307:1087–1091.

Salama, Walid, M. M. El Aref, & Reinhard Gaupp. 2012. Mineralogical and geochemical investigations of the Middle Eocene ironstones, El Bahariya Depression, Western Desert, Egypt. Gondwana Research 22:717–736.

Salama, Walid., M. M. El Aref, & Reinhard Gaupp. 2013. Mineral evolution and processes of ferruginous microbialite accretion: An example from the Middle Eocene stromatolitic and ooidal ironstones of the Bahariya Depression, Western Desert, Egypt. Geobiology 11:15–28.

Schopf, J. W. 2006. Fossil evidence of Archean life. Philosophical Transactions Royal Society B 361:869–886.

Schwertmann, U., & R. M. Cornell. 1991. Iron oxides in the laboratory; Preparation and characterization. VCH, Weinheim, Federal Republic of Germany. 137 p.

Severmann, Silke, C. M. Johnson, B. L. Beard, & James McManus. 2006. The effect of early diagenesis on the Fe isotope compositions of porewaters and authigenic minerals in continental margin sediments. Geochimica et Cosmochimica Acta 70:2006–2022.

Shields, Graham, & Ján Veizer. 2002. Precambrian marine carbonate isotope database: version 1.1. Geochemistry Geophysics Geosystems (online journal). Vol. 3. [doi:10.1029/2001GC000266].

Shimojo, M., S. Yamamoto, S. Aoki, S. Sakata, K. Maki, K. Koshida, A. Ishikawa, T. Hirata, K. D. Collerson, & T. Komiya. 2013. Occurrence of >3.9 Ga "Nanok" gneiss from Saglek Block, northern Labrador, Canada. Mineralogical Magazine (abstract) 77:2202.

Siever, Raymond. 1992. The silica cycle in the Precambrian. Geochimica et Cosmochimica Acta 56:3265–3272.

Simonson, B. M. 1985. Sedimentological constraints on the origins of Precambrian iron-formations. Geological Society of America Bulletin 96:244–252.

Simonson, B. M. 2003. Origin and evolution of large Precambrian iron formations. Geological Society of America Special Paper 370:231–244.

Simonson, B. M., & S. W. Hassler. 1996. Was the deposition of large Precambrian iron formations linked to major marine transgressions? Journal of Geology 104:665–676.

Slack, J. F., Tor Grenne, & Andrey Bekker. 2009. Seafloor-hydrothermal Si-Fe-Mn exhalites in the Pecos greenstone belt, New Mexico, and the redox state of the ca. 1720 Ma deep seawater. Geosphere 5:302–314.

Søgaard, E. G., Robin Medenwaldt, & J. V. Abraham-Peskir. 2000. Conditions and rates of biotic and abiotic iron precipitation in selected Danish freshwater plants and microscopic analysis of precipitate morphology. Water Research 34:2675–2682.

Sommers, M. G., S. M. Awramik, & K. S. Woo. 2000. Evidence for initial calcite-aragonite composition of Lower Algal Chert Member ooids and stromatolites, Paleoproterozoic Gunflint Formation, Ontario, Canada. Canadian Journal Earth Sciences 37:1229–1243.

Spry, P. G., J. M. Peter, & J. F. Slack. 2000. Metaexhalites as exploration guides to ore. Reviews in Economic Geology 11:163–201.

Stanton, R. L. 1972. A preliminary account of chemical relationships between sulfide lode and "banded iron formation" at Broken Hill, New South Wales. Economic Geology 67:1128–1145.

Stanton, R. L. 1976. Petrochemical studies of the ore environment at Broken Hill, N.S.W.: 3- banded iron formations and sulphide ore bodies: constitutional and genetic ties. Transactions of the Institution of Mining and Metallurgy 85:B132–B141.

Steinhoefel, Grit, Ingo Horn, & F. von Blanckenburg. 2009. Micro-scale tracing of Fe and Si isotope

signatures in banded iron formation using femtosecond laser ablation. Geochimica et Cosmochimica Acta 73:5343–5360.

Straub, K. L., F. A. Rainey, & Friedrich Widdel. 1999. Rhodovulum iodosum sp. nov. and Rhodovulum robiginosum sp. nov., two new marine phototrophic ferrous-iron-oxidizing purple bacteria. International Journal of Systematic Bacteriology 49:729–735.

Sturesson, Ulf. 2003. Lower Palaeozoic iron oolites and volcanism from a Baltoscandian perspective. Sedimentary Geology 159:241–256.

Sturesson, Ulf, Andrei Dronov & Tönis Saadre. 1999. Lower Ordovician iron ooids and associated oolitic clays in Russia and Estonia: A clue to the origin of iron oolites? Sedimentary Geology 123:63–80.

Summons, R. E., L. L. Jahnke, J. M. Hope, & G. A. Logan. 1999. 2-Methylhopanoids as biomarkers for cyanobacterial oxygenic photosynthesis. Nature 400:554–557.

Sverjensky, D. A. 1984. Europium equilibria in aqueous solution. Earth and Planetary Science Letters 67:70–78.

Taitel-Goldman, Nurit, V. Ezrsky, & D. Mogilyanski. 2009. High-resolution transmission electron microscopy study of Fe-Mn oxides in the hydrothermal sediments of the Red Sea deeps system. Clay and Clay Minerals 57:465–475.

Tangalos, G. E., B. L. Beard, , C. M. Johnson, C. N. Alpers, E. S. Shelobolina, Xu H., H. Konishi, & E. E. Roden. 2010. Microbial production of isotopically light iron(II) in a modern chemically precipitated sediment and implications for isotopic variations in ancient rocks. Geobiology 8:197–208.

Taylor, S. R., & S. M. McLennan. 1986. The chemical composition of the Archaean crust. *In* The nature of the lower continental crust. Geological Society Special Publications 24:173–178.

Taylor, K. G., J. A. Simo, D. Yakum, & D. A. Leckie. 2002. Stratigraphic significance of ooidal ironstones from the Cretaceous western interior seaway: The Peace River Formation, Alberta, Canada, and the Castlegate Sandstone, Utah, U.S.A. Journal of Sedimentary Research 72:316–327.

Teutsch, Nadya, Martin Schmid, Beat Müller, A. N. Halliday, Helmut Bürgmann, & Bernhard Wehrli. 2009. Large iron isotope fractionation at the oxic–anoxic boundary in Lake Nyos. Earth and Planetary Science Letters 285:52–60.

Thamdrup, Bo. 2000. Bacterial manganese and iron reduction in aquatic sediments. Advances in Microbial Ecology 16:41–84.

Thompson, J. B., & F. G. Ferris. 1990. Cyanobacterial precipitation of gypsum, calcite, and magnesite from natural alkaline lake water. Applied and Environmental Microbiology 62:1458–1460.

Tice, M. M. 2008. Paleontology: Modern life in ancient mats. Nature 452:40–41.

Tice, M. M., & D. R. Lowe. 2004. Photosynthetic microbial mats in the 3,416-Myr-old ocean. Nature 431:549–552.

Toner, B. M., C. M. Santelli, M. A. Marcus, R. Smith, C. S. Chan, T. McCollom, Wolfgang Bach, & K. J. Edwards. 2009. Biogenic iron oxyhydroxide formation at mid-ocean ridge hydrothermal vents; Juan de Fuca Ridge. Geochimica et Cosmochimica Acta 73:388–403.

Trendall, A. F. 1968. Three great basins of Precambrian banded iron formation deposition: A systematic comparison. Geological Society of America Bulletin 79:1527–1544.

Trendall, A. F. 2002. The significance of iron-formation in the Precambrian stratigraphic record. Special Publication International Association of Sedimentologists 33:33–66.

Trendall, A. F., & J. G. Blockley. 1970. The iron formations of the Precambrian Hamersley group, Western Australia; with special reference to the crocidolite. Bulletin, Geological Survey of Western Australia 119:1–366.

Trendall, A. F., W. Compston, D. R. Nelson, J. R. De Laeter, & V. C. Bennett. 2004. SHRIMP zircon ages constraining the depositional chronology of the Hamersley Group, Western Australia. Australian Journal of Earth Sciences 51:621–644.

Trompette, R., C. J. S. Alvarenga, & D.de Walde. 1998. Geological evolution of the Neoproterozoic Corumbá graben system (Brazil): Depositional context of the stratified Fe and Mn ores of the Jacadigo Group. Journal of South American Earth Sciences 11:587–597.

Trouwborst, R. E., Anne Johnston, Gretchen Koch, G. W. Luther, & B. K. Pierson. 2007. Biogeochemistry of Fe(II) oxidation in a photosynthetic microbial mat: Implications for Precambrian Fe(II) oxidation. Geochimica et Cosmochimica Acta 71:4629–4643.

Tsikos, Harilaos, Alan Matthews, Yigal Erel, & J. M. Moore. 2010. Iron isotopes constrain biogeochemical redox cycling of iron and manganese in a Palaeoproterozoic stratified basin. Earth and Planetary Science Letters 298:125–134.

Tunnicliffe, Verena, & A. R. Fontaine. 1987. Faunal composition and organic surface encrustations at hydrothermal vents on the southern Juan de Fuca Ridge. Journal of Geophysical Research 92:11303–11314.

Tyler, S. A., & E. S. Barghoorn. 1954. Occurrence of structurally preserved plants in Pre-Cambrian rocks of the Canadian Shield. Science 11:606–608.

Van Houten, F. B. 1985. Oolitic ironstones and contrasting Ordovician and Jurassic paleogeography. Geology 13:722–724.

Van Houten, F. B., & M. A. Arthur. 1989. Temporal patterns among Phanerozoic oolitic ironstones and oceanic anoxia. Geological Society Special Publication 46:33–49.

Vargas, M. M., Kazem Kashefi, E. L. Blunt-Harris, & D. R. Lovley. 1998. Microbiological evidence for Fe(III) reduction on early Earth. Nature 395:65–67.

Veizer, J. 1976. Evolution of ores of sedimentary affiliation through geologic history: Relations to the general tendencies in evolution of the crust, hydrosphere, atmosphere, and biosphere. *In* K. H. Wolf, ed., Handbook of Strata-bound and Stratiform Ore Deposits. Elsevier. Amsterdam. 3:1–41.

Veizer, J. 1983. Geologic evolution of the Archean-early Proterozoic earth. *In* J. W. Schopf, ed., Earth's

Earliest Biosphere: Its Origin and Evolution. Princeton University Press. Princeton. p. 240–259.

Waldbauer, J. R., L. S. Sherman, D. Y. Sumner, & R. E. Summons. 2009. Late Archean molecular fossils from the Transvaal Supergroup record the antiquity of microbial diversity and aerobiosis. Precambrian Research 169:28–47.

Walker, J. C. G. 1984. Suboxic diagenesis in banded iron formations. Nature 309:340–342.

Walter, M. R., John Bauld, & T. D. Brock. 1972. Siliceous algal and bacterial stromatolites in hot spring and geyser effluents of Yellowstone National Park. Science 178:402–405.

Walter, M. R., John Bauld, D. J. Des Marais, & J. W. Schopf. 1992. A general comparison of microbial mats and microbial stromatolites: Bridging the gap between the modern and the fossil. *In* J. W. Schopf & C. Klein, eds., The Proterozoic Biosphere. Cambridge University Press. Cambridge, UK. p. 335–338.

Walter, M. R., & H. J. Hoffman. 1983. The palaeontology and palaeoecology of Precambrian iron-formations. *In* A. F. Trendall & R. C. Morris, eds., Iron-Formation: Facts and Problems. Elsevier. Amsterdam. p. 373–400.

Walter, X. A., Antonio Picazo, R. M. Miracle, Eduardo Vicente, Antonio Camacho, Michel Aragno, & Jakob Zopfi. 2009. Anaerobic microbial iron oxidation in an iron-meromictic lake. Geochimica et Cosmochimica Acta 73(Supplement 1):A1405.

Weidman, Samuel. 1904. The Baraboo iron-bearing district of Wisconsin. Wisconsin Geological and Natural History Survey Bulletin 13:1–190.

Whitehouse, M. J., & C. M. Fedo. 2007. Microscale heterogeneity of Fe isotopes in >3.71 Ga banded iron formation from the Isua greenstone belt, southwest Greenland. Geology 35:719–722.

Widdel, Friedrich, Sylvia Schnell, Silke Heising, Armin Ehrenreich, Bernhard Assmus, & Bernhard Schink. 1993. Ferrous iron oxidation by anoxygenic phototrophic bacteria. Nature 362:834–836.

Winogradsky, S. J. 1888. Ueber Eisenbacterien. Botanische Zeitschrift. 46:261–270.

Winter, B. L., & L. P. Knauth. 1992. Stable isotope geochemistry of cherts and carbonates from the 2.0 Ga Gunflint Iron Formation: Implications for the depositional setting, and the effects of diagenesis and metamorphism. Precambrian Research 59:283–313.

Wu, Lingling, R. P. Brucker, B. L. Beard, E. E. Roden, & C. M. Johnson. 2013. Iron isotope characteristics of hot springs at Chocolate Pots, Yellowstone National Park. Astrobiology 13:1091–1101 [doi:10.1089/ast.2013.0996].

Wu Lingling, E. M. Percak-Dennett, B. L. Beard, E. E. Roden, & C. M. Johnson. 2012. Stable iron isotope fractionation between aqueous Fe(II) and model Archean ocean Fe–Si coprecipitates and implications for iron isotope variations in the ancient rock record. Geochimica et Cosmochimica Acta 84:14–28.

Xiong, Jin. 2006. Photosynthesis: What color was its origin? Genome Biology 7:245.

Yamaguchi, K.E., C. M. Johnson, B.L. Beard, & Hiroshi Ohmoto. 2005. Biogeochemical cycling of iron in the Archean-Paleoproterozoic Earth: Constraints from iron isotope variations in sedimentary rocks from the Kaapvaal and Pilbara Cratons. Chemical Geology 218:135–169.

Zegers, T. E., M. J. de Wit, J. Dann, & S. H. White. 1998. Vaalbara, Earth's oldest assembled continent? A combined structural, geochronological, and palaeomagnetic test. Terra Nova 10:250–259.

ZoBell, C. E. 1943. The effect of solid surfaces upon bacterial activity. Journal of Bacteriology 46: 39–56.